

ATMOSPHERIC TRANSFORMATION OF POLYCYCLIC AROMATIC
COMPOUNDS

**ATMOSPHERIC TRANSFORMATION OF POLYCYCLIC AROMATIC
COMPOUNDS**

By

SUJAN FERNANDO, B.Sc.

A Thesis

Submitted to the School of Graduate Studies

In Partial Fulfilment of the Requirements

for the Degree

Master of Science

McMaster University

© Copyright by Sujan Fernando, September 2007

MASTER OF SCIENCE (2007)
(Chemistry)

McMaster University
Hamilton, Ontario

TITLE: ATMOSPHERIC TRANSFORMATION OF POLYCYCLIC
 AROMATIC COMPOUNDS

AUTHOR: Sujan Fernando, B.Sc. (University of Toronto)

SUPERVISOR: Professor B.E. McCarry

NUMBER OF PAGES: xvii, 138

ABSTRACT

The profiles of polycyclic aromatic compounds (PAC) were compared in three separate studies involving air samples collected in urban and rural locations across Canada. In the Freelton/Pier 25 study (conducted near Hamilton, Ontario) a total of 32 NPAH were analyzed for in 12 composite air particulate samples from Freelton (a rural site) and Pier 25 (an urban site) using negative ion chemical ionization gas chromatography-mass spectrometry.

The NPAH levels at the two sites were found to be similar except for the two samples at Pier 25. These results were consistent with the PAH levels determined previously which showed significantly increased levels at Pier 25 under the same condition when the sampling site was downwind of the urban/industrial core. NPAH may be significant contributors to mutation induction due to exposures to ambient air since the offspring of male mice from the Pier 25 site exposed to ambient air showed inherited mutation rates about 2 times greater than offspring of mice exposed at the Freelton site. NPAH are highly mutagenic and carcinogenic compounds that act via reductive metabolism and can be readily metabolized to potent reactive intermediates within all cells.

Concentration data for a set of polycyclic aromatic compounds were obtained for samples collected during the day and night during a study in Simcoe (rural) and Toronto (urban) as well as at three sites in British Columbia as part of the Pacific 2001 study (Slocan (urban), Langley (suburban/rural) and Sumas (rural)). The conversion of these concentration data into particulate loadings data (using elemental carbon data) enabled us

to perform a number of unique interpretations and analyses of the data sets. Since particulate loadings values are not affected by air dispersion it was possible to compare samples and individual PAC across a range of samples.

Principal components analysis of the loadings data showed dramatic differences between the urban and rural sites from each study. Day-night samples at the rural sites also showed dramatic profile differences. The urban sites showed significantly less differences in profiles, consistent with lesser degree of air transformation and closer proximities to sources.

ACKNOWLEDGEMENTS

I would like to take this opportunity to express my gratitude to Dr. B. E. McCarry, my supervisor. This thesis would not have been possible without his guidance, patience and encouragement. Thank you sincerely for all your time and effort and for making the past few years a memorable experience. I would also like to thank Dr. Jeff Brook from Environment Canada for providing the elemental carbon data for both the Toronto/Simcoe study and the Pacific 2001 study.

I would also like to acknowledge all members of the research group with whom I share a special friendship. Uwayemi Sofowote, Catherine Amoateng, Tarlika Persaud, Libia Saborido, Brita Asfaw, Ed Sverko, and David Dam have truly made my time in the research group pleasant and enjoyable. Thank you all for the help and encouragement and I wish you all success in the future.

Lastly and most importantly I would like to thank my family. To my mom and dad, thank you for providing me with the opportunities that I needed to succeed. Your efforts and sacrifices have helped me become a better man. To my loving wife Ruwani, thank you for your encouragement and patience. This thesis would not have been possible without your love and support.

TABLE OF CONTENTS

	Page
ABSTRACT	iii
ACKNOWLEDGEMENTS	v
TABLE OF CONTENTS	vi
LIST OF FIGURES	ix
LIST OF TABLES	xiv
ABBREVIATIONS	xvi
1.0 INTRODUCTION	1
1.1 Particulate material	1
1.2 Polycyclic Aromatic Compounds	3
1.3 Atmospheric Transformation of PAH to Nitrated PAH	4
1.4 Photodegradation of PAH and NitroPAH	6
1.5 Toxicological properties of PAH and NPAH	8
1.6 Freelton/Pier 25 study	11
1.7 Research Objectives	13
2.0 EXPERIMENTAL	15
2.1 Chemicals	15
2.2 Gases and Solvents	15
2.3 Instrumentation	18

2.4 Samples	19
2.4.1 Pier 25/Freelton Samples	19
2.4.2 Pacific 2001 Samples	21
2.4.3 Toronto/Simcoe Samples	23
2.5 Sample Extraction and Cleanup	25
2.6 Synthesis of NPAH	26
2.7 Negative Ion Chemical Ionization Mass Spectrometry	30
2.8 NICI Method Parameters	32
2.9 Calibration and Detection Limits	35
2.10 Tandem Mass Spectrometry	39
2.11 Principal Components Analysis	47
3.0 RESULTS AND DISCUSSION	50
3.1 GC-MS Analysis of Freelton and Pier 25 Air Filter Extracts	51
3.1.1 Principal Components Analysis of the Freelton and Pier 25 Data Sets.	60
3.1 Elemental Carbon and Organic Carbon Concentrations at Toronto & Simcoe.	69
3.2 Loadings of Polycyclic Aromatic Carbons on Air Particulate at Toronto and Simcoe Sites.	72
3.2.1 Principal Component Analysis of PAC Data from Toronto and Simcoe.	77
3.3.2 Mean Relative Loadings of PAC at Toronto and Simcoe	89
3.4 Loadings of Polycyclic Aromatic Carbons on Air Particulate at Slocan, Langley and Sumas Sites.	93

3.4.1	Principal Components Analysis of PAC Data from Slokan, Langley and Sumas	97
3.4.2	Mean Relative Loadings of PAC at Slokan, Langley and Sumas Sites.	108
4.0	CONCLUSIONS	113
5.0	REFERENCES	117
6.0	APPENDICES	122
Appendix A.	Compound Names, Molecular Masses and Structures of Selected Polycyclic Aromatic Compounds	122
Appendix B.	Concentrations (pg/m ³) of the 23 NPAH compounds detected in the Freelton and Pier 25 samples.	127
Appendix C.	Relative Loadings (µg/g C) of PAC in PM _{2.5} collected at Simcoe and Toronto	129
Appendix D.	Relative Loadings (µg/g C) of PAC in PM _{2.5} collected at Slokan, Langley and Sumas	133

LIST OF FIGURES

Figure 1-1	OH radical pathway for the nitration of fluoranthene to 2-nitrofluoranthene.	Page 5
Figure 2-1	GC-MS total ion chromatogram of 32-compound NPAH standard under NICI-SIM mode.	Page 17
Figure 2-2	An aerial map of the Pier 25 and Freelon (Ontario, Canada) sampling sites obtained from GoogleEarth.	Page 20
Figure 2-3	An Aerial map of the sampling sites at the Lower Fraser Valley in British Columbia, Canada.	Page 21
Figure 2-4	An Aerial map of Toronto and Simcoe sampling sites in Ontario, Canada obtained from GoogleEarth.	Page 24
Figure 2-5	Analytical scheme for air sample extraction and cleanup.	Page 25
Figure 2-6	Total ion chromatogram (full scan mode) of the nitrated fluoranthene crude reaction mixture, fraction A, B and C collected from solid phase extraction cleanup method.	Page 28
Figure 2-7	GC-MS mass chromatograms (m/z 247) of a suburban air filter extract analyzed using EI^+ and NICI modes.	Page 30
Figure 2-8	Mass spectra of 1-nitropyrene analyzed using NICI and EI^+ modes.	Page 31
Figure 2-9	The eight 247MW NPAH isomers separated on a DB-17ht column under NICI-SIM mode.	Page 33
Figure 2-10	The average signal to noise ratio (S/N) of the 247MW isomers over a CI gas pressure range of 6.5 to 9.5 Torr.	Page 34
Figure 2-11	Calibration plot of 3-, 4-, 9-nitrophenanthrene and 1-nitropyrene- d_9 over the concentration range from 10 – 5000pg/ μ L.	Page 35
Figure 2-12	Schematic of a daughter ion scan.	Page 39

Figure 2-13	MS/MS mass spectra of 1-nitropyrene at 30eV, 40eV and 50eV collision.	Page 41
Figure 2-14	MS/MS mass spectrum of 1-Nitropyrene, 4-Nitropyrene and 2-Nitrofluoranthene at 50eV collision energy.	Page 42
Figure 2-15	GC-MS analyses of an air filter extract.	Page 45
Figure 2-16	Detection limits (pg/ μ L) of the 247MW NPAH under MRM and SIM conditions.	Page 47
Figure 3-1	Total NPAH concentrations (pg/m ³) of the six composite samples collected at Freelton and Pier 25 sites.	Page 56
Figure 3-2	The ratio of selected NPAH total levels in the 19-24hr samples to the 0-18hrs samples.	Page 57
Figure 3-3	The net concentrations at Pier 25 (Pier 25 – Freelton) of 2-NFA, 1-NP and 2-NP.	Page 59
Figure 3-4(a)	Principal components plot of the Freelton and Pier 25 data matrix that excludes the 19-23hrs and 24hrs data from Pier 25 (Components 1, 2, and 3).	Page 62
Figure 3-4(b)	Principal components plot of the complete data matrix from Freelton and Pier 25 (Components 1, 2, and 3).	Page 63
Figure 3-4(c)	Principal components plot of complete data matrix from Freelton and Pier 25 (Components 1 and 2).	Page 64
Figure 3-4(d)	Principal components plot of complete data matrix from Freelton and Pier 25 (components 1 and 3).	Page 65
Figure 3-4(e)	Principal components plot of the data matrix from Freelton and Pier 25 (components 1, 2 and 3) after the removal of the newly synthesized NPAH from all samples.	Page 67
Figure 3-5	Elemental Carbon (EC) concentrations from Toronto & Simcoe samples.	Page 69

Figure 3-6	Organic Carbon concentrations from Toronto and Simcoe samples.	Page 70
Figure 3-7(a)	Absolute loadings of 2-NP, BeP and Picene from Simcoe and Toronto samples.	Page 73
Figure 3-7(b)	Relative loadings of 2-NP, BeP and Picene from Simcoe and Toronto samples.	Page 73
Figure 3-8(a)	Relative loading ratio of BbF, BkF, BjF, BeP & BghiP to PAH5 composite from Toronto and Simcoe samples.	Page 74
Figure 3-8(b)	Relative loading ratio of BD, 2-NP and 2-NFA to PAH5 composite from Toronto and Simcoe samples.	Page 75
Figure 3-9	Relative loadings values of PAH5 composite at Simcoe and Toronto.	Page 77
Figure 3-10(a)	Principal components plot of data matrix from Toronto and Simcoe (Components 1, 2 and 3).	Page 79
Figure 3-10(b)	Principal components plot of data matrix from Toronto and Simcoe (Component 1 and 2).	Page 80
Figure 3-10(c)	Principal components plot of data matrix from Toronto and Simcoe (components 1, 2 and 3) highlighting the distribution of the non-PAH with respect to the PAH cluster at Simcoe day and night.	Page 81
Figure 3-10(d)	Principal components plot of data matrix from Toronto and Simcoe (components 1, 2 and 3) highlighting the distribution of the non-PAH with respect to the PAH cluster at Toronto day.	Page 82
Figure 3-10(e)	Principal components plot of data matrix from Toronto and Simcoe (components 1, 2 and 3) highlighting the distribution of the non-PAH with respect to the PAH cluster at Toronto night.	Page 83

Figure 3-10(f)	Principal components plot of only PAH data from Toronto and Simcoe (components 1, 2 and 3).	Page 84
Figure 3-11	Relative loadings profile of 1-NP and PAH5 composite at Simcoe and Toronto during the sampling period.	Page 88
Figure 3-12	Mean relative loadings values of the PAC in the Toronto day (TD) and Toronto night (TN) samples along with the differences in loadings (green line).	Page 89
Figure 3-13	Mean relative loadings values of the PAC in the Toronto day (TD) and Toronto night (TN) samples along with the differences in loadings (green line).	Page 90
Figure 3-14	Day and night difference in the relative loadings values of the PAC at Toronto and Simcoe.	Page 91
Figure 3-15	Relative loading ratio of BbF, BkF, BjF, BeP & BghiP to PAH5 composite at Slocan, Langley and Sumas.	Page 94
Figure 3-16	Relative loading ratio of BD, 2-NP and 2-NFA to the PAH5 composite at Slocan, Langley and Sumas.	Page 95
Figure 3-17	The transformation pattern of the PAH5 composite based on relative loadings data at Slocan, Langley and Sumas. 'D' indicates day samples where as 'N' indicated night samples.	Page 96
Figure 3-18(a)	Principal component plot of the data matrix from the Pacific 2001(Components1, 2, and 3).	Page 99
Figure 3-18(b)	Principal components plot of the data matrix from the Slocan, Langley and Sumas sites (Components 1, 2, and 3) highlighting the distribution of the non-PAH with respect to the PAH cluster at Slocan day and night.	Page 100
Figure 3-18(c)	Principal components plot of the data matrix from the Slocan, Langley and Sumas sites (Components 1, 2, and 3) highlighting the distribution of the non-PAH with respect to the PAH cluster at Langley day and night.	Page 101

Figure 3-18(d)	Principal components plot of the data matrix from the Slocan, Langley and Sumas sites (Components 1, 2, and 3) highlighting the distribution of the non-PAH with respect to the PAH cluster at Sumas day and night.	Page 102
Figure 3-19	Principal components plot of the PAH data from the Slocan, Langley and Sumas sites (Components 1, 2, and 3).	Page 104
Figure 3-20	Mean relative loadings values of the PAC in the Langley Day (LD) and Langley Night (LN) samples along with the differences in loadings (green line).	Page 108
Figure 3-21	Mean relative loading value of the PAC in the Slocan Day (SID) and Slocan Night (SIN) samples along with the differences in loadings (green line).	Page 109
Figure 3-22	Mean relative loading value of the PAC in the Sumas Day (SuD) and Sumas Night (SuN) samples along with the differences in loadings (green line).	Page 110
Figure 3-23	Day and night difference in the relative loadings values of the PAC at Langley, Slocan and Sumas.	Page 111

LIST OF TABLES

Table 1-1	List of major PAH from identified sources.	Page 3
Table 1-2	PAH half-lives on wood soot particles in the chamber atmosphere at varying solar intensities, humidities and temperatures.	Page 6
Table 1-3	Calculated atmospheric lifetimes of PAH and NPAH due to photolysis and gas phase reaction with OH and NO ₃ radicals and O ₃ .	Page 6
Table 1-4	Mutagenic activity (revs/nmol) of selected PAC in <i>S. typimurium</i> strain YG 1021.	Page 9
Table 2-1	Nitro-polycyclic aromatic hydrocarbons (NPAH) in the 32-compound standard along with their molecular masses listed in the order of elution on a DB-17ht column.	Page 16
Table 2-2	The composite samples from Freelton and Pier 25 collected for the analysis of NPAH.	Page 20
Table 2-3	Parent PAH along with the NPAH products from the N ₂ O ₅ reaction pathway.	Page 29
Table 2-4	Relative response factors (RRF) of the NPAH compounds in the standard relative to 1-NP-d ₉ under NICI-SIM mode listed in their order of elution.	Page 37
Table 2-5	Detection limit (pg/μL) of the NPAH compounds in the standard determined under NICI-SIM mode listed in their order of elution.	Page 38
Table 2-6	Detection limits (pg/μL) of selected NPAH under MRM technique and NICI- SIM technique along with the ratio of MRM to SIM.	Page 46
Table 3-1	Detection limits (pg/μl) of the 23 NPAH from the Pier 25/Freelton air filter extracts compared to that of the NPAH standard determined under NICI-SIM mode.	Page 53
Table 3-2	Concentration (pg/m ³) of the 23 NPAH compounds detected in the Freelton samples.	Page 54

Table 3-3	Concentration (pg/m^3) of the 23 NPAH compounds detected in the Pier 25 samples.	Page 55
Table 3-4	The 5 principal components for the Freerton/Pier 25 data set along with the percentage variance.	Page 61
Table 3-5	The 7 principal components for the Toronto/Simcoe data set along with the percentage variance.	Page 78
Table 3-6	Rotated components matrix for the PAH data from the Toronto and Simcoe samples.	Page 86
Table 3-7	The 5 principal components for the Slocan, Langley and Sumas data set along with the percentage variance.	Page 98
Table 3-8	Rotated components matrix for the PAH from Pacific 2001 samples.	Page 106

ABBREVIATIONS

PAC	(Polycyclic Aromatic Compound)
GC-MS	(Gas Chromatography-Mass Spectrometry)
SIM	(Selected Ion Monitoring)
MS/MS	(Tandem mass spectrometry)
EI	(Electron Ionization)
NICI	(Negative Ion Chemical Ionization)
MW	(Molecular Weight)
MRM	(Multiple Reaction Monitoring)
TSP	(Total Suspended Particulate)
RRF	(Relative Response Factor)
PCA	(Principal Component Analysis)
pg	(pico-gram)
μl	(micro-liter)
m ³	(cubic-meter)
PAH	(Polycyclic Aromatic Hydrocarbon)
BghiF	(Benzo[ghi]fluoranthene)
BaA	(Benz[a]anthracene)
Chr	(Chrysene)
BD	(Benz[a]anthracene-7,12-dione)
BbF	(Benzo[b]fluoranthene)
BjF	(Benzo[j]fluoranthene)

BkF	(Benzo[k]fluoranthene)
BeP	(Benzo[e]pyrene)
BaP	(Benzo[a]pyrene)
Per	(Perylene)
IcdP	(Indeno[1,2,3-cd]pyrene)
BghiP	(Benzo[ghi]perylene)
Cor	(Coronene)
NPAH	(Nitro-Polycyclic Aromatic Hydrocarbon)
9-NA	(9-nitroanthracene)
4-Nphe	(4-nitrophenanthrene)
9-Nphe	(9-nitrophenanthrene)
3-Nphe	(3-nitrophenanthrene)
1-NFA	(1-nitrofluoranthene)
7-NFA	(7-nitrofluoranthene)
2-NFA	(2-nitrofluoranthene)
3-NFA	(3-nitrofluoranthene)
4-NP	(4-nitropyrene)
8-NFA	(8-nitrofluoranthene)
1-NP	(1-nitropyrene)
2-NP	(2-nitropyrene)

1.0 INTRODUCTION

1.1 Particulate material

Particulate material (PM) is the term used to refer to particles found in the air including dust, dirt, soot, smoke, and liquid droplets. Some particles are directly emitted into the air. They come from a variety of sources such as cars, trucks, buses, factories, construction sites, tilled fields, unpaved roads, stone crushing, and burning of wood⁶⁰. Other particles may be formed in the air from the chemical reactions of gases. Particles are indirectly formed when gases such as SO₂ and NO_x react with sunlight and water vapor to form salts. SO₂ and NO_x are produced mainly from fuel combustion in motor vehicles, at power plants and in other industrial processes⁶¹.

Individual particles tend to vary significantly in size, geometry, chemical composition and physical properties. Particle size can range from 0.005 μm to 500 μm⁶². Particulate matter in the air is commonly referred to as total suspended particulate matter (TSP). Particulate matter from industrial processes tend to be larger in size (>1 μm) whereas those from combustion and photochemical reactions tend to be smaller in size (<1 μm)⁶⁴.

Particulate matter is constituted into an inorganic fraction and a carbonaceous fraction⁶⁰. The inorganic component is comprised of a mixture of substances that can have a primary origin (metals like Pb, Ni, and V) and a secondary component (sulfate, nitrate and ammonium salts). The carbonaceous fraction is constituted by a complex mixture of species that are normally classified into two principal components: organic carbon (OC) and elemental carbon (EC). Elemental carbon is a primary pollutant directly

emitted by combustion processes. Organic carbon is a complex mixture of different compound classes (hydrocarbons, aldehydes, ketones, polycyclic aromatic hydrocarbons and derivatives) and it has both primary and secondary origin.

Since particulate matter is formed from a large number of sources, its composition greatly varies. In general, it is found that fine particles (mean aerodynamic diameter smaller than $10\ \mu\text{m}$) contain high levels of sulfate, ammonium, nitrate, elemental carbon, and condensed organic compounds as well as heavy metals⁶⁴. Larger particles which tend to arise from the soil, ash, unpaved roads, wood ash and soot contains mostly minerals, including aluminum, potassium, iron, calcium, and other alkaline metals.

It is observed that air polluted with particulate matter causes asthma and aggravates numerous respiratory as well as cardio diseases especially in children and elderly individuals. Particulate matter with aerodynamic diameter smaller than $10\ \mu\text{m}$ (PM_{10}) were classified by the environmental protection agency (EPA) as having adverse human health affects since its ability to reach the lower regions of the respiratory tract⁶⁴. Recent studies indicate that it is the $\text{PM}_{2.5}$ (mean aerodynamic diameter smaller than $2.5\ \mu\text{m}$) that poses the most severe threat to human health due to its ability to penetrate into the deeper parts of the respiratory tract where it is absorbed into the bloodstream or remain within the body for long period of time (45-46). PAH and heavy metals are predominantly associated with small particles, which is of concern because some PAH, such as benzo(a)pyrene, are known carcinogens⁴³.

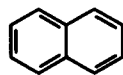
1.2 Polycyclic Aromatic Compounds

Polycyclic aromatic compounds (PAC) are a class of organic contaminants that are formed as primary combustion products of carbonaceous fuels such as gasoline, diesel, kerosene, wood, and coal¹⁻³. PAC consists of polycyclic aromatic hydrocarbons (PAH) and various PAH derivatives such as oxygen-containing PAH, sulfur-containing PAH and nitrogen-containing PAH.

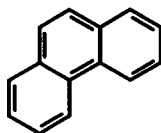
Table 1-1. List of major PAH from identified sources^{3,4}.

Sources	Principal PAH
Coal combustion	Phenanthrene, Fluoranthene, Pyrene
Coke Production	Anthracene, Phenanthrene, Benzo(a)pyrene
Incineration	Pyrene, Phenanthrene, Fluoranthene
Wood combustion	Benzo(a)pyrene, Fluoranthene
Industrial oil burning	Fluoranthene, Pyrene, Chrysene
Petrol/Diesel powered vehicles	Fluoranthene, Pyrene, Benzo(b)Fluoranthene, Benzo(k)Fluoranthene

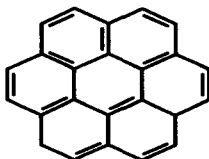
Common PAH range from naphthalene (2 rings, 128 Da) to coronene (7 rings, 300 Da).



Naphthalene (M.W. 128)



Phenanthrene (M.W. 178)



Coronene (M.W. 300)

1.3 Atmospheric Transformation of PAH to Nitrated PAH

PAH are present both in the gas and particle phase. They are known to undergo atmospheric transformations leading to the production of nitrated PAH (NPAH) ^{5,15}.

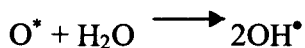
NPAH are formed from PAH by three different mechanisms:

- 1) Atmospheric transformation during the day-time via OH radicals ¹⁰.
- 2) Atmospheric transformation during the night via NO₃ radicals ¹¹.
- 3) Electrophilic nitration during combustion processes ¹¹.

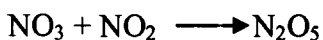
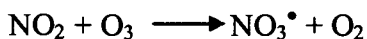
It is known from studies conducted by Atkinson and Arey ²³⁻²⁷ that PAH in the atmosphere undergo nitration via two different radical-mediated mechanisms. In the day-time PAH undergo nitration initiated by OH radicals and at night the transformation process is initiated by the NO₃ radical in the presence of oxides of nitrogen.

OH radicals (OH[•]) are formed in the atmosphere during the day-time by the photolysis of ozone to form dioxygen and the electronically excited form of O atom (O^{*}).

Subsequent reaction of O^{*} with H₂O leads to the production of two OH radicals ¹²:



NO₃ radicals (NO₃[•]) are formed in the atmosphere during the night-time by the following reaction ¹²:



Since NO_3 radical decays rapidly in sunlight this pathway is only significant in the night-time. Thus, the NO_3 pathway is of minor importance compared to the OH radical pathway^{55,56}.

Arey et al. proposed that the OH and NO_3 radicals attack the aromatic rings of the PAH at the position of highest electron density¹⁶. This is followed by the addition of NO_2 (g) at the ortho position and the subsequent loss of water or nitric acid.

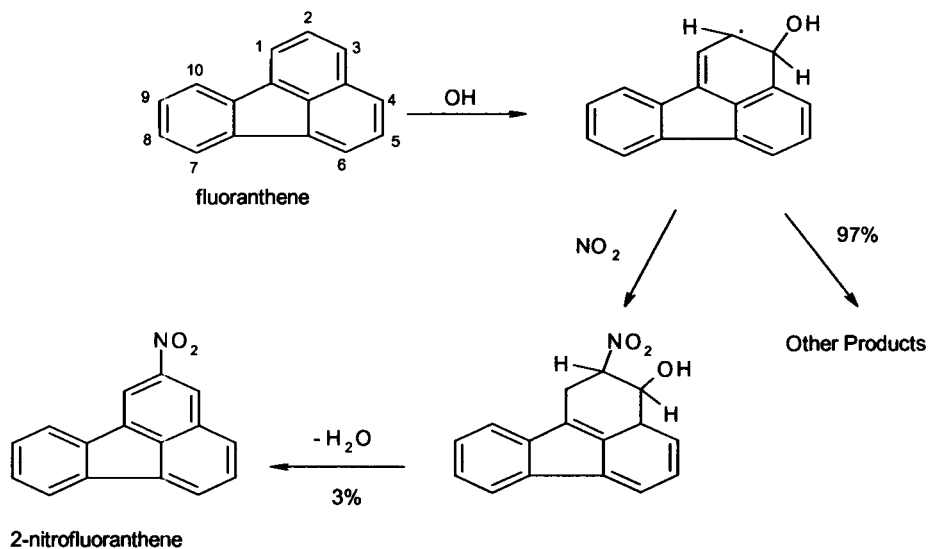


Figure 1-1. OH radical pathway for the nitration of fluoranthene to 2-nitrofluoranthene.

It is known that fluoranthene and pyrene undergo nitration at different rates depending on the pathway which is available (OH vs. NO_3). Thus the ratio of the nitrated products of these PAH (2-nitrofluoranthene/2-nitropyrene) has been used as indicators of the day-time vs. night-time transformation processes in previous work³¹.

In addition to atmospheric formation, NPAH are also formed in exhaust gases by high temperature fuel combustion. In this case, PAH undergo electrophilic reactions in the presence of NO_2 during combustion. A major product of this pathway is 1-nitropyrene (1-NP) in diesel exhaust. Studies conducted by Pitts et al. have identified 9-nitroanthracene (9-NA) and 6-nitrobenzo[a]pyrene (6-NBaP) in addition to 1-NP in organic extracts of diesel exhaust particulate⁴⁸. Also the 3-, 8-, and 1-nitrofluoranthene (NFA) have been found on diesel exhaust particles⁴⁹.

Since 1-NP found in the atmosphere is produced predominantly from the electrophilic reaction pathway, it serves as a surrogate for total NPAH released into the air via direct emission sources. Since 2-nitrofluoranthene (2NFA) is formed exclusively in the atmosphere, the ratio of 2NFA/1NP has been used as an indicator of overall atmospheric transformation processes³¹.

1.4 Photodegradation of PAH and NitroPAH

The gaseous as well as particle-associated PAC in the air may be removed by wet and dry deposition, photolysis and reactions with hydroxyl radicals, nitrate radicals and ozone. Table 1-2 lists the photolysis rates and half-lives for several particle-bound PAH measured by Kamens et al.¹³. The results in Table 1-2 clearly show that photolysis is dependent on atmospheric conditions such as light intensity, temperature and humidity.

Table 1-2. PAH half-lives on wood soot particles in the chamber atmosphere at varying solar intensities, humidities and temperatures ¹³.

PAH	Rate constant	Half-life, h		
		Light = 1 10g/m ³ H ₂ O 20°C	Light = 0.8 4g/m ³ H ₂ O 0°C	Light = 0.4 2g/m ³ H ₂ O -10°C
CcdP	0.0458	0.3	0.7	2
BaA	0.0265	0.4	2.2	7
Chry	0.0092	1.3	7.7	25
BbF	0.0091	1.3	3.7	10
BkF	0.0138	0.8	3.2	11
BaP	0.0234	0.5	2.1	6
IcdP	0.0153	0.8	8.8	39
BghiP	0.0179	0.6	3.1	12

Rate constant estimated at 1 cal cm⁻² min⁻¹, 10g/m³ H₂O, and 20°C. Units of light are cal cm⁻² min⁻¹

The most important mechanism for the loss of gas phase PAC in the atmosphere is the reaction with OH radicals. While reactions occur with other photo-oxidants such as the NO₃ radical and O₃, the rates of the reaction are orders of magnitude lower ³⁵. Table 1-3 lists the lifetimes of selected PAH and PAH derivatives due to gas phase reaction with OH and NO₃ radicals and O₃.

Table 1-3. Calculated atmospheric lifetimes of PAH and NPAH due to photolysis and gas phase reaction with OH and NO₃ radicals and O₃.

PAH	Lifetime due to reaction with		
	OH ^a	NO ₃ ^b	O ₃ ^c
Naphthalene	8hr	1.5yrs	80days
Acenaphthene	1.7hr	1.2yrs	30days
Fluoranthene	3.5hr	85days	
Pyrene	3.5hr	30days	
1-nitronaphthalene	2.7days	18yrs	28days
2-nitronaphthalene	2.6days	20yrs	28days

^a For a 12-hr day-time average OH radical concentration of 1.6 x 10⁶ molecule cm⁻³

^b For a 12-hr average night-time NO₃ radical concentration of 5 x 10⁸ molecule cm⁻³

^c For a 24-hr average O₃ concentration of 7 x 10¹¹ molecule cm⁻³

1.5 Toxicological properties of PAH and NPAH

Several PAH, including benz[a]anthracene, benzo[a]pyrene, benzo[b]fluoranthene, benzo[j]fluoranthene, benzo[k]fluoranthene, chrysene, dibenz[a,h]anthracene, and indeno[1,2,3-c,d]pyrene, have been shown to cause tumors in laboratory animals when they were exposed to these substances, through ingestion, injection or as a result of extended periods of skin contact. Studies of people show that individuals exposed by breathing or skin contact for long periods to mixtures that contain PAH can also develop cancer ¹⁴.

NPAH levels in the atmosphere are 1 to 3 orders of magnitude lower than that of PAH levels. However, NPAH are known to be highly mutagenic and carcinogenic when compared to the un-substituted PAH ⁵⁹. NPAH as well as PAH require metabolic activation in order to become toxic ¹⁴. NPAH metabolism can proceed through either of two pathways: oxidation of the aromatic ring system or reduction of the nitro group or a combination of the two pathways.

It is known that in *Salmonella typhimurium* strains the NPAH are reduced via nitroreductase to three major metabolites: nitroso-PAH, N-hydroxyamino-PAH and amino-PAH. It is the N-hydroxyamino-PAH that is believed to covalently bind to the bacterial cellular DNA and cause mutation. Chemicals such as NPAH that are readily reduced within cells and exhibit mutagenic responses are referred to as direct-acting mutagens.

Many recent publications have stated that certain features of the NPAH affect the mutagenic activity of these species ^{67,68}. One such feature is the dihedral angle of nitro

groups in relation to the aromatic ring plane. It has been stated that in the case of nitrobenzanthrone isomers, the ease of attacking the nitro groups with nitroreductase was found to be a major factor in determining the most mutagenic isomers⁶⁷. Studies conducted by Debnath et al. have shown that the reduction potential of the nitro groups on compounds is directly correlated with increased mutagenicity of these compounds⁶⁹.

Table 1-4. Mutagenic activity (revs/nmol) of selected PAC in *S. typhimurium* strain YG 1021⁶⁵.

Compound	Mutagenic Activity (revs/nmol)
Fluoranthene	0.39
Pyrene	0.37
benzo[a]pyrene	0.40
2-nitrofluoranthene	7900
2-nitropyrene	18800
3,7-dinitrofluoranthene	117,000
1,8-dinitropyrene	2,550,000

Benzo[a]pyrene is classified as a highly mutagenic compound among PAH⁴⁵. However, its mutagenic activity (revs/nmol) in *S. typhimurium* strain YG1021 is considerably lower when compared with the four member ring NPAH (2-nitrofluoranthene, 2-nitropyrene) as well as the dinitro-PAH (Table 1-4). The addition of a mono nitro group to fluoranthene and pyrene increases its mutagenic activity by more than three orders of magnitude.

The metabolism of NPAH has been studied in mammalian systems. In vitro metabolism of NPAH has been conducted with rat liver microsomes and S9 enzyme systems. It was found that metabolism of 1-NP proceeded via the reductive pathway with the N-hydroxyamino-pyrene being the reactive intermediate leading to the DNA adduct formation⁶⁶. Metabolism of 1-NP has also been studied in human tissues. Human liver microsomal metabolism of 1-NP has also yielded the N-hydroxyamino-pyrene as the predominant product.

Certain PAH and NPAH exhibits semi-volatile behavior. As a result they are known to partition between the gas and particle phase depending on the vapor pressures. The most genotoxic NPAH are those consisting of four and five rings. These NPAH are almost exclusively associated with particulate matter. Majority of the particle-bound PAC are adsorbed onto fine particles of diameter 2.5 μ m or less¹⁴. This raises a serious health issue since particulate matter of small sizes can readily penetrate the respiratory system and deposit in the bronchioles and alveoli of the lungs. These particles are known to deposit slowly from the atmosphere and depending on atmospheric conditions may be airborne for days being transported over long distances²². Species associated with particulate matter can be analyzed much more easily than those in the gas phase.

1.6 Freelton/Pier 25 study

In a study conducted in collaboration with Dr. James S. Quinn (Department of Biology, McMaster University), sentinel laboratory mice were exposed to ambient outdoor air for 10 weeks at two different sites²⁸. One site was representative of an urban/industrial location: Pier 25, in the east end of Hamilton (Ontario, Canada) lies to the east of two integrated steel mills and to the west of a major highway (Queen Elizabeth Way). The second site, located in Freelton 30 km north of the Pier 25 site, was representative of a rural area. At each site, 2 groups of mice (both males and females) were housed concurrently for 10 weeks. One group was exposed to the ambient air while the second group was housed inside a chamber equipped with a high efficiency particulate-air (HEPA) filtration system.

A HEPA filter functions by filtering particulate matter in the air and removes up to 99.99% of particles down to 0.1µm in diameter. As a result, at each site one group of mice was exposed to the ambient air (gas + particles) while the other group was protected from exposure to particulate matter, with the exception of the smallest ultra-fine particles. The exposed male and female mice were mated with unexposed mice. The germ-line mutation rates of the resulting offspring were then compared using pedigree DNA profiling at ESTR loci.

The results from this study showed that the offspring from the urban-industrial males exposed to ambient air inherited mutation rates 2 times more frequently than offspring from the other three treatment groups. In fact, the mutation rates of offspring from the males at the urban-industrial site which were housed in the HEPA filtered

chamber had paternal mutation rates 52% lower than compared to offspring from males exposed to ambient air. Furthermore, the mutation rates from the males are 2 times as frequent compared to that from females at the urban-industrial site exposed to ambient air.

These observations led Somers et al. to conclude that exposure to air particulate matter was a key contributing factor to mutation rates of males at the urban-industrial site. Furthermore it was concluded that the particulate exposure affected ESTR mutation induction primarily in the paternal germ line affecting the premeiotic male germ cells. The amount of airborne particulate matter was measured at both sites on the same 25 days during the mouse exposure study. Mean total suspended particulate (TSP), which consists of the respirable fraction as well as larger particles, was 2 to 10 times as high at the urban industrial site compared to the rural site.

Further analysis was performed on the air samples that were collected from both sites to examine the levels of 26 PAH which included seven carcinogens identified by the U.S. Environmental Protection Agency (USEPA). It was found that the PAH concentrations at the urban-industrial site were significantly higher compared to those at the rural site. In fact the weighted daily PAH exposure was found to be 33-fold higher at the urban site compared to the rural site; the mean exposures at the two sites were 13.4 ng/m³ and 0.4 ng/m³, respectively.

1.7 Research Objectives

Although a set of PAH have been identified and quantified in the Freelton/Pier 25 study, the NPAH levels had not been determined. The first overall goal of this thesis was to develop a selective and sensitive method for the detection of NPAH in air samples collected in the Hamilton area, specifically at Freelton and Pier 25. The following approaches were undertaken to achieve this goal:

- 1) A set of NPAH standards would be synthesized to increase the number of NPAH standards in the collection of authentic standards
- 2) The use of tandem mass spectrometry techniques would be explored for the identification and quantification of NPAH in environmental samples. Tandem mass spectrometry methods have not been reported for the analysis of NPAH in air filter extracts. The selectivity and sensitivity of the tandem mass spectrometry technique would be compared to negative ion chemical ionization methods.
- 3) The resulting NPAH data set would be examined using principal components analysis to explore trends in the data set and to look for differences in the urban and rural sites.

The second major goal of the thesis was to analyze polycyclic aromatic compound (PAC) data (both PAH and NPAH) that had been collected during two large-scale sampling programs; both data sets had day-night samples from urban and rural areas. Elemental carbon data was provided to us which allowed us to calculate particulate loadings of each PAH and NPAH. The following approaches were undertaken to achieve this goal:

- 1) The data would be examined to determine whether there were unique atmospheric transformation profiles in the urban and rural areas and whether differences were observed during the day and night.
- 2) The loadings data would be explored from the context of the use of relative loadings to compare profiles of PAH and NPAH.
- 3) This data would also be used as the basis for principal components analysis to determine whether there are differences between sampling sites and day-night profiles.

2.0 EXPERIMENTAL

2.1 Chemicals

A 32-compound NPAH mixture was prepared from commercially available and synthetic standards and was used as a qualitative standard for the identification of target analytes in air filter extracts. Seven NPAH were synthesized in order to expand the existing 25-compound NPAH standard to 32 compounds. The 7 NPAH synthesized included 3-nitrophenanthrene, 4-nitrophenanthrene, and 9-nitrophenanthrene, 7-nitrobenz[a]anthracene, 12-nitrobenz[a]anthracene, 1-nitrotriphenylene and 2-nitrotriphenylene. Two deuterated compounds, 1-nitropyrene-d₉ and 2-nitrofluoranthene-d₉ were also synthesized. 1-Nitropyrene-d₉ was used as the internal standard in all NPAH analyses. Refer to Table 2-1 for complete list of compounds.

2.2 Gases and Solvents

High purity helium gas was purchased from VitalAire and was used as the carrier gas in all GC-MS experiments. Methane was used as the chemical ionization gas in the negative ion chemical ionization (NICI) experiments. Argon was used as the collision gas in the tandem mass spectrometry (MS/MS) experiments. Methane and argon were purchased from VitalAire. Distilled-in-glass grade of dichloromethane (DCM), methanol, acetone, and carbontetrachloride (CCl₄) were purchased from Caledon Laboratories. PCA grade toluene was purchased from Aldrich Chemical Co. (St. Louis, MO, USA).

Table 2-1. Nitro-polycyclic aromatic hydrocarbons (NPAH) in the 32-compound standard along with their molecular masses listed in the order of elution on a DB-17ht column.

Peak No.	Compound	Source	M.W.
1	1-nitronaphthalene	c	173
2	2-methyl-1-nitronaphthalene	a	187
3	2-nitronaphthalene	a	173
4	2-nitrobiphenyl	c	199
5	3-nitrobiphenyl	c	199
6	4-nitrobiphenyl	c	199
7	1,5-dinitronaphthalene	a	218
8	5-nitroacenaphthene	c	199
9	2-nitrofluorene	a	211
10	9-nitrofluorene	c	211
11	1,8-dinitronaphthalene	a	218
12	9-nitroanthracene	a	223
13	4-nitrophenanthrene	e	223
14	9-nitrophenanthrene	e	223
15	3-nitrophenanthrene	e	223
16	1-nitrofluoranthene	b	247
17	7-nitrofluoranthene	b	247
18	2-nitrofluoranthene	b	247
19	3-nitrofluoranthene	b	247
20	4-nitropyrene	d	247
21	8-nitrofluoranthene	c	247
22	1-nitropyrene-d ₉	e	256
23	1-nitropyrene	b	247
24	2-nitropyrene	b	247
25	12-nitrobenzanthracene	e	273
26	7-nitrobenzanthracene	e	273
27	1-nitrotriphenylene	e	273
28	6-nitrochrysene	d	273
29	2-nitrotriphenylene	e	273
30	3-nitrobenzanthrone	d	275
31	6-nitrobenzo[a]pyrene	d	297
32	3-nitroperylene	c	297

^a compounds purchased from Aldrich Chemical Company Inc. (Milwaukee, WI).

^b compounds purchased from Chemsyn Ltd. (Lenexa, KS).

^c compounds received from Dr. M. L. Lee (Brigham Young University, Provo, UT) and Dr. William Vance (California Environmental Protection Agency, Sacramento, CA).

^d compounds synthesized and purified using preparative HPLC by previous members of our research group.

^e compounds synthesized by author according to procedures described in section 2.6.

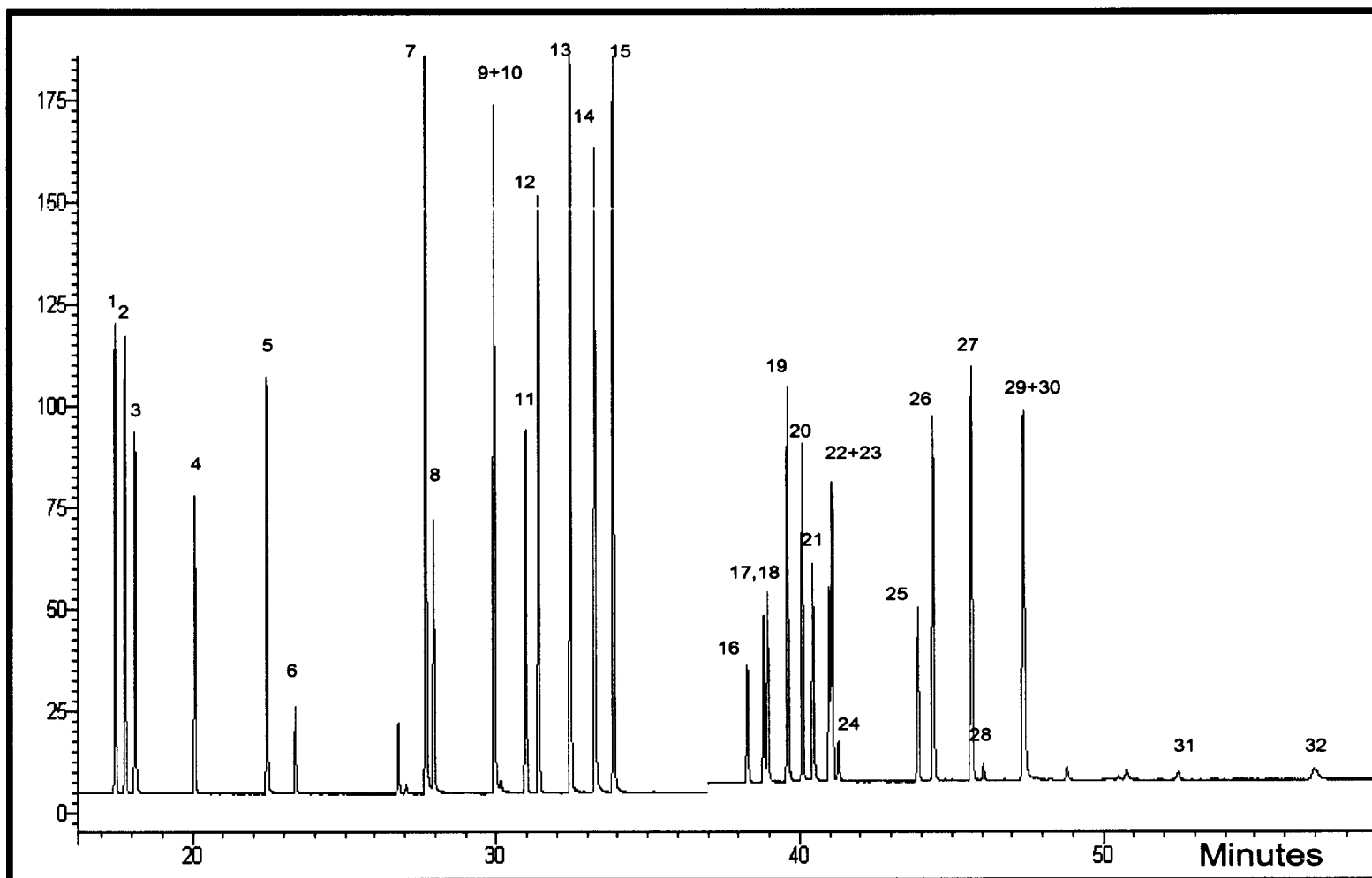


Figure 2-1. GC-MS total ion chromatogram of 32-compound NPAH standard under NICI-SIM mode (Refer to Table 2-1 for peak identification).

2.3 Instrumentation

Gas chromatography-mass spectrometry (GC-MS) analyses under NICI mode were conducted using Varian CP 3800 gas chromatograph connected to a Varian 1200L mass spectrometer. The Varian 1200L mass spectrometer is equipped with a triple quadrupole mass analyzer capable of tandem mass spectrometry (MS/MS) experiments.

Most GC-MS analyses under EI^+ mode was carried out using a HP 5890 series II gas chromatograph connected to a HP 5971A mass spectrometer. The HP 5971A mass spectrometer is equipped with a quadrupole mass analyzer. A DB-17ht capillary column (30m x 0.25mm i.d. x 0.15um film, J & W Scientific) was used for analysis in both the NICI and EI modes.

2.4 Samples

2.4.1 Pier 25/Freelton Samples

Air particulate samples were collected at the Freelton and Pier 25 sites by Somers et al. and analyzed for PAH levels²⁸. Freelton is a rural site located north of Hamilton (Ontario, Canada). Pier 25 is an urban-industrial site located near the Hamilton harbor and is in close proximity to steel manufacturing plants as well as a major highway.

High-volume air samplers were used for the collection of total suspended particulate matter (TSP) from both sites. The mouse exposure study was conducted during a 70-day time period during which the samplers were operational simultaneously for 24 hours on 25 of the 70 days. Based on wind direction data for Hamilton obtained from the Ontario Ministry of the Environment at station 29026 (a site about 1.5km from Pier 25 site), samples were grouped together depending on the number of hours the mice at the urban-industrial site (Pier 25) were downwind from the industrial core of Hamilton on each sampling day. The corresponding samples collected from the rural site (Freelton) were similarly grouped together. Six composite samples were prepared from the samples collected at each site and the equivalent sample volume they represent is presented in Table 2-2.

Table 2-2. The composite samples from Freelon and Pier 25 collected for the analysis of NPAH.

Sample	Hours downwind from industrial site	Representative sample volume (m ³) at Freelon	Representative sample volume (m ³) at Pier 25
1	0	400	400
2	1-3	800	400
3	4-9	800	320
4	10-18	800	400
5	19-23	800	80
6	24	800	130

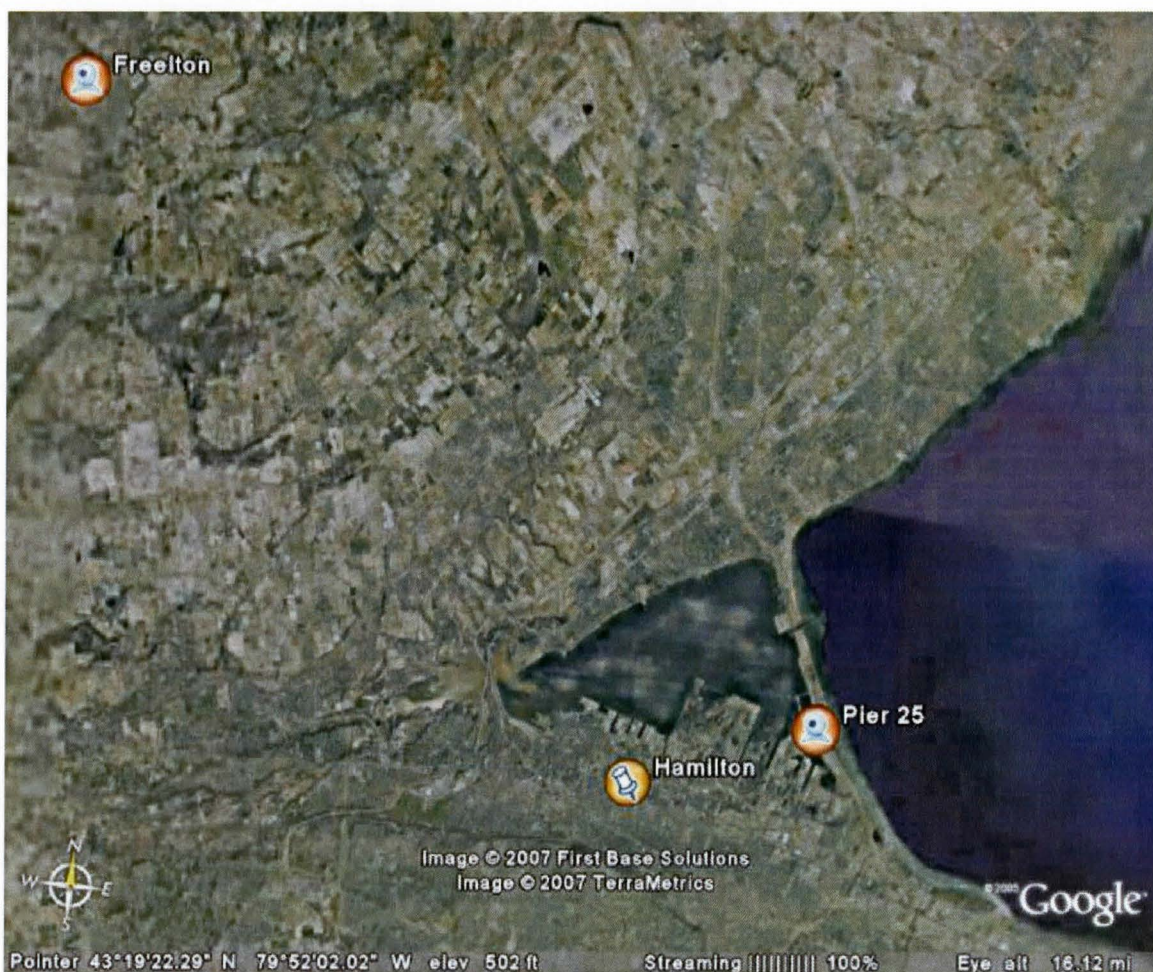


Figure 2-2. An aerial map of the Pier 25 and Freelon (Ontario, Canada) sampling sites obtained from GoogleEarth.

2.4.2 Pacific 2001 Samples

The Pacific 2001 Air Quality Study was carried out in the Lower Fraser Valley region of British Columbia, Canada. The Lower Fraser Valley is referred to as one of the ‘smog corridors’ in Canada. Located in close proximity to the Pacific Ocean, the air moving into the valley from the Pacific Ocean is regarded as relatively clean. Thus, the Pacific 2001 study allows for the analysis of local impacts in the region. Local emission sources in the region include transportation, industry, marine activities and agricultural activities.



Figure 2-3. An Aerial map of the sampling sites at the Lower Fraser Valley in British Columbia, Canada.

The Pacific 2001 air particulate samples were collected as day and night samples at four different sites between August 15 and 31, 2001. The four sites were Cassiar tunnel, Slokan, Langley and Sumas (Figure 2-3). Cassiar Tunnel is a short tunnel with mostly light-duty traffic. Slokan is regarded to be an urban site in the city of Vancouver. Langley is in a transition zone between a suburban/rural and an urban/suburban area. The Sumas site is in a rural area and was expected to offer a good monitoring site for samples with considerable atmospheric transformation.

High-volume air samplers with size-selective inlets were used for the collection of $PM_{2.5}$ at the four sites. A total of 75 air particulate samples were collected during the 2001 study from all 4 sites. Air filter sample collection was carried out by staff associated with the Pacific 2001 study and supervised by Dr. Rob McLaren from York University. The samples were extracted and analyzed for PAC and NPAH by Rong Yang. The concentrations (pg/m^3) of a number of PAC and NPAH from each site were determined by Rong Yang. In addition, total elemental carbon (EC) data was obtained from samples collected concurrently at the Slokan, Langley and Sumas site and were provided by Dr. J. Brook of Environment Canada. Since particulate matter contains both organic carbon (OC) and elemental carbon (EC), the particulate matter was heated sequentially such that the volatilizable organic compounds were driven off initially leaving behind elemental carbon. The sample was then further heated in the presence of oxygen which results in the conversion of the remaining elemental carbon into carbon dioxide. By measuring the changes in the mass of air particulate through the sequential

heating periods it is possible to derive the elemental carbon level defined in unit of $\mu\text{g carbon/m}^3$.

The elemental carbon data ($\mu\text{g carbon/m}^3$) was used to convert the concentration values of PAC and NPAH (pg/m^3) into particulate loadings of PAC and NPAH on elemental carbon, which is defined as microgram PAC or NPAH per gram elemental carbon ($\mu\text{g/g C}$). However, elemental carbon data from the Cassiar Tunnel site was not available and thus only the loadings data from the Slocan, Langley and Sumas sites have been used in the current thesis to examine the transformation profile of the PAC and NPAH based on the relative stability in the atmosphere.

2.4.3 Toronto/Simcoe Samples

Air particulate samples were collected in Toronto and Simcoe between 16th and 28th of July 2001. The samples from Toronto were collected on the roof of the Gage Institute at the corner of College and Huron street and are considered to be representative of an urban site. Simcoe is a rural area located about 150km southwest of Toronto and is classified as a rural site. Day and night $\text{PM}_{2.5}$ samples were collected from both Toronto and Simcoe using high-volume air samplers with size-selective inlets.

There are few local sources in Simcoe. The Simcoe site is impacted by long-range transport across the transcontinental border. Toronto is one of Canada's largest urban cities and is home to a number of local emission sources. Similar to the Pacific 2001 samples (section 2.4.2) concentration data of PAH and NPAH had been determined previously by members of our research group; elemental carbon data was provided by Dr.

J. Brook and was used to calculate loadings data for a set of PAC and NPAH. The loadings data was used to examine the transformation profiles of PAC and NPAH at the urban site compared to that from the rural site.



Figure 2-4. An aerial map of Toronto and Simcoe sampling sites in Ontario, Canada obtained from GoogleEarth.

2.5 Sample Extraction and Cleanup

The air samples from the Pier 25/Freelton sites were extracted and cleaned up according to the scheme described in Figure 2-5 by Quinn et al. Air filters were extracted with DCM²¹ followed by silica Sep-Pak (SPE) purification⁵⁸. The silica tends to capture and retain the highly polar compounds in the crude extract. Next, the extract was put through a sephadex LH20 separation. The Sephadex method effectively separates the hydrocarbon (alkane) fraction from the PAC fraction which consists of both PAH as well as NPAH. The PAC fraction was analyzed for NPAH using GC-MS.

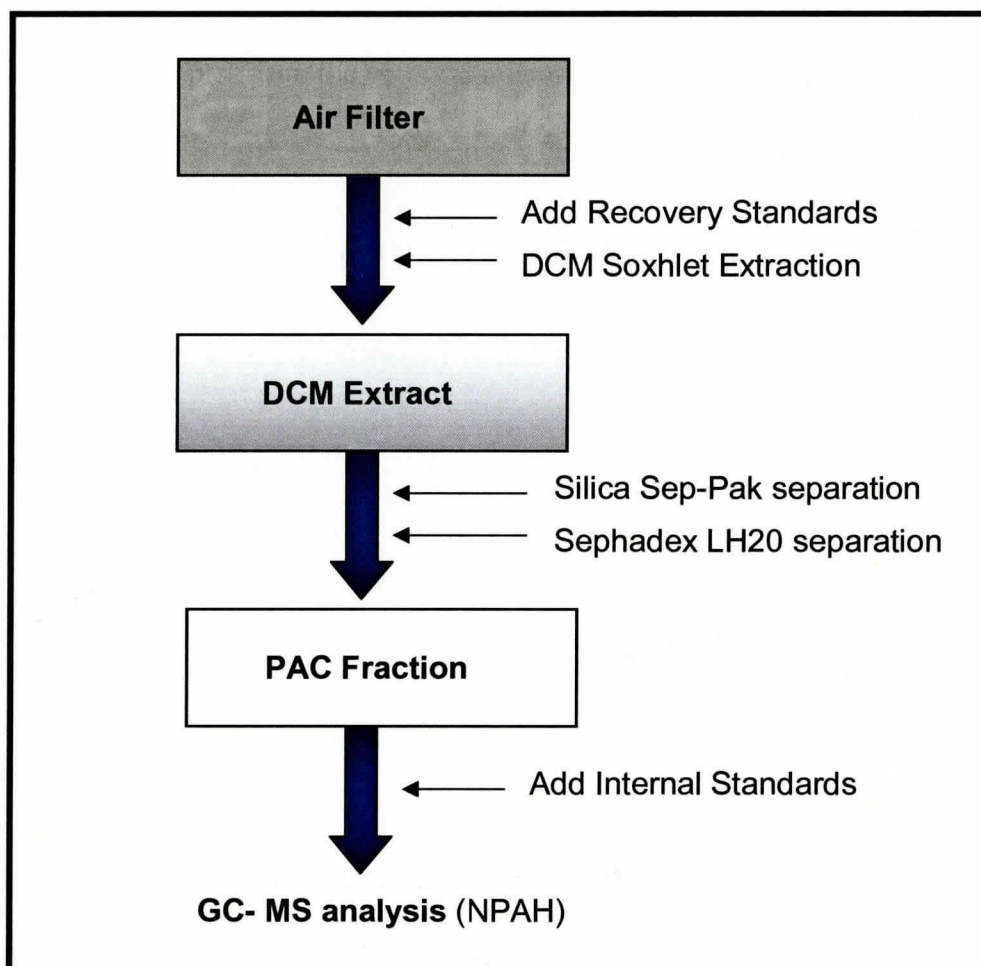
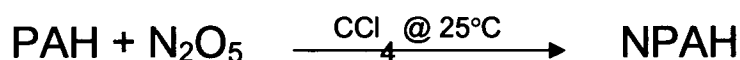


Figure 2-5. Analytical scheme for air sample extraction and cleanup.

2.6 Synthesis of NPAH

The major purpose of the synthesis was to produce stocks of commercially unavailable NPAH standards as well as some deuterated NPAH standards. N_2O_5 was used as the nitrating agent and the reactions were carried out at room temperature in dry carbon tetrachloride^{17, 56}.



N_2O_5 readily reacts with water to form nitric acid and thus the reaction was carried out in distilled CCl_4 . A group of 12 PAH (Table 2-3) were nitrated using N_2O_5 in CCl_4 solution. Approximately 5mg of each PAH was measured out and dissolved in 15mL of CCl_4 . Since N_2O_5 was the limiting reagent, it was added such that the molar ratio between PAH and N_2O_5 was 1 to 0.75. The reactions were instantaneous once the N_2O_5 was added to the PAH in CCl_4 at room temperature. Each reaction was allowed to proceed for no more than 5 minutes at which time NaHCO_3 (5%v/v) was added to quench the reaction. The resulting reaction mixtures were then evaporated to dryness. The dried crude reaction mixtures varied in colour from yellow to brown and orange.

The mass of the crude reaction mixture from each reaction varied between 10 to 20mg. Each crude reaction mixture was dissolved in approximately 2mL of DCM and filtered through a silica solid phase extraction cartridge to separate the synthesized NPAH from any un-reacted PAH. PAH and NPAH show high solubility in DCM. Solid phase extraction was carried out with the use of Sep-Pak (plus silica model) cartridges which contains 690mg of sorbent and was purchased from Waters. Each crude mixture in DCM was loaded onto a sep-pak cartridge uniformly. The loaded cartridges were allowed to sit

at room temperature for 15 minutes to allow the DCM to evaporate and thus leaving only the crude reaction mixture on the cartridge. The loaded cartridges were then attached to a vacuum filter and eluted with the following wash solvents in the order specified and the corresponding fractions were collected:

Elution order	Volume (mL)	Composition	Fraction collected
1	10	100% hexane	A
2	25	2.5%DCM/hexane	B
3	10	5%DCM/hexane	C
4	10	10%DCM/hexane	D
5	10	20%DCM/hexane	E
6	10	100%DCM	F

Increasing the relative polarity of the wash solvent helped separate the PAH from the NPAH. It was found that most of un-reacted PAH were washed off the cartridge with 10ml of 100% hexane solution (fraction A) meanwhile the NPAH compounds were found mostly in fraction B and C (Figure 2-6). The isolated NPAH were identified by comparison with authentic standards and were used to expand the existing NPAH standard (Table 2-3).

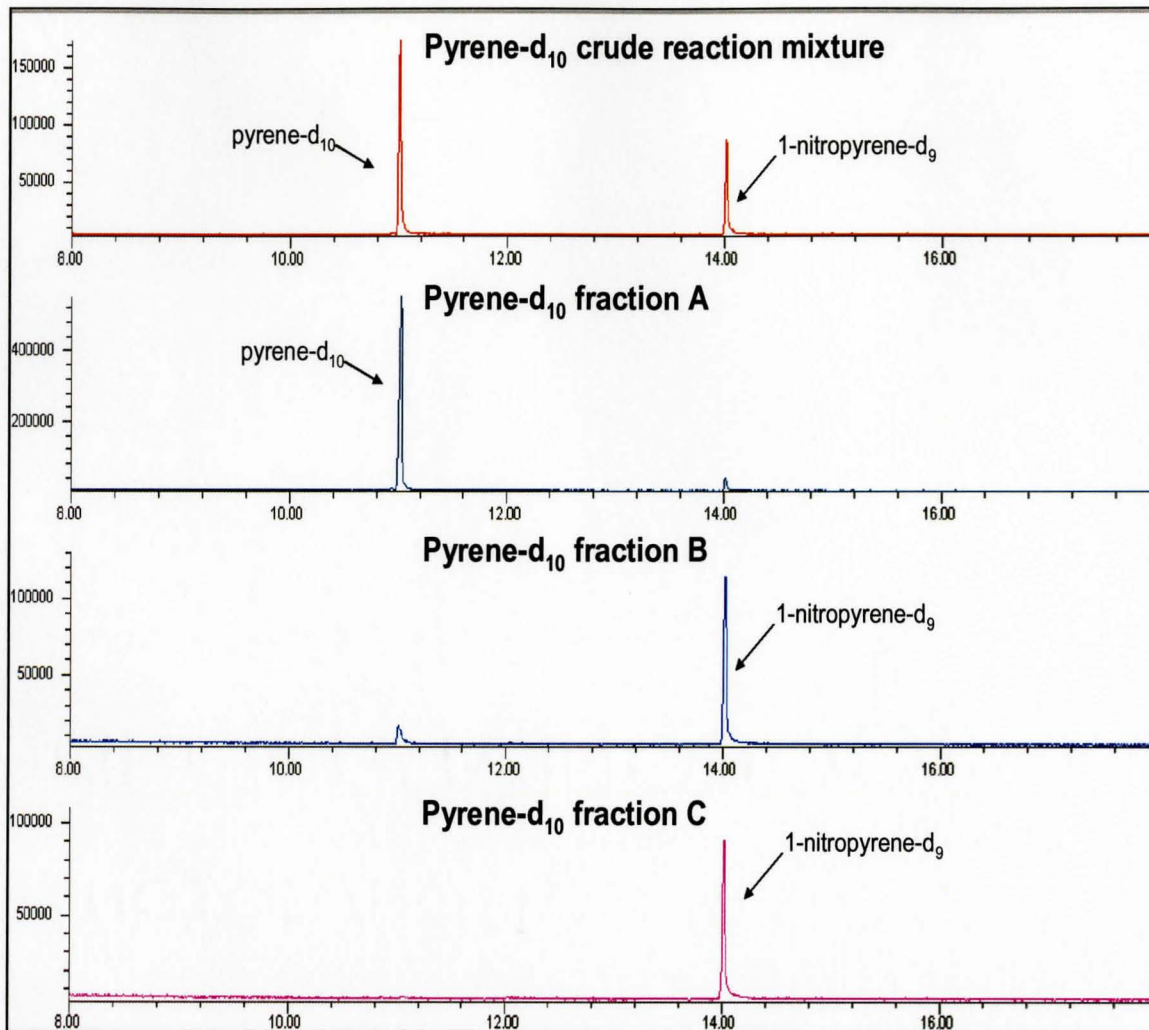


Figure 2-6. Total ion chromatogram (full scan mode) of the GC-MS analysis of the crude nitrated fluoranthene reaction mixture, along with fractions A, B and C collected from elution of the solid phase extraction cartridge.

Table 2-3. Parent PAH along with the NPAH products from the N₂O₅ reaction pathway.

Parent PAH	Number of mono-nitro isomers in crude reaction mixture	Identified NPAH
MW 178		MW 223
Phenanthrene	5	3-nitrophenanthrene 4-nitrophenanthrene 9-nitrophenanthrene
Anthracene	1	9-nitroanthracene
MW 202		MW 247
Pyrene	1	1-nitropyrene
Pyrene-d ₁₀	1	1-nitropyrene-d ₉
Fluoranthene	1	2-nitrofluoranthene
Fluoranthene-d ₁₀	1	2-nitrofluoranthene-d ₉
MW 228		MW 273
Benz[a]anthracene	2	7-nitrobenz[a]anthracene 12-nitrobenz[a]anthracene
Chrysene	2	6-nitrochrysene
Triphenylene	2	1-nitrotriphenylene 2-nitrotriphenylene
MW 252		MW 297
Benzo[a]pyrene	1	6-nitrobenzo[a]pyrene
Benzo[e]pyrene	2	Not identified
Perylene	2	3-nitroperylene

2.7 Negative Ion Chemical Ionization Mass Spectrometry

Gas chromatography-mass spectrometry (GC-MS) analysis using negative ion chemical ionization (NICI) mode was carried out using a Varian 1200L instrument. Though high-performance liquid chromatography (HPLC) techniques have been used for the analysis of PAH and NPAH GC-MS has been the method of choice due to its greater separation efficiency for complex non-polar compounds^{4,19,59}. It was known from previous work and the literature that NICI is more sensitive towards the analysis of NPAH than EI^+ ^{3,30,57}. The result is a more highly selective and sensitive chromatogram for the target NPAH species.

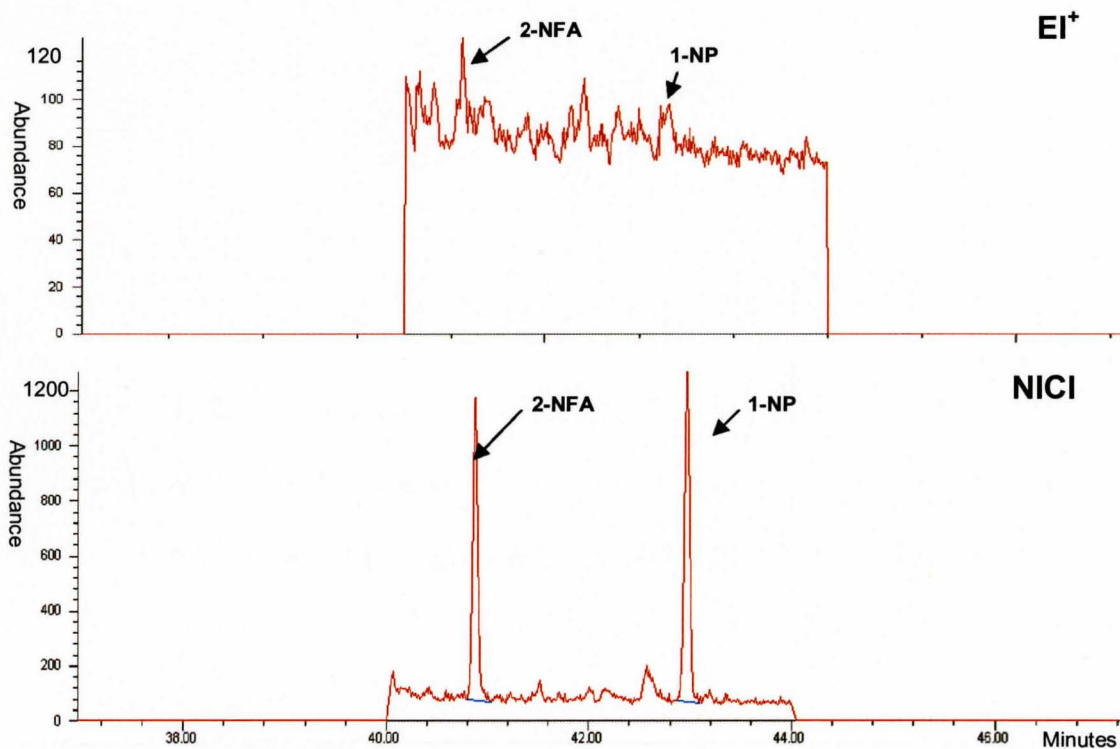


Figure 2-7. GC-MS mass chromatograms (m/z 247) of a suburban air filter extract analyzed using EI^+ and NICI modes.

Since NICI is a soft ionization technique, the molecular ion is always the base peak in the mass spectrum.

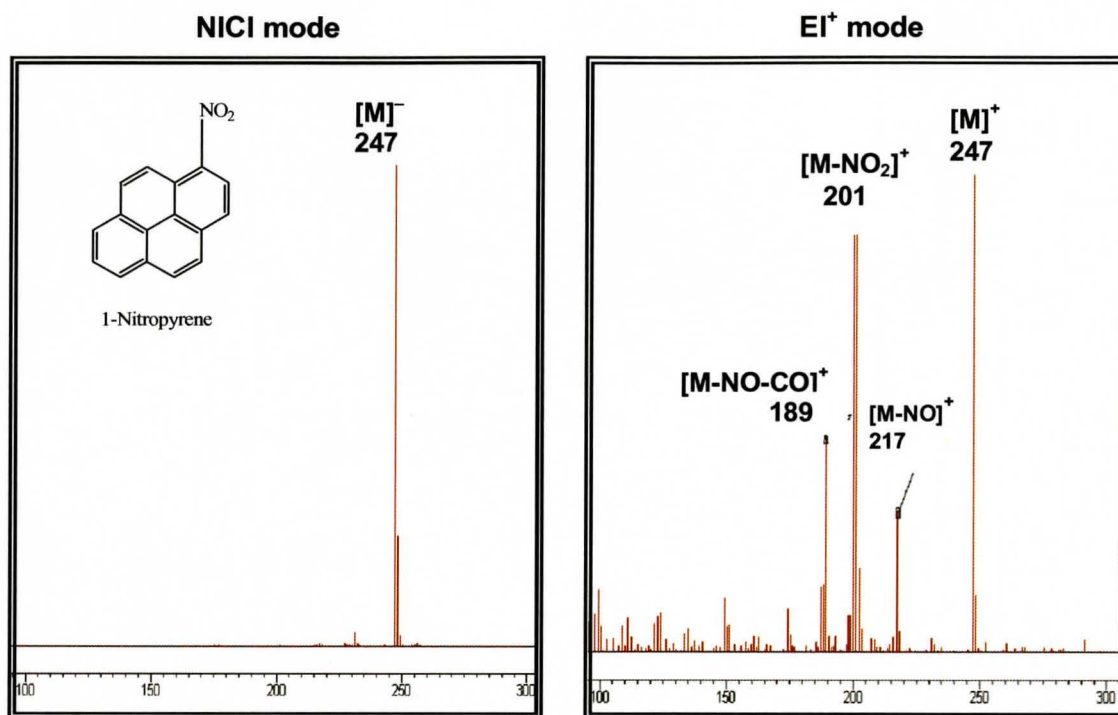


Figure 2-8. Mass spectra of 1-nitropyrene analyzed using NICI and EI^+ modes.

2.8 NICI Method Parameters

A selected ion monitoring (SIM) program was developed using the m/z values of the molecular ions of each target NPAH compound.

Source Conditions Electron energy: 70eV Chemical ionization gas: Methane Ion source pressure: 8.5Torr Ion source temperature: 200°C Transfer line temperature: 300°C	
Temperature Program Column: DB-17ht (30m x 0.25mm) Initial temperature: 90°C Rate 8°C/min Final temperature: 300°C Hold 46.25 min Total run time: 72.5 minutes	
Time Segment	SIM ions (m/z)
<i>Ion group 1</i> (start time 4.5 min)	173, 187, 199, 218, 223
<i>Ion group 2</i> (start time 37 min)	247, 256, 273, 275, 297

An 8°C/minute temperature program using a DB-17ht (50% phenyl substituted methylsiloxane stationary phase) column allowed for baseline resolution of all 32 compounds in the NPAH standard with the exception of 2-nitrofluorene and 9-nitrofluorene. The major advantage in utilizing the DB-17ht column with the above temperature program is that it allows for the baseline resolution of all 8 247MW NPAH isomers (Figure 2-9). By contrast, a DB-5MS (5% phenyl substituted methylsiloxane stationary phase) column cannot attain the complete separation of the 247MW NPAH isomers; in particular the 2- and 3-nitrofluoranthene isomers which co-elute⁵⁸.

The complete separation of the 247MW NPAH species is important in that the 2-nitrofluoranthene isomer serves as a surrogate for atmospherically transformed NPAH meanwhile the 3-nitrofluoranthene is a direct emission product.

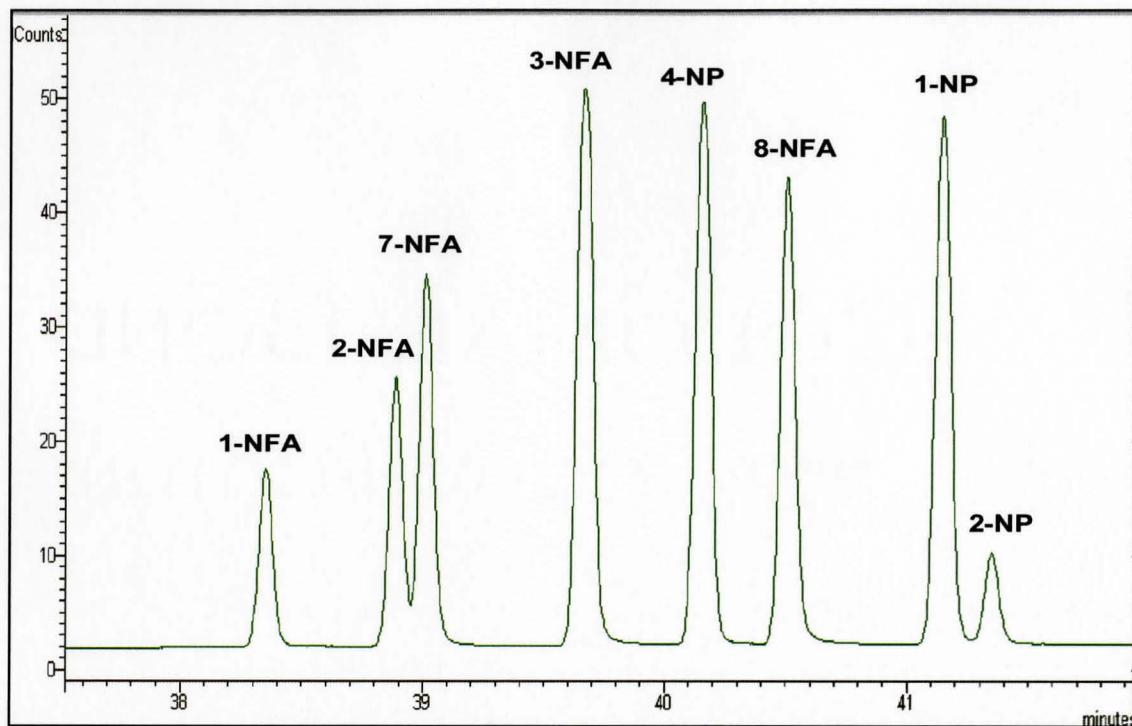


Figure 2-9. The eight 247MW NPAH isomers separated on a DB-17ht column under NICI-SIM mode.

NICI Ion Source Pressure

A major parameter that was optimized for NICI analysis was that of gas pressure in the ion source. Methane was examined as the CI gas at a range of pressures to determine its affect on the sensitivity of the NPAH species. Generally, it was found that the sensitivity increased with increasing CI gas pressure and reached a maximum at pressures between 8 and 9 Torr (Figure 2-10).

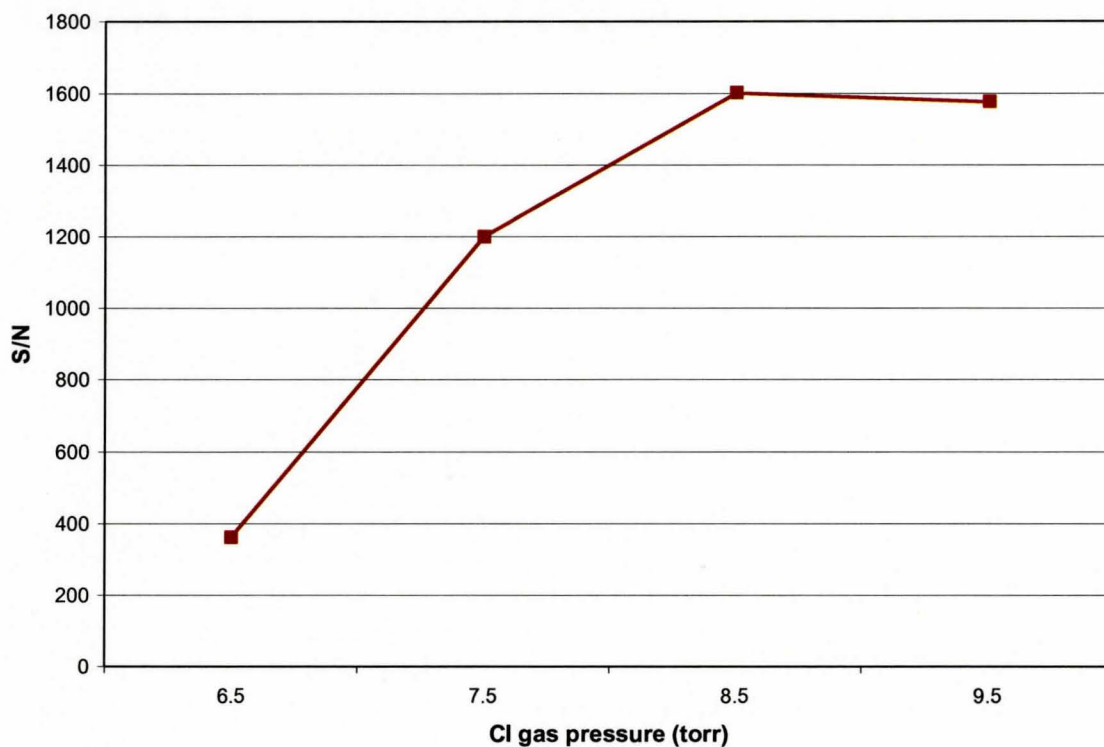


Figure 2-10. The average signal to noise ratio (S/N) of the 247MW isomers over a CI gas pressure range of 6.5 to 9.5 Torr.

2.9 Calibration and Detection Limits

The 32-compound NPAH standard (Table 2-1) was used to monitor the performance of the GC-MS system under NICI-SIM conditions. The linearity and performance of NPAH compounds in the standard was first determined over a range from 10 to 5000 pg/μL. The relative response factors (RRF) of the NPAH compounds were calculated relative to that of 1-nitropyrene-d₉ which was assigned a response factor of 1.0.

Compounds	Concentration Range	R ² values
4-nitrophenanthrene	0.01-5ng/ul	0.996
9-nitrophenanthrene	0.01-5ng/ul	0.993
3-nitrophenanthrene	0.01-5ng/ul	0.994
1-nitropyrene-d ₉	0.01-5ng/ul	0.996

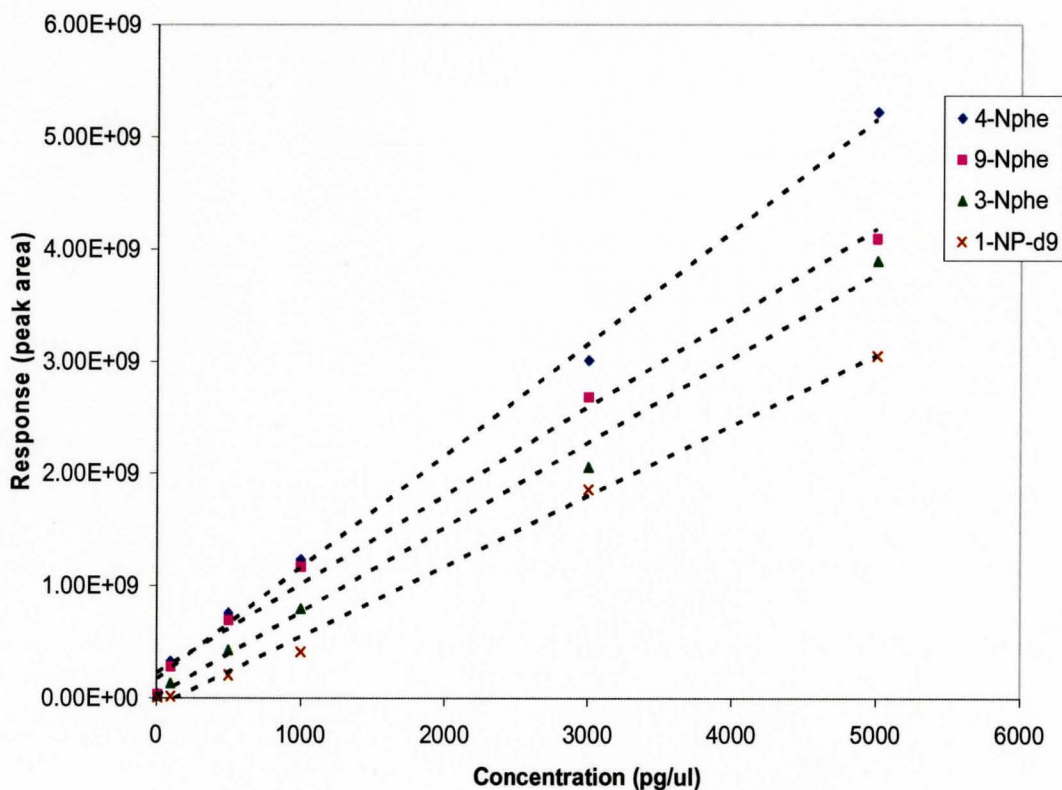


Figure 2-11. Calibration plot of 3-, 4-, 9-nitrophenanthrene and 1-nitropyrene-d₉ over the concentration range from 10 – 5000pg/μL.

The RRF of the NPAH compounds were determined based on the peak area of the M^+ ion for each species under NICI-SIM conditions. The following equation was utilized to calculate RRF values:

$$RRF = A_x/A_{I.S.} \times C_{I.S.}/C_x$$

A_x represents the area under the M^+ ion peak of the target NPAH, $A_{I.S.}$ represents the area of the internal standard (1-NP-d₉), $C_{I.S.}$ represents the concentration of the internal standard and C_x represents the concentration of the target NPAH.

The detection limits of the 32 NPAH were determined by injecting a 35pg/ μ L standard solution and determining S/N ratio of all peaks (Table 2-5). A 35pg/ μ L standard solution was used due to the wide distribution of RRF of the NPAH (Table 2-4). The 32-compound NPAH standard was used routinely to monitor the performance of the instrument and as a qualitative standard to identify target NAPH in air filter extract analysis.

Table 2-4. Relative response factors (RRF) of the NPAH compounds in the standard relative to 1-NP-d₉ under NICI-SIM mode listed in their order of elution.

Peak No.	Compound	M.W.	Mean RRF (N=10)	Std. Dev.
1	1-nitronaphthalene	173	0.4	0.08
2	2-methyl-1-nitronaphthalene	187	0.2	0.03
3	2-nitronaphthalene	173	0.6	0.07
4	2-nitrobiphenyl	199	0.4	0.06
5	3-nitrobiphenyl	199	0.4	0.04
6	4-nitrobiphenyl	199	3.1	0.6
7	1,5-dinitronaphthalene	218	a	-
8	5-nitroacenaphthene	199	1.3	0.1
9	2-nitrofluorene	211	a	-
10	9-nitrofluorene	211	a	-
11	1,8-dinitronaphthalene	218	0.2	0.02
12	9-nitroanthracene	223	0.7	0.1
13	4-nitrophenanthrene	223	1.7	0.1
14	9-nitrophenanthrene	223	1.4	0.1
15	3-nitrophenanthrene	223	1.2	0.1
16	1-nitrofluoranthene	247	1.8	0.2
17	7-nitrofluoranthene	247	2.7	0.3
18	2-nitrofluoranthene	247	1.1	0.04
19	3-nitrofluoranthene	247	0.5	0.03
20	4-nitropyrene	247	0.5	0.03
21	8-nitrofluoranthene	247	0.9	0.1
22	1-nitropyrene-d ₉	256	1.0	-
23	1-nitropyrene	247	0.6	0.02
24	2-nitropyrene	247	5.7	1.2
25	12-nitrobenzanthracene	273	b	-
26	7-nitrobenzanthracene	273	b	-
27	1-nitrotriphenylene	273	3.7	0.3
28	6-nitrochrysene	273	8.3	0.4
29	2-nitrotriphenylene	273	3.1	0.5
30	3-nitrobenzanthrone	275	1.9	0.5
31	6-nitrobenzo[a]pyrene	297	3.8	0.9
32	3-nitroperylene	297	3.7	1.5

^a RRF of 1,5-dinitronaphthalene, 2- and 3-nitrofluorene was assumed to be equivalent to that of 1,8-dinitronaphthalene.

^b RRF of 12- and 7-nitrobenzanthracene was assumed to be equivalent to that of 1-nitrotriphenylene.

Table 2-5. Detection limits (pg/ μ L) of the NPAH compounds in the standard determined under NCI-SIM mode listed in their order of elution.

Peak No.	Compound	M.W.	Detection limit (pg/ μ L)	Std. Dev.
1	1-nitronaphthalene	173	0.16	0.09
2	2-methyl-1-nitronaphthalene	187	0.09	0.04
3	2-nitronaphthalene	173	0.23	0.12
4	2-nitrobiphenyl	199	0.13	0.02
5	3-nitrobiphenyl	199	0.14	0.02
6	4-nitrobiphenyl	199	0.96	0.08
7	1,5-dinitronaphthalene	218	0.26	0.16
8	5-nitroacenaphthene	199	0.40	0.02
9	2-nitrofluorene	211	0.33	0.07
10	9-nitrofluorene	211	0.33	0.07
11	1,8-dinitronaphthalene	218	0.19	0.05
12	9-nitroanthracene	223	0.16	0.03
13	4-nitrophenanthrene	223	0.20	0.04
14	9-nitrophenanthrene	223	0.23	0.02
15	3-nitrophenanthrene	223	0.21	0.02
16	1-nitrofluoranthene	247	0.50	0.16
17	7-nitrofluoranthene	247	0.70	0.23
18	2-nitrofluoranthene	247	0.50	0.23
19	3-nitrofluoranthene	247	0.15	0.05
20	4-nitropyrene	247	0.14	0.04
21	8-nitrofluoranthene	247	0.28	0.10
22	1-nitropyrene-d ₉	256	0.11	0.05
23	1-nitropyrene	247	0.18	0.06
24	2-nitropyrene	247	1.59	0.55
25	12-nitrobenzanthracene	273	1.00	0.09
26	7-nitrobenzanthracene	273	0.74	0.09
27	1-nitrotriphenylene	273	1.74	0.28
28	6-nitrochrysene	273	3.06	0.69
29	2-nitrotriphenylene	273	2.28	0.93
30	3-nitrobenzanthrone	275	2.22	1.68
31	6-nitrobenzo[a]pyrene	297	1.90	0.86
32	3-nitroperylene	297	4.42	1.38

*Detection limit is defined as signal to noise ratio of 3.

**Detection limit represents the mean of 6 analyses using a 35 pg/ μ L NAPH standard.

2.10 Tandem Mass Spectrometry

The Varian 1200L with its triple quadrupole mass analyzer was utilized to explore the effectiveness of tandem mass spectrometry (MS/MS) techniques for the analysis of target NPAH. It is known from the EI^+ mass spectra of NPAH that they can readily lose a NO group (M-30) as well as a NO_2 group (M-46). As a result, a set of MS/MS experiments were conducted on target NPAH to determine the potential effectiveness and efficiency of such a technique.

The first step in the MS/MS approach was to investigate the characteristic fragment ions that result due to collision with argon gas in the collision cell. Thus, a daughter ion scan was set up such that the first quadrupole was selected to allow the parent ions to pass through while the third quadrupole scans for any fragmented (daughter) ions as a result of collision with argon. A set of daughter ion scans were conducted over a range of collision energies to determine the optimal energy needed to attain a set of fragment ions.

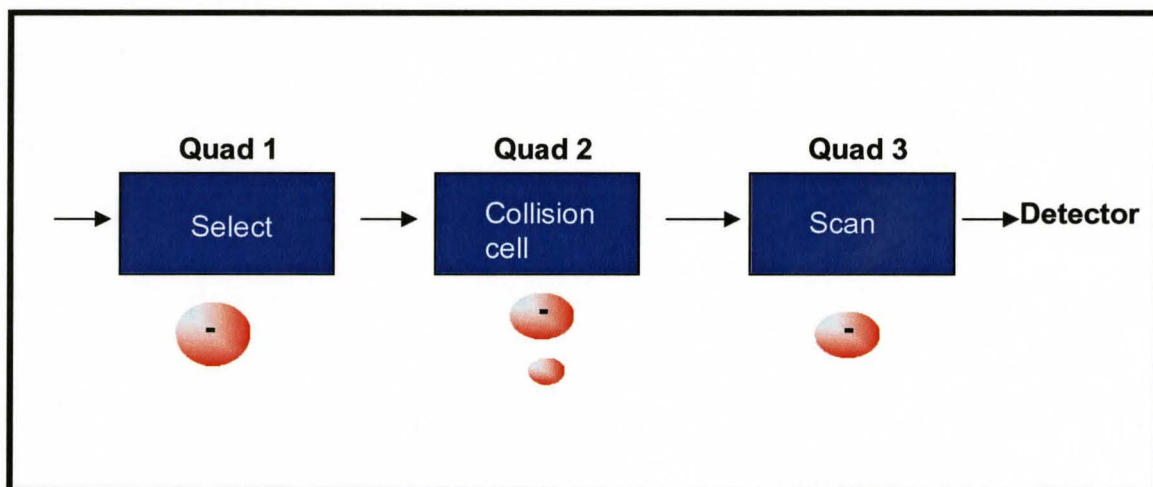


Figure 2-12. Schematic of a daughter ion scan.

The most prominent fragment ion for the 247 molecular weight (MW) NPAH was that of the M-30 ion at m/z 217 which results from the loss of a NO molecule. The energy of the collision gas was varied from 5eV to a maximum of 50eV. As expected, the energy of the collision gas increased the intensities of the fragment ions increased. From Figure 2-13 it can be seen that a collision energy of 30eV provided little fragmentation which at 50eV very little of the parent ion remained for 1-nitropyrene. At 40eV there are sufficient intensities of both the parent ion at m/z 247 as well as the daughter ion at m/z 217. Since the presence of a parent ion peak is useful in the identification of a compound, collision energy of 40eV was used for the MS/MS analysis of all 247MW NPAH compounds.

However, it was observed that not all of the 247 MW NPAH fragmented in a similar fashion. For example, although 1-nitropyrene fragmented readily at 40eV, 2-nitropyrene and 2-nitrofluoranthene did not yield any significant proportion of daughter ions even at the maximum collision energy of 50eV (Figure 2-14).

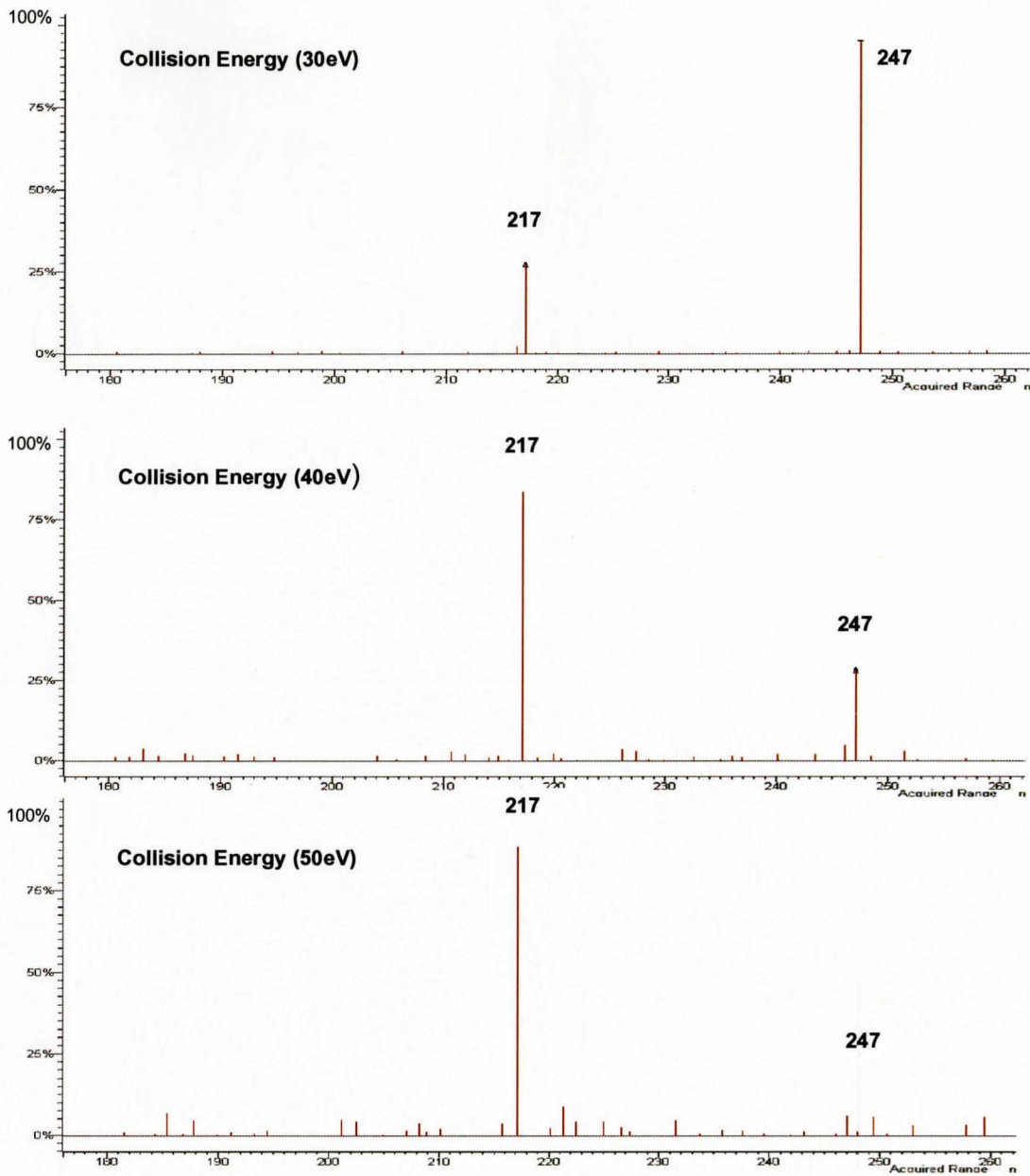


Figure 2-13. MS/MS mass spectra of 1-nitropyrene at 30eV, 40eV and 50eV collision

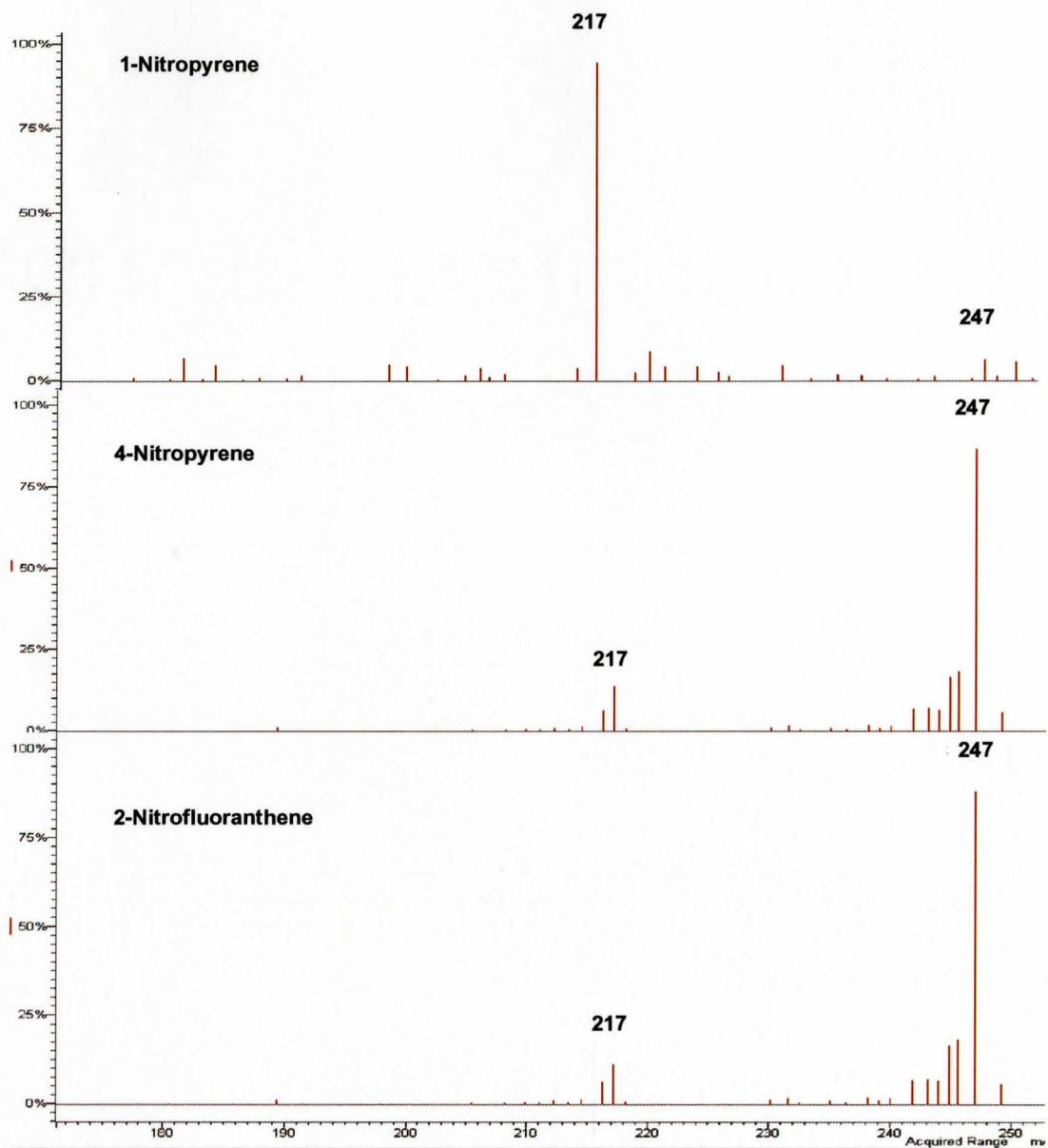


Figure 2-14. MS/MS mass spectra of 1-Nitropyrene, 4-Nitropyrene and 2-nitrofluoranthene at 50eV collision energy.

Similar observations were also made for the 173MW species as well as the 187MW and 199MW species of the NPAH standard. Therefore, a MS/MS method was developed that targeted selected NPAH species.

In order to improve the sensitivity of the MS/MS technique (daughter ion scan), a Multiple Reaction Monitoring (MRM) technique was developed. In a MRM technique the first quadrupole is selected to allow the parent ion to pass through and the third quadrupole is also set to allow the resulting fragment ion(s) to pass through. MRM technique is more sensitive than the daughter ion scan technique since the third quadrupole in MRM does not scan and thus reduces the overall noise of the method. The most prominent fragment ion of each parent NPAH observed from the daughter ion scan was used along with the optimum collision energy to derive an ideal MRM method.

Source Conditions			
Electron energy: 70eV			
Chemical ionization gas: Methane			
Ion source pressure: 8.5Torr			
Ion source temperature: 200°C			
Transfer line temperature: 300°C			
Collision gas: Argon			
Collision cell pressure: 2Torr			
Temperature Program			
Column: DB-17ht (30m x 0.25mm)			
Initial temperature: 90°C			
Rate 8°C/min			
Final temperature: 300°C			
Hold 20 min			
Total run time 72.5 minutes			
Time Segment	Collision Energy (eV)	Parent Ion (m/z)	Daughter Ion(s) (m/z)
<i>Time segment 1</i>	30	218	188, 172, 158
<i>Time segment 2</i>	40	223	199,193
<i>Time segment 3</i>	40	247 256	217 226
<i>Time segment 4</i>	40	273 275	243 245
<i>Time segment 5</i>	40	297	267

The major advantage of the MS/MS technique is displayed in Figure 2-15. In this case the top chromatogram displays the NICI-SIM 256 mass chromatogram of an air filter extract which has been cleaned-up using the aforementioned silica and Sephadex LH20 methodology. The only compound of interest in this chromatogram is the deuterated 1-nitropyrene species. The other peaks correspond to species in the matrix. The bottom chromatogram in Figure 2-15 corresponds to the NICI-MRM 256→226 transition of the same air filter extract. Since the defined transition is a characteristic loss of a NO

molecule which is common only among NPAH compounds the only peak that is observed is that of the deuterated 1-nitropyrene species.

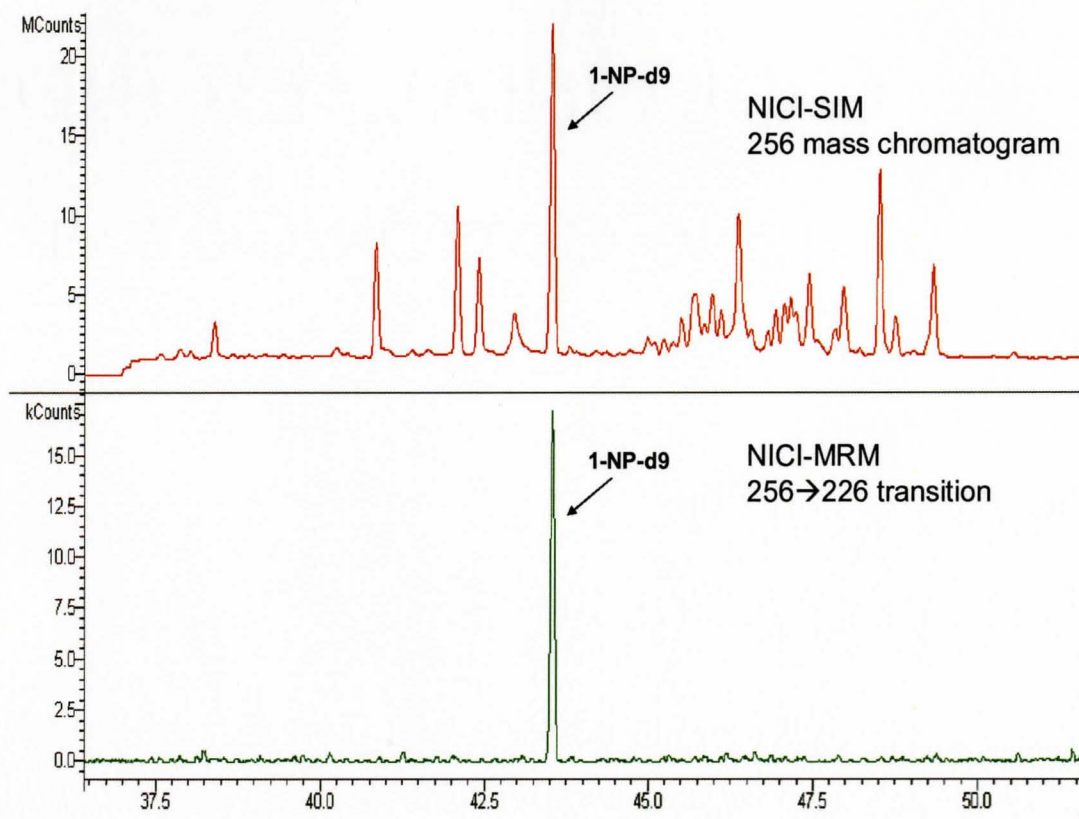


Figure 2-14. GC-MS analyses of an air filter extract.

Although MS/MS techniques provide an added degree of selectivity, sensitivities varied a great deal and were generally poorer than that of the SIM method. This fact was most dramatic for NPAH in the 247MW group. As a result, air filter extract analyses for the Freelton and Pier 25 sites were carried out under NICI-SIM conditions. The ratio of detection limits of the MRM to SIM method in Table 2-6 shows that while the sensitivity was poor for the low molecular weight species it was not too different for the high mass species (273MW and 297MW groups). Therefore the MRM method does have potential

for the analysis of these high molecular mass species in samples. The selectivity of the MRM method holds great potential in that it allows for the analysis of samples with minimal cleanup.

Table 2-6. Detection limits (pg/ μ L) of selected NPAH under MRM technique and NICI- SIM technique along with the ratio of MRM to SIM.

Compound	M.W.	SIM ^a	MRM ^b	MRM/SIM
1,5-dinitronaphthalene	218	0.26	2.1	8.1
1,8-dinitronaphthalene	218	0.19	2.5	13.2
9-nitroanthracene	223	0.16	6.1	38.1
1-nitrofluoranthene	247	0.50	1.3	2.6
7-nitrofluoranthene	247	0.70	15.1	21.6
2-nitrofluoranthene	247	0.50	12.9	25.8
3-nitrofluoranthene	247	0.15	0.64	4.3
4-nitropyrene	247	0.14	6.0	42.9
8-nitrofluoranthene	247	0.28	22.6	80.7
1-nitropyrene	247	0.18	1.2	6.7
2-nitropyrene	247	1.59	30.1	18.9
6-nitrochrysene	273	3.06	4.8	1.6
3-nitrobenzanthrone	275	2.22	2.75	1.2
6-nitrobenzo[a]pyrene	297	1.90	3.61	1.9
3-nitroperylene	297	4.42	3.25	0.7

*Detection limit is defined as signal to noise ratio of 3.

^a Detection limit represents the mean of 6 analyses using a 35 pg/ μ L NAPH standard.

^b Detection limit represents the mean of 6 analyses using a 1 ng/ μ L NAPH standard.

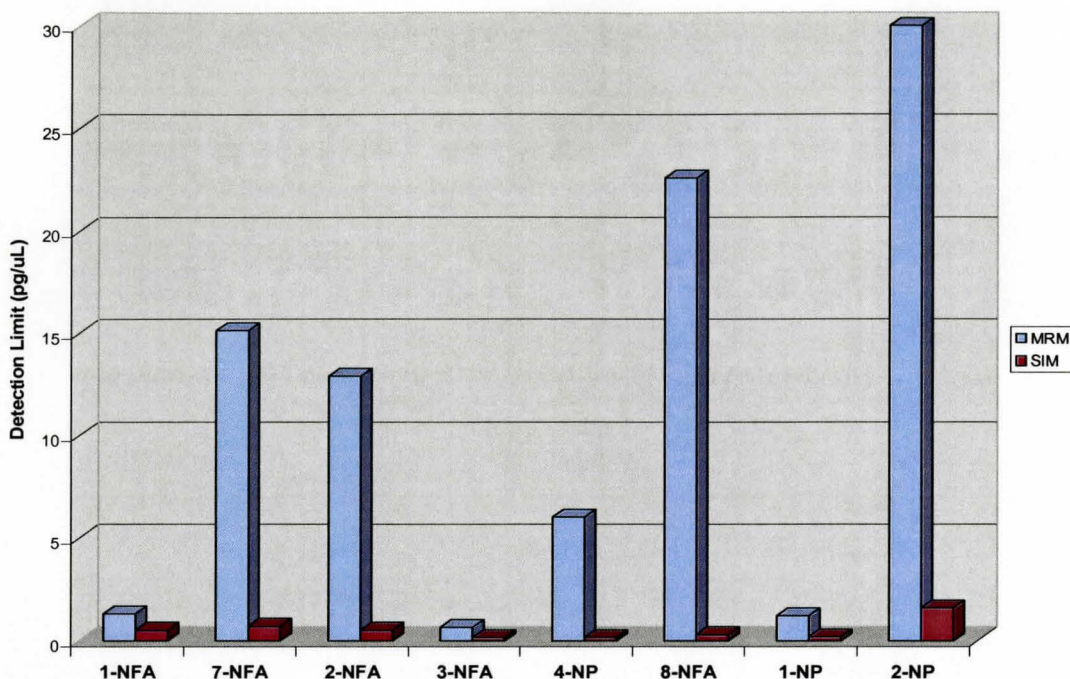


Figure 2-15. Detection limits (pg/μL) of the 247MW NPAH under MRM and SIM conditions.

2.11 Principal Components Analysis

Concentration data from the Freelon/Pier 25 study along with loadings data from the Pacific 2001 and Toronto/Simcoe study were analyzed using the statistical package for social sciences (SPSS) version 15. The SPSS program was used to conduct Principal Components Analysis (PCA) of the data matrix. PCA allows one to determine the correlations between a large numbers of variables in a data set.

Since the samples collected in each study vary with respect to time (day/night) and place (industrial, urban, rural), a PCA was performed to compare the transformation profile of each analyte among the samples collected. Three dimensional principal components plots were used to display the correlations among the variables in a given data set. The variables in this case included both NPAH as well as PAH. PCA was

carried out with Varimax rotation. The purpose of Varimax rotation was to produce final factors as distinct as possible from each other⁶.

In the case of the Freelon/Pier 25 study, concentration data (pg/m^3) was used for principal components analysis of the NPAH. For the Pacific 2001 and Toronto/Simcoe study loading values were used. Loading value of a given PAH is defined as the microgram of PAH that is present on a gram of elemental carbon of air particulate ($\mu\text{g PAH}/\text{g C}$). Furthermore, the loadings data from the two studies were converted to relative loadings data. Relative loadings data allow for the direct comparison of a number of variables by means of a single scale.

In order to obtain relative loading values, the loading values for each analyte from each study were first sorted from highest to lowest. In the case of the Pacific 2001 study, it was noticed that 3 samples from the Langley site were consistently the top 3 loadings values for each target analyte during the sampling period. Furthermore, the loading values of the top 3 samples were significantly higher compared to the other samples. As a result, it was decided to take the average of the top 3 samples for each analyte and refer to it as the “100% relative loading” sample. All remaining samples were assigned relative loading values based on comparison to the average value of these top 3 samples.

A similar approach was undertaken to convert loading values from the Toronto/Simcoe study to relative loading values. From the samples collected at Toronto/Simcoe, it was noticed that 2 samples at Simcoe were consistently the top loadings values for each target analyte. Since the value of the top 2 loadings was

significantly higher than the rest of the samples, the average of these samples was assigned the “100% relative loading” value. The remaining samples were assigned relative loading values based on the average value of these top 2 samples.

3.0 RESULTS AND DISCUSSION

The first part of the results and discussion section of the thesis focuses on the identification and quantification of NPAH from air filter extracts collected at the Freelton and Pier 25 sites. Based on wind direction data for Hamilton obtained from the Ontario Ministry of the Environment at station 29026, samples collected were grouped together depending on the number of hours the mice at the urban-industrial site (Pier 25) were downwind from the industrial core on each sampling day. The corresponding samples collected at the rural site (Freelton) were grouped together. Six composite samples were prepared from the samples collected at each site (Section 2.4.1). A 32-compound authentic standard of NPAH was used for the positive identification of NPAH in these samples.

It is of interest to see the differences in the levels of NPAH at an urban-industrial site (Pier 25) compared to a rural site (Freelton). It is known that the offspring from the urban-industrial males exposed to ambient air inherited mutation rates 2 times more frequently than offspring from the other three treatment groups in the study conducted by Somers et al.²⁸.

The second part of the results and discussion section of the thesis focuses on the data analysis and interpretation of two separate day/night air sampling studies conducted across multiple sites in Canada. Concentrations of polycyclic aromatic compounds (PAC) in samples collected during the day and night from Simcoe and Toronto as well as three sites in the Pacific 2001 study were converted to particulate loadings values. These data were analyzed to explore differences in the day and night profiles and chemistries of

the PAC. Principal components analysis was used as the statistical tool to examine the differences in the transformation of PAC during the day and night at the different sites.

3.1 GC-MS Analysis of Freelon and Pier 25 Air Filter Extracts

A total of 12 air filter extract samples were analyzed by a NICI-SIM method which targeted 32 NPAH compounds. A total of 23 NPAH compounds were identified at least once in the 12 samples (see Tables 3-2 and 3-3). A total of 9 NPAH were identified in all 12 samples (see compounds with asterisks in Table 3-2 and 3-3).

The following criteria were used for the positive identification and quantification of the target NPAH species:

1. NPAH were identified based on the observation of a mass spectral peak in the negative ion GC-MS mode corresponding to the molecular ion of a target analyte.
2. NPAH were identified based on correspondence between the retention time of a peak and the retention time of the authentic standard.
3. NPAH were quantified with the use of the internal standard, 1-nitropyrene-d₉.

High molecular mass NPAH such as 6-nitrochrysene, 2-nitrotriphenylene, 6-nitrobenz[a]pyrene and 3-nitroperylene are amongst the target compounds that were not detected in any of the samples. Sensitivity of the NICI-SIM method was inadequate to detect many of the high molecular mass species since their levels were low and the relative response factors (RRF) were much poorer than 1-nitropyrene-d₉.

In addition to the 9 NPAH which were detected in all samples, another 5 NPAH were detected in all but 2 (or less) samples (see compounds with degree symbol in Table 3-2 and 3-3). These 14 NPAH were used for data analysis. The sample detection limit of

each NPAH was substituted for the non-detected values for these 5 NPAH for data analysis purposes.

Of the 7 newly synthesized NPAH (Table 2-1), the 3-, 4-, and 9-nitrophenanthrene as well as 7-nitrobenzanthracene were detected in all 12 samples. The 12-nitrobenzanthracene along with 1-nitrotriphenylene was detected in 9 of the 12 samples. 2-Nitrotriphenylene was the only newly synthesized NPAH which was not detected in any of the samples. Thus the expansion of the standard list to include the new NPAH has shown to be important in that a wider range of NPAH have now been identified and quantified than in previous studies conducted by our group.

Table 3-1. Detection limits (pg/ μ L) of the 23 NPAH from the Pier 25/Freelton air filter extracts compared to that of the NPAH standard determined under NICI-SIM mode.

Compound	M.W.	Sample D.L. (pg/ μ L)	Standard D.L. (pg/ μ L)
1-nitronaphthalene	173	0.44	0.16
2-methyl-1-nitronaphthalene	187	0.14	0.09
2-nitronaphthalene	173	0.46	0.23
2-nitrobiphenyl	199	0.32	0.13
3-nitrobiphenyl	199	0.36	0.14
4-nitrobiphenyl	199	4.07	0.96
1,5-dinitronaphthalene	218	ND	0.26
5-nitroacenaphthene	199	1.2	0.40
2-nitrofluorene	211	ND	0.33
9-nitrofluorene	211	ND	0.33
1,8-dinitronaphthalene	218	0.16	0.19
9-nitroanthracene	223	0.50	0.16
4-nitrophenanthrene	223	0.42	0.20
9-nitrophenanthrene	223	0.40	0.23
3-nitrophenanthrene	223	0.20	0.21
1-nitrofluoranthene	247	ND	0.50
7-nitrofluoranthene	247	ND	0.70
2-nitrofluoranthene	247	1.08	0.50
3-nitrofluoranthene	247	0.49	0.15
4-nitropyrene	247	0.38	0.14
8-nitrofluoranthene	247	0.62	0.28
1-nitropyrene	247	0.62	0.18
2-nitropyrene	247	4.25	1.59
12-nitrobenzanthracene	273	2.22	1.00
7-nitrobenzanthracene	273	2.05	0.74
1-nitrotriphenylene	273	4.10	1.74
6-nitrochrysene	273	11.76	3.06
2-nitrotriphenylene	273	ND	2.28
3-nitrobenzanthrone	275	2.94	2.22
6-nitrobenzo[a]pyrene	297	ND	1.90
3-nitroperylene	297	ND	4.42

*Detection limit is defined as signal to noise ratio of 3.

**Detection limit represents the mean of 6 analyses for the standard and the mean of 6-12 analyses for the samples.

***Compounds listed in order of elution on a DB-17ht column

Table 3-2. Concentrations (pg/m³) of the 23 NPAH compounds detected in the Freelton samples.

* denotes those NPAH detected in all samples.

° denotes those NPAH with 2 or less non-detect samples (the detection limit value was substituted for ND for data analysis).

NPAH	Hours Downwind of Industrial Site					
	0hrs	1-3hrs	4-9hrs	10-18hrs	19-23hrs	24hrs
1-nitronaphthalene	ND	ND	0.22	0.11	ND	ND
2-methyl-1-nitronaphthalene	0.26	ND	0.01	0.01	0.12	0.19
2-nitronaphthalene	0.04	ND	0.18	0.11	ND	ND
2-nitrobiphenyl °	ND	0.14	0.08	0.07	0.07	0.09
3-nitrobiphenyl °	ND	0.14	0.06	0.06	0.09	0.07
4-nitrobiphenyl	2.04	ND	0.38	0.39	0.28	0.4
5-nitroacenaphthene °	ND	3.54	0.09	0.09	0.11	0.14
1,8-dinitronaphthalene °	0.06	0.05	0.05	0.02	0.05	0.12
9-nitroanthracene*	1.74	5.29	1.1	0.86	0.99	1.07
4-nitrophenanthrene*	0.29	0.14	0.03	0.02	0.07	0.1
9-nitrophenanthrene*	0.07	0.16	0.05	0.04	0.09	0.16
3-nitrophenanthrene*	0.78	1.36	0.48	0.42	0.38	0.57
2-nitrofluoranthene*	12.49	18.92	6.38	11.83	4.08	13.8
3-nitrofluoranthene*	0.74	1.92	2.32	0.19	0.27	0.36
4-nitropyrene	0.07	0.06	ND	ND	ND	0.16
8-nitrofluoranthene	0.54	ND	ND	ND	ND	0.25
1-nitropyrene*	1.29	2.07	1.08	0.38	0.38	0.56
2-nitropyrene	0.64	1.98	ND	ND	ND	0.48
12-nitrobenzanthracene	0.23	0.16	ND	0.11	0.07	0.61
7-nitrobenzanthracene*	0.8	0.81	0.22	0.43	0.14	1.21
1-nitrotriphenylene	0.27	0.66	ND	0.1	0.16	2.13
6-nitrochrysene °	6.83	0.61	ND	0.35	0.55	0.53
3-nitrobenzanthrone*	4.99	0.51	1.67	0.51	0.82	0.7
Total	34.17	38.52	14.4	16.08	8.72	23.69

Table 3-3. Concentrations (pg/m³) of the 23 NPAH compounds detected in the Pier 25 samples.

* denotes those NPAH detected in all samples.

° denotes those NPAH with 2 or less none detect samples (the detection limit was substituted for ND for data analysis).

NPAH	Hours Downwind of Industrial Site					
	0hrs	1-3hrs	4-9hrs	10-18hrs	19-23hrs	24hrs
1-nitronaphthalene	ND	ND	0.13	0.04	1.28	15.86
2-methyl-1-nitronaphthalene	ND	ND	0.01	ND	0.12	0.23
2-nitronaphthalene	ND	ND	0.13	0.03	0.65	0.56
2-nitrobiphenyl °	0.07	0.04	0.05	ND	0.17	0.18
3-nitrobiphenyl °	0.11	0.07	0.09	0.03	0.29	0.25
4-nitrobiphenyl	ND	ND	0.43	ND	ND	0.71
5-nitroacenaphthene °	3.4	0.46	0.47	0.5	2.14	23.78
1,8-dinitronaphthalene °	0.05	ND	0.13	0.03	0.13	0.2
9-nitroanthracene*	7.35	5.51	7.18	0.65	35.75	60.28
4-nitrophenanthrene*	0.2	0.16	0.22	0.07	0.55	1.58
9-nitrophenanthrene*	0.32	0.18	0.36	0.12	0.64	2.45
3-nitrophenanthrene*	1.57	1.03	1.65	0.44	5.56	5.45
2-nitrofluoranthene*	12.76	18.73	17.4	5.29	53.37	60.06
3-nitrofluoranthene*	1.84	0.83	2.02	1.75	1.51	10.88
4-nitropyrene	0.11	0.21	0.33	0.11	ND	0.65
8-nitrofluoranthene	0.23	ND	0.48	ND	ND	ND
1-nitropyrene*	4.06	2.83	2.71	1.53	8.19	15.6
2-nitropyrene	2.96	1.57	2.2	ND	7.63	18.2
12-nitrobenzanthracene	0.15	0.17	0.91	ND	1.91	ND
7-nitrobenzanthracene*	1.13	1.23	2.98	0.47	9.37	7.84
1-nitrotriphenylene	0.29	0.12	1.21	0.59	ND	ND
6-nitrochrysene °	2.61	0.48	2.65	ND	6.01	7.27
3-nitrobenzanthrone*	2.41	0.43	1.37	0.32	2.13	2.43
Total	41.61	34.04	45.12	11.97	137.38	234.45

The total NPAH levels were the same at the two sampling sites except for the 19-23hour and the 24hour samples at the Pier 25 site. The sum of the 6 samples collected from Freelton and Pier 25 are 136 pg/m^3 and 505 pg/m^3 , respectively. The difference in the NPAH levels is most prominent in the 19-23hrs and 24hrs samples in which the total concentration levels are on average 10 times higher at Pier 25 compared to Freelton (Figure 3-1). Figure 3-2 shows the ratio of NPAH levels in the 19-24hrs samples relative to the 0-18hrs samples. The ratio at Freelton for all NPAH is below 1 which indicates that there is no significant increase in NPAH levels in the 19-24hrs samples compared with the 0-18hrs samples. The ratio at Pier 25 however is well above 1 in all cases which indicates elevated levels of NPAH in the 19-24hrs samples.

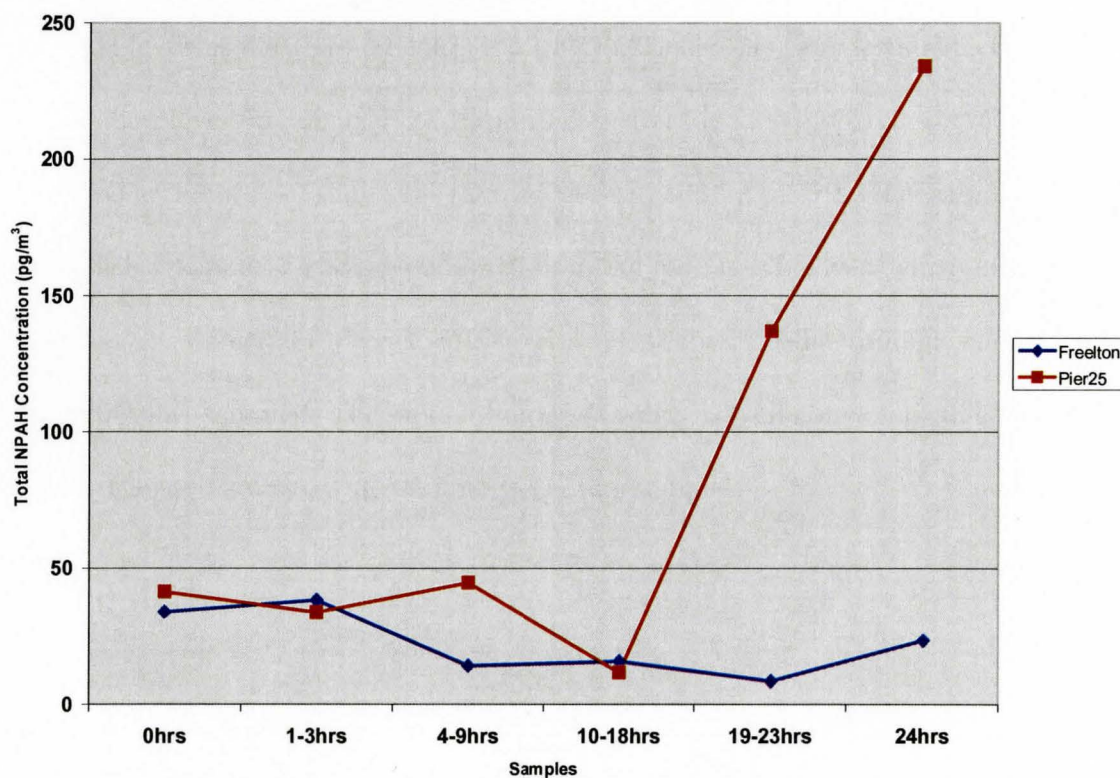


Figure 3-1. Total NPAH concentrations (pg/m^3) of the 6 composite samples collected at Freelton and Pier 25 sites.

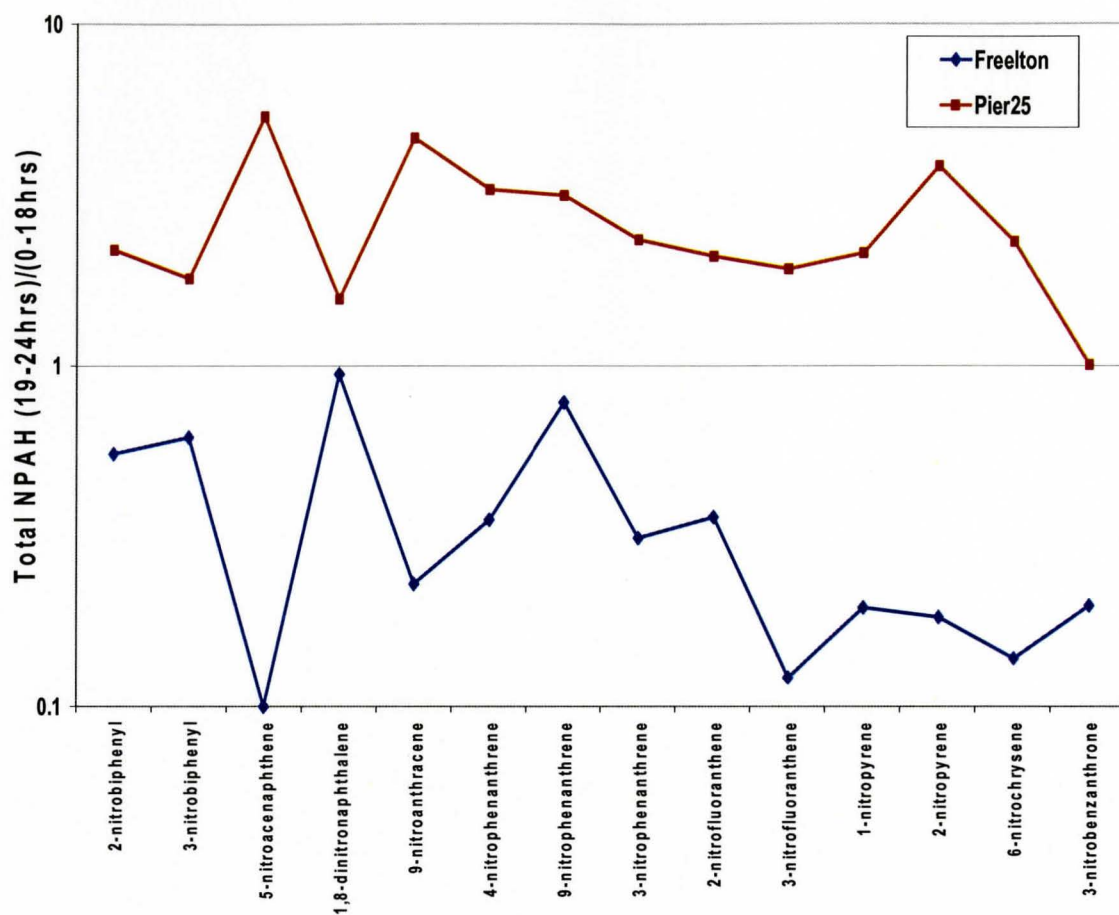


Figure 3-2. The ratio of total NPAH levels in the 19-24hr samples compared to the 0-18hrs samples of selected NPAH.

The 2-NFA, 1-NP and 2-NP concentrations show a similar trend to that of the total NPAH levels (Figure 3-3). There are increased levels of these three NPAH at Pier 25 compared to Freelton with a clear distinction in the 19-23hrs and 24hrs samples. It is known from Atkinson and Arey that a 2-NFA/2-NP concentration ratio of 6 or less is an indicator of OH radical-dominated transformations of PAH to NPAH¹⁰⁻¹². A 2-NFA/2-NP ratio close to 100 is an indicator of a NO₃ radical dominated transformation pathway which occurs at night. The average 2-NFA/2-NP ratio calculated from the 19-23hrs and 24hrs samples from Pier 25 and Freelton are 8 and 20, respectively. This finding indicates that the nitration process at the Pier 25 is dominated by the OH radical pathway meanwhile the nitration process at Freelton is influenced by both the OH radical chemistry as well as NO₃ radical chemistry.

Pier 25 is an industrial site located 1.5-3.5 km downwind of 2 steel mills and the city of Hamilton. It is likely that the 2-NFA and 2-NP species are produced primarily in the atmosphere from their precursor PAH. Since the pathway of NPAH synthesis seems to be dominated by the OH radical pathway, it is likely that PAH emitted in Hamilton would be transformed and collected a short time later. Since there are no major local sources of PAH at Freelton, it is highly likely that NPAH have been formed some distance from Freelton. As a result, the 2-NFA and 2-NP species detected at the Freelton site are those that are produced in the atmosphere during long range transport of PAH. Therefore PAH transformation to NPAH is affected by both OH radical during the day-time as well as NO₃ radical during the night-time.

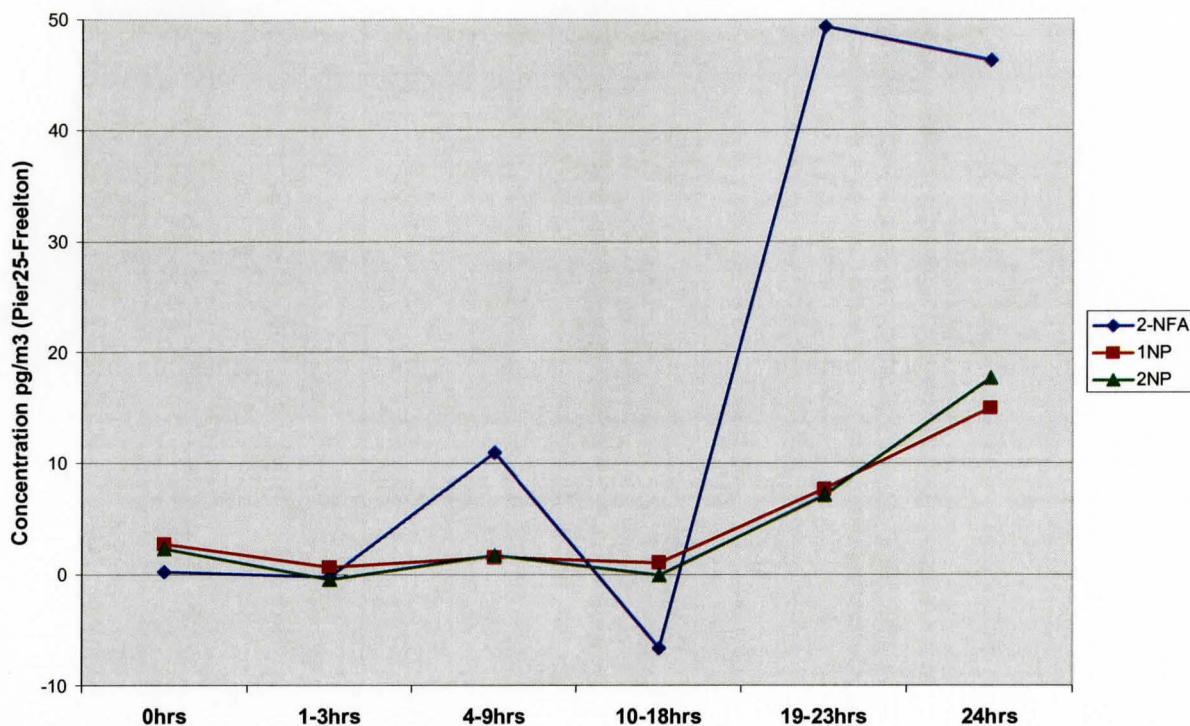


Figure 3-3. The net concentrations at Pier 25 (Pier 25 – Freelton) of 2-NFA, 1-NP and 2-NP.

The 2-NFA/1-NP ratio serves as an indicator of the overall atmospheric transformation at a given site since 2-NFA is produced in the atmosphere and 1-NP is only found in exhaust gases by high temperature fuel combustion⁵³. The average 2-NFA/1-NP ratio calculated from the 19-23hrs and 24hrs samples from Pier 25 and Freelton are 5 and 18 respectively. Although the actual concentrations of 2-NFA and 1-NP are higher at Pier 25 the ratio of the two species is lower than that at Freelton. A lower ratio is an indicator that there is a higher contribution from direct emission sources and a lesser contribution from atmospheric transformation. This finding is not surprising given that the Pier 25 site is located in close proximity to the steel industry, a large city and a major highway (QEW); 1-NP is a primary emission product from diesel engines.

The higher 2-NFA/1-NP ratio observed at Freelton indicates that there is a higher degree of atmospheric transformation at the rural site compared to the industrial site in Hamilton where direct emissions from sources such as diesel engines predominate.

3.1.1 Principal Components Analysis of the Freelton and Pier 25 Data Sets.

To further explore the differences in transformation profiles of NPAH between Freelton and Pier 25 sites, a principal components analysis (PCA) was conducted. PCA is a commonly used multivariate statistical tool that helps to reduce the dimensionality of a large data set⁷⁰. In order to perform PCA, a complete data matrix was utilized. As a result, only 14 of the 23 NPAH detected at the sampling sites were used. For compounds with non-detectable levels, the detection limit values were substituted (see compounds with asterisks and symbols in Tables 3-2 and 3-2).

The data set was comprised of the concentration values for each variable (pg/m^3), which in this case were the individual NPAH. In PCA, variables are correlated against each other in the same sample as well as against all other samples. A number of principal components are obtained from the analysis that accounts for the greatest amount of variability among the variables. In this case 5 principal components were obtained which accounted for 100% of the variability in the data set (see Table 3-3). The first 3 components, which accounted for 88% of the total variance, were used to create plots in a reduced sub-space which permits for the visualization of the correlations amongst the defined variables.

Table 3-4. The 5 principal components for the Freelton/Pier 25 data set along with the percentage variance.

Component	% of Variance	Cumulative %
1	53.3	53.3
2	22.7	76.0
3	12.0	88.0
4	7.7	95.7
5	4.3	100.0

In the principal component plots each marker represents a given NPAH from samples collected at Pier 25 and Freelton. Since it has already been shown that the NPAH levels in the 19-23hr and 24hrs samples at Pier 25 are significantly greater than NPAH from any other sample (Figure 3-1, Tables 3-2 and 3-3), the first principal components plot was obtained using a data matrix of 10 samples that excluded the data from these latter two samples at Pier 25. The resulting principal components plot is displayed in Figure 3-4(a). Although there is some separation between the NPAH at Freelton and Pier 25, the NPAH from both sites are well dispersed moderately overlapped in the plot. Figure 3-4(b) displays the principal components plot of all 12 samples collected at Freelton and Pier 25. In this case the separation of NPAH at Freelton and Pier 25 is dramatic. These results show that there is a significant difference between the air masses at the Pier 25 has and Freelton sites. The NPAH at Pier 25 appear to have a transformation profile that is rather different from that of Freelton when the 19-23hrs and 24hrs samples are taken into account.

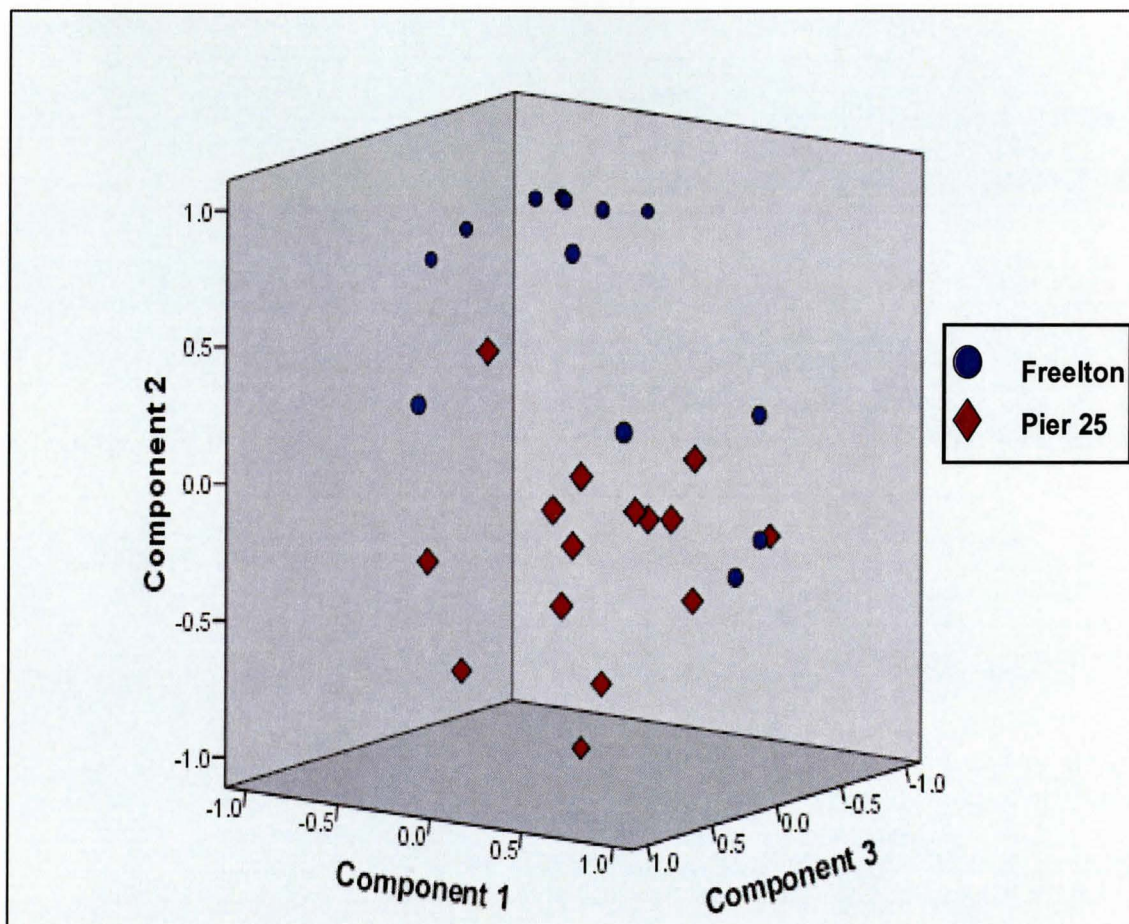


Figure 3-4(a) Principal components plot of the Frelton and Pier 25 data matrix that excludes the 19-23hrs and 24hrs data from Pier 25 (Components 1, 2, and 3).

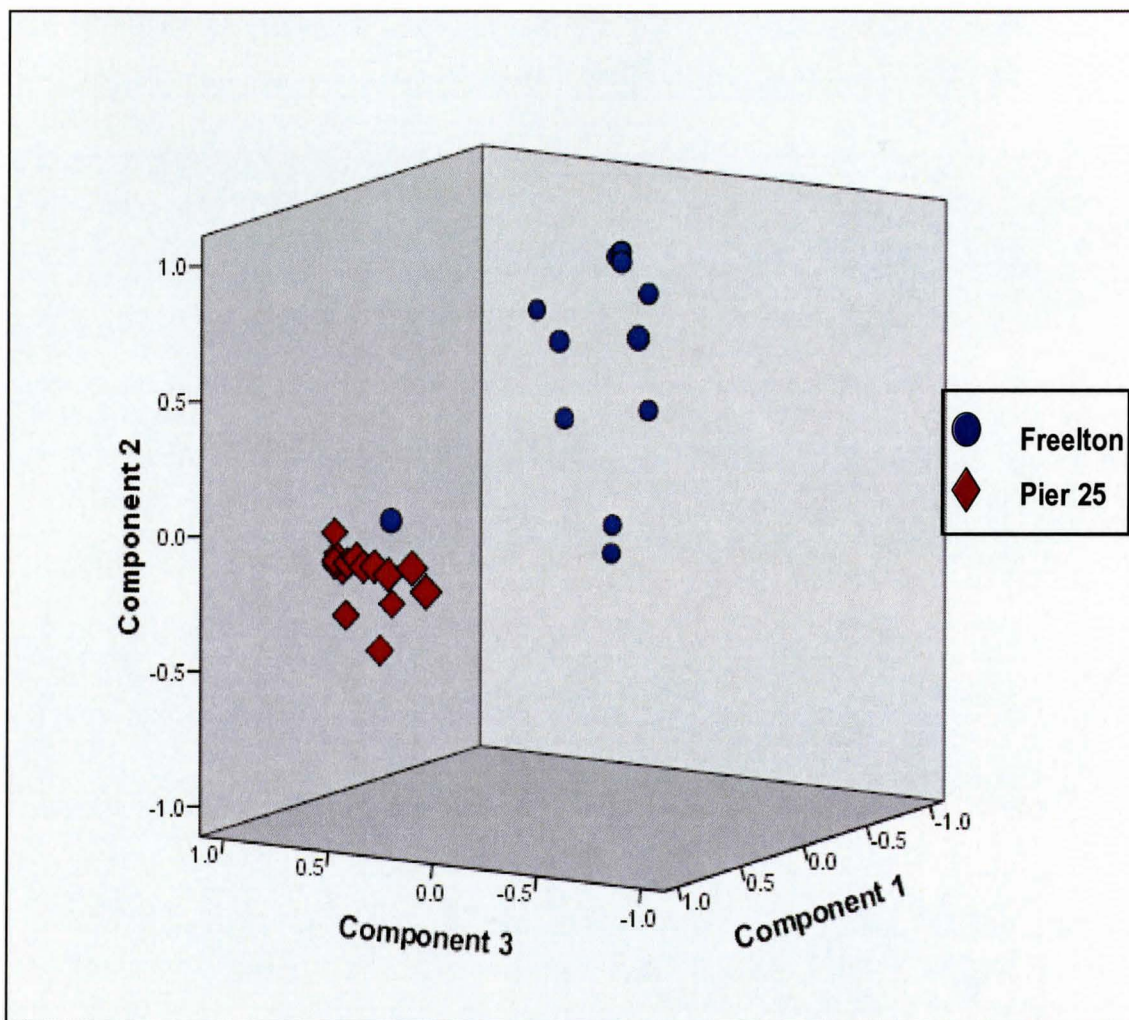


Figure 3-4(b) Principal components plot of the complete data matrix from Frelton and Pier 25 (Components 1, 2, and 3).

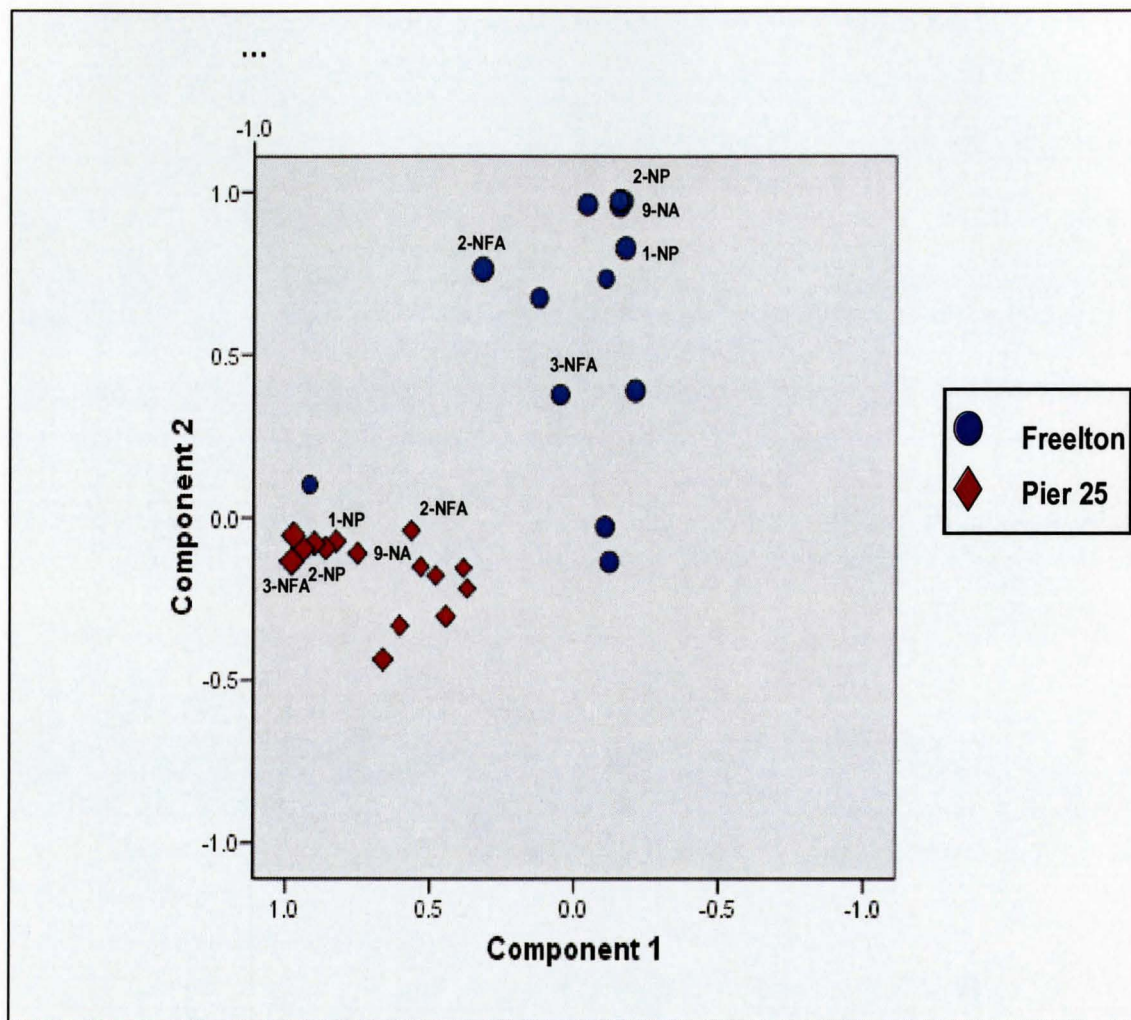


Figure 3-4(c) Principal components plot of complete data matrix from Frelton and Pier 25 (Components 1 and 2).

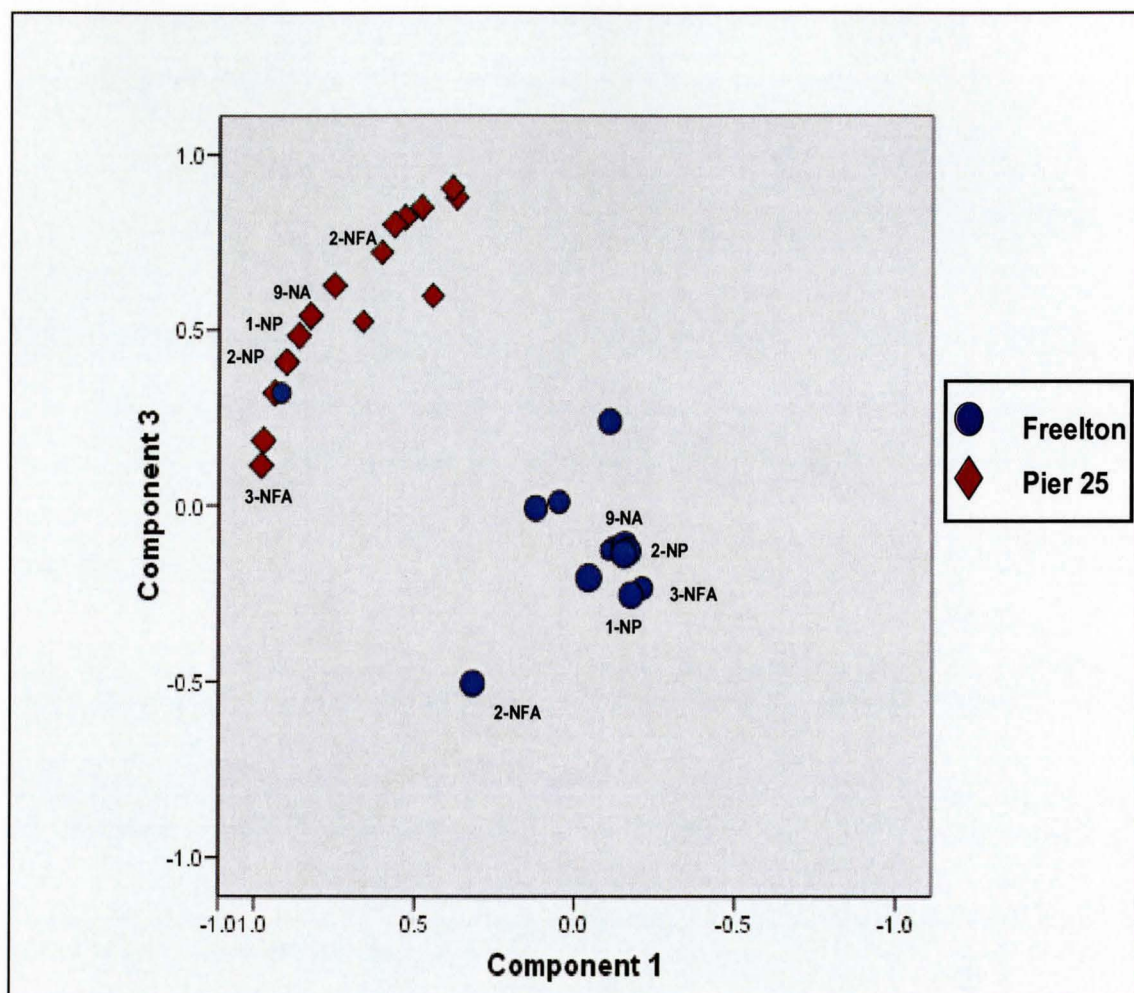


Figure 3-4(d) Principal components plot of complete data matrix from Frelton and Pier 25 (components 1 and 3).

It can be seen from the principal components plots that two major source emission products, 9-nitroanthracene (9-NA) and 1-nitropyrene (1-NP), are grouped together at both the Freelton and Pier 25 sites (Figure 3-4c). 2-Nitrofluoranthene (2-NFA), a major transformation product, seems to be distant from 1-nitropyrene, a major emission product at both the Freelton and Pier 25 sites (Figure 3-4d). Furthermore, 2-nitrofluoranthene is distant from 2-nitropyrene at both Freelton and Pier 25. The PCA plots indicate differences in day/night chemistry at Freelton and Pier 25. The tighter clustering of the NPAH at Pier 25 compared to Freelton is consistent with a site located in close proximity to a local source. The air mass moving onto Freelton seems to have been influenced by both day and night transformation and thus is less tightly clustered.

Figure 3-4 (e) shows the grouping the NPAH at Freelton and Pier 25 once the 6 new NPAH analytes had been removed from the data set. The removal of these 6 NPAH does not have any significant effect on the outcome of the PCA. The NPAH clusters at Pier 25 and Freelton remain well separated from each other. Thus, inclusion of these 6 NPAH in the data set is valid and does not alter the outcome of the statistical analysis.

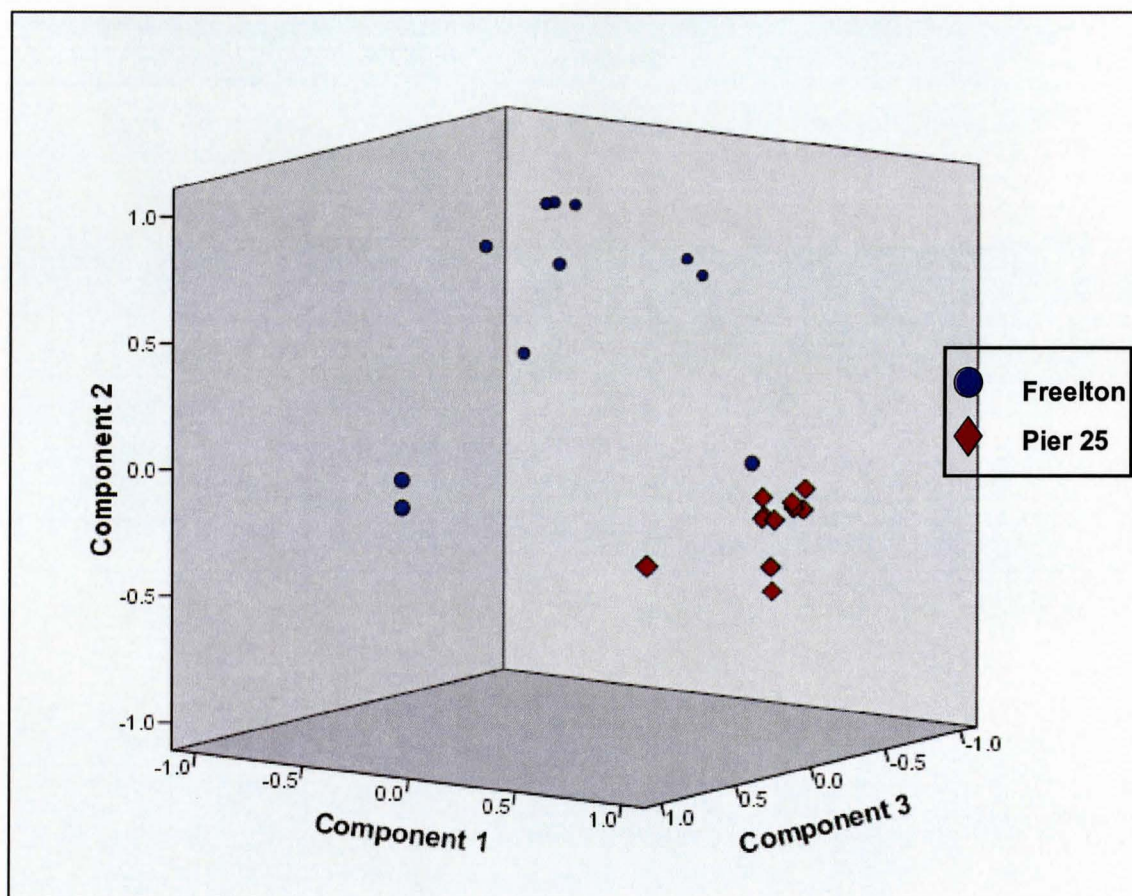


Figure 3-4(e) Principal components plot of the data matrix from Freelton and Pier 25 (components 1, 2 and 3) after the removal of the newly synthesized NPAH from all samples.

The expansion of the NPAH standard to include 7 newly synthesized NAPH proved to be valuable since all but 1 NPAH were detected and quantified in the samples analyzed. Thus including these NAPH to determine the total NPAH levels allowed for a more accurate representation of the total NPAH levels at Pier 25 and Freelton. The total NPAH levels at Pier 25 were on the average 5 times as high as in Freelton with the most significant differences in the 19-23hrs and 24hrs samples.

The principal components analysis showed that the NPAH at Freelton and Pier 25 are not significantly different when the 19-23hrs and 24hrs samples from the Pier 25 site were removed. It is known that the prevailing winds during the sampling period at Pier 25 were from the south-westerly direction and would bring pollutant from the Ohio Valley. Since Pier 25 is in close proximity to numerous PAH emission sources nitrogen oxides in the air can react with PAH to form NPAH in the presence of nitrate and/or hydroxyl radical. Thus the NPAH levels increased as the percentage of winds coming from the urban-industrial core increased. It is believed that the air mass at Pier 25 is affected by not only local sources such as the steel industries and vehicle emissions but from long range transport of matter across the transcontinental border.

3.2 Elemental Carbon and Organic Carbon Concentrations at Toronto & Simcoe.

The Elemental Carbon (EC) and Organic Carbon (OC) concentration data from Toronto and Simcoe were made available for the day and night samples collected in July 2001 by Dr. Jeff Brook from Environment Canada. A comparison of the elemental carbon levels between Toronto and Simcoe during the sampling period is displayed in Figure 3-5. The figure clearly shows the elevated levels of EC at Toronto. Since Toronto is an urban site there are many local sources which could account for the increased levels of EC. Simcoe is a rural site near Lake Erie and thus displays a relatively flat EC profile compared to Toronto during the sampling period.

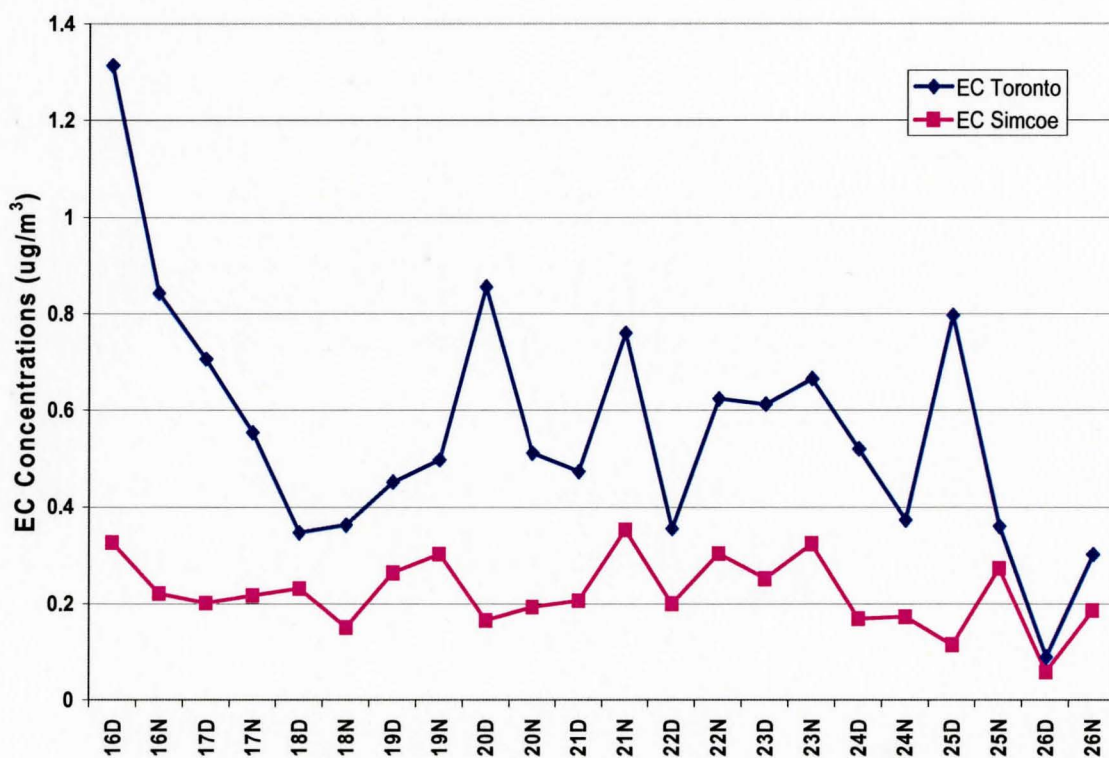


Figure 3-5. Elemental Carbon (EC) concentrations from Toronto & Simcoe samples.

Similarly, with the exception of a few samples the Organic Carbon (OC) concentrations at Toronto were always greater than at Simcoe (Figure 3-6). These results are consistent when comparing the emissions from an urban site (Toronto) to that from a rural site (Simcoe). The higher levels of elemental carbon and organic carbon in Toronto are indicative of the high levels of organic compounds and air particulate present during the summer months in an urban centre like Toronto.

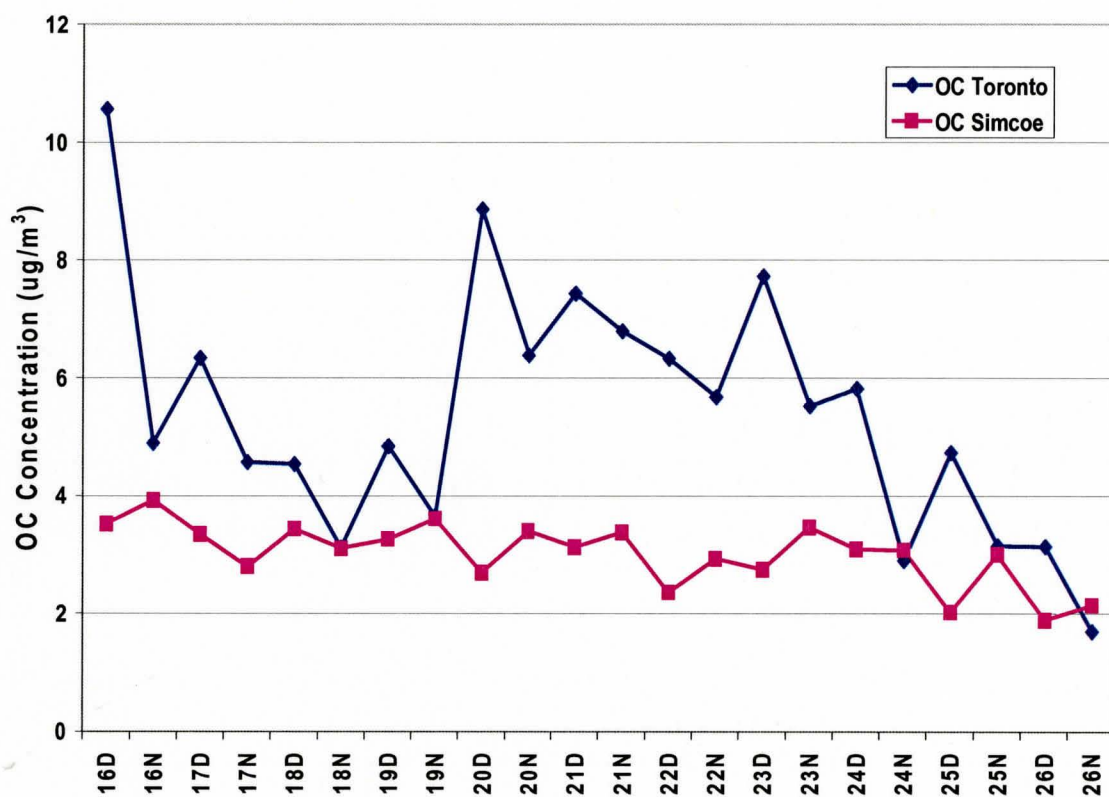


Figure 3-6. Organic Carbon concentrations from Toronto and Simcoe samples.

The prevailing air flow in southern Ontario is from the south-west from the Ohio Valley across Lake Erie, over Simcoe and on towards Toronto. Thus, subtracting the EC and OC concentrations at Simcoe from the levels in Toronto samples enables one to account for the net amounts of EC and OC at the urban site in Toronto. The EC concentration levels (average of $0.213 \pm 0.071 \text{ ug/m}^3$) and OC concentration levels (average of $2.92 \pm 0.56 \text{ ug/m}^3$) at Simcoe are fairly consistent throughout the sampling period. The emissions at Toronto however vary during the sampling period. The time periods with increased EC and OC levels at Toronto may be due to any number of factors such as increased emissions or smog events. Without the proper meteorological data it is uncertain as to which specific factors are responsible for the elevated emissions.

3.3 Loadings of Polycyclic Aromatic Carbons on Air Particulate at Toronto and Simcoe Sites.

One of the major disadvantages of using concentration values to assess the degree of transformation of airborne species is that concentration values of airborne species may change due to chemical transformations and to dispersion in the air. The use of loadings values on air particulate tends to compensate for the effects of dispersion. Loadings values of a given PAH are defined as the mass of a given PAH present on a gram of elemental carbon air particulate ($\mu\text{g PAH/g C}$). The loadings value for a given species is therefore only affected by atmospheric transformation and volatilization and not by dispersion.

Instead of using absolute loadings values the levels of each species are expressed in terms of relative loadings in this thesis since absolute loadings of PAH and NPAH vary by about 1000-fold. Relative loadings values allow for the direct comparison of a number of species using a single scale (see Figure 3-7(a) and (b)) and form the basis for statistical comparisons. The loadings values for each compound from Simcoe and Toronto were sorted from highest to lowest. It was noticed that the same 2 samples at Simcoe always had the highest absolute loadings values for every target analyte. Since the values of the highest loadings were significantly higher than the loadings of the rest of the samples, the average of the two highest samples was assigned the "100% relative" loading value for each PAH and NPAH. The remaining samples were assigned relative loadings values based on the average value of these top 2 samples. This procedure was applied to each PAH and NPAH to attain a relative loading.

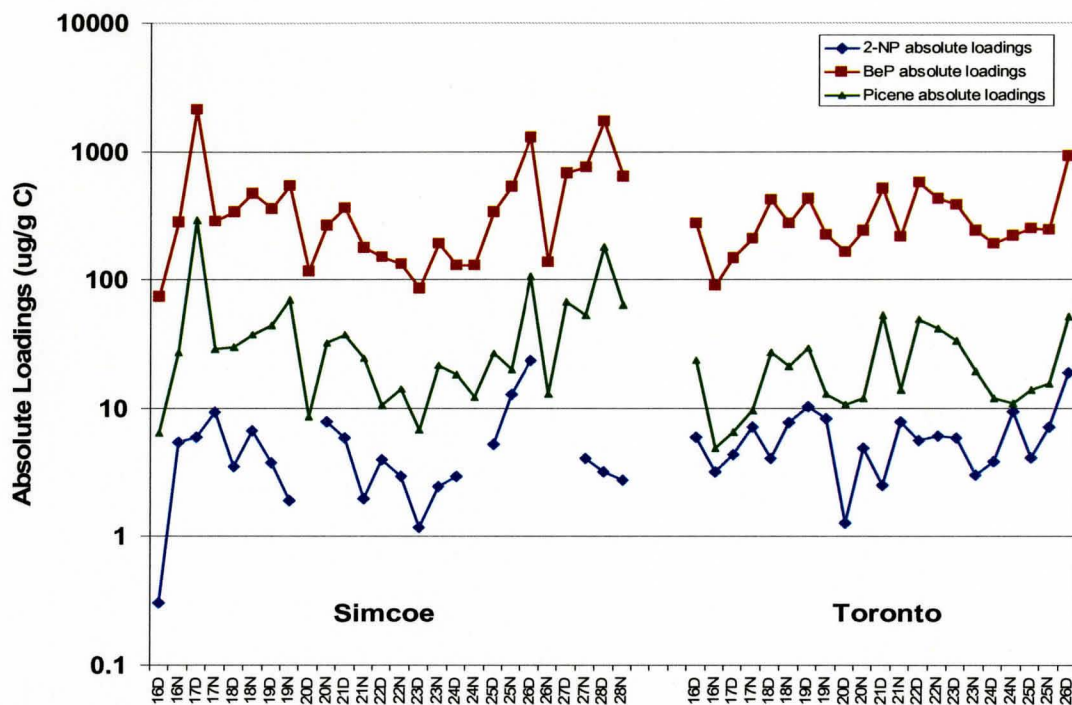


Figure 3-7(a) Absolute loadings of 2-NP, BeP and Picene from Simcoe and Toronto samples.

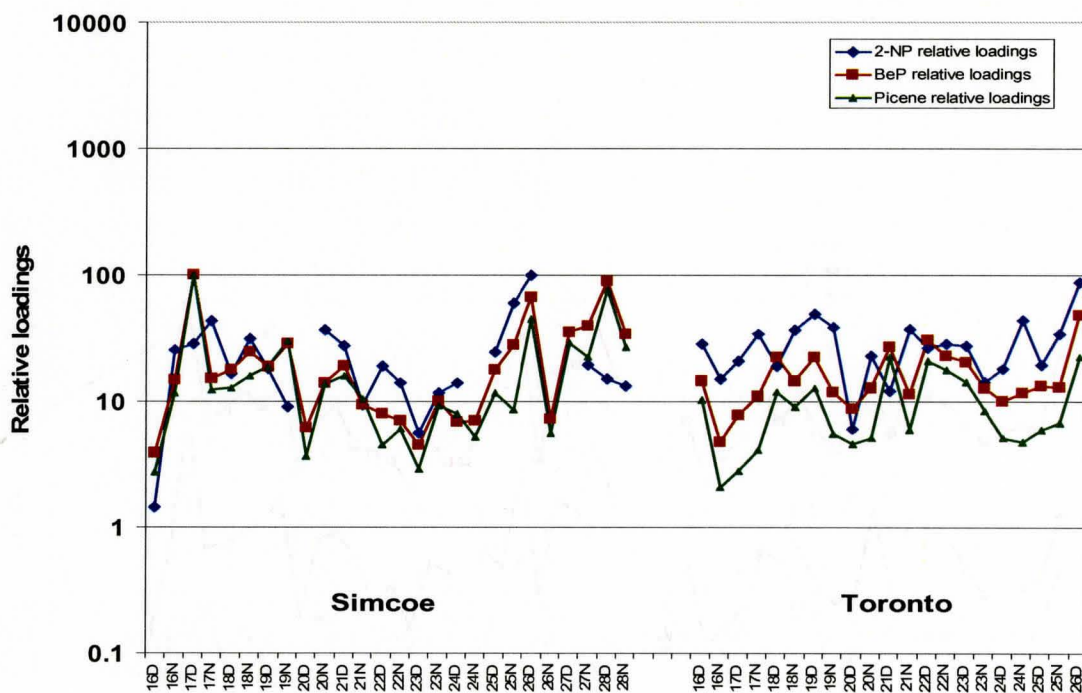


Figure 3-7(b) Relative loadings of 2-NP, BeP and Picene from Simcoe and Toronto samples.

From the relative loadings values of each species in the Simcoe and Toronto samples, it observed that five PAH had very similar patterns. The relative loadings of these five PAH were averaged and the mean value was referred to as the 'PAH5' composite value. The PAH5 composite is representative of the average relative loading values of the following five PAH species: B_jF, B_kF, B_bF, B_eP and B_{ghi}P. These five PAH are known to undergo relatively low level of transformation in air¹³. Figure 3-8(a) shows the relative loadings ratios of each of these individual PAH compared to the PAH5 composite value. The ratio in almost all cases is very close to 1, consistent with the similarity in the relative loadings and thus the transformation patterns of these five PAH during the sampling period. The ratio at the Simcoe site was extremely consistent.

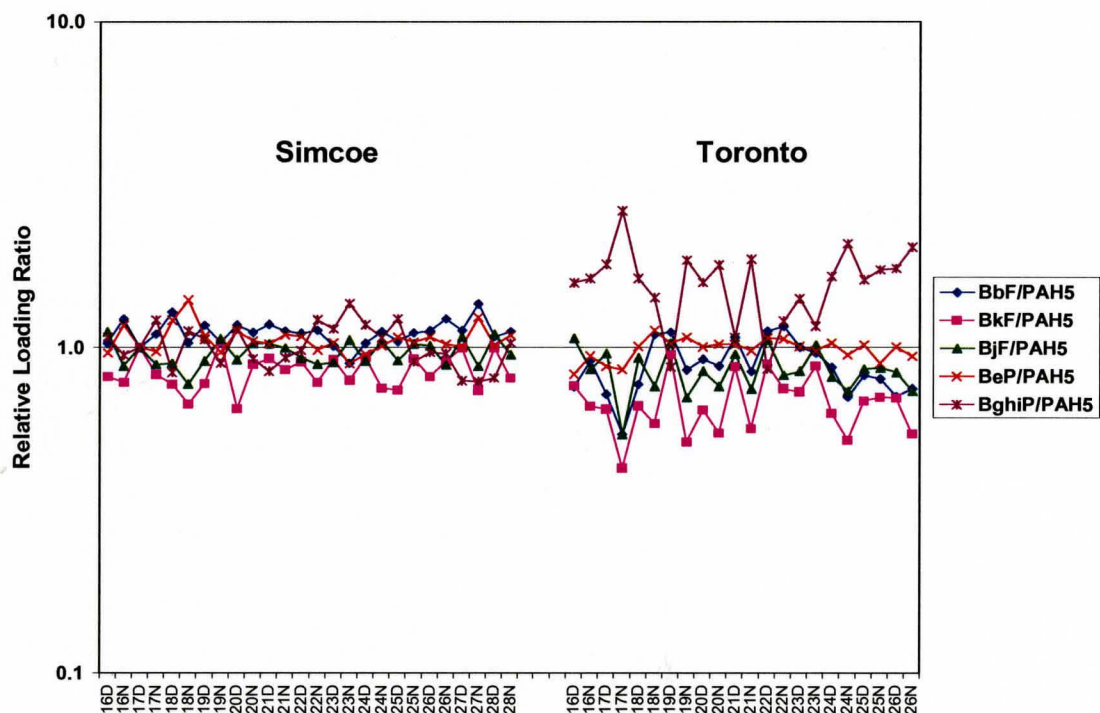


Figure 3-8(a) Relative loading ratio of B_bF, B_kF, B_jF, B_eP & B_{ghi}P to PAH5 composite from Toronto and Simcoe samples.

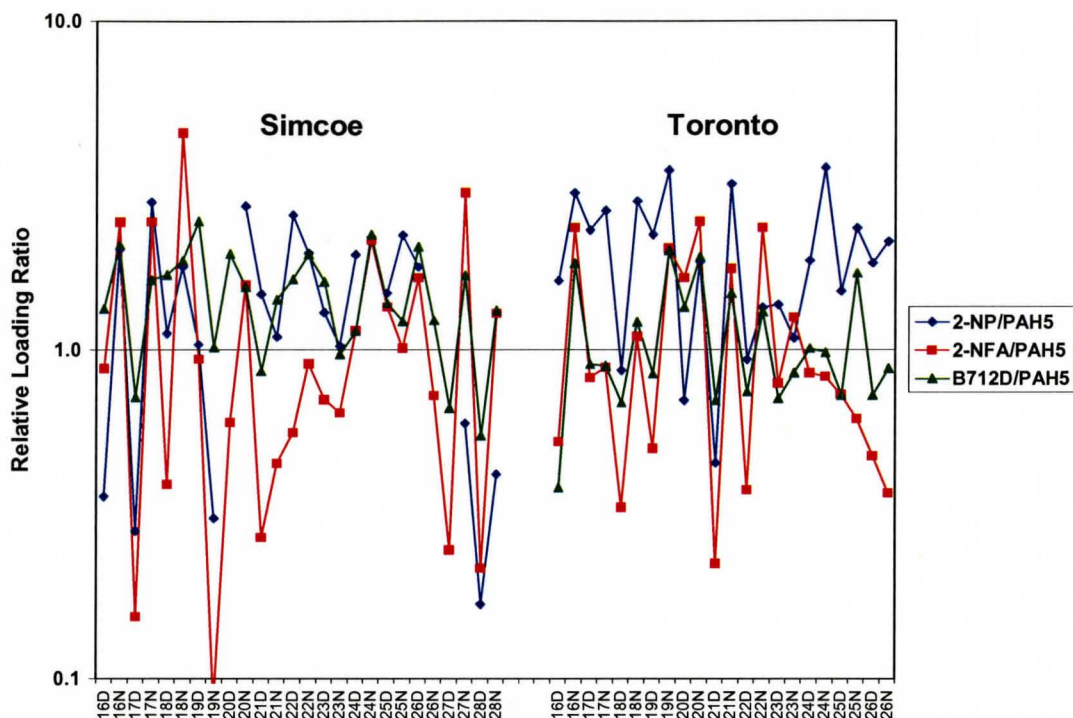


Figure 3-8(b) Relative loading ratio of BD, 2-NP and 2-NFA to PAH5 composite from Toronto and Simcoe samples.

The PAH that constitute the PAH5 composite all have molecular masses of 252 Da with the exception of BghiP (276 Da). All five members of the PAH5 composite are emission products from anthropogenic sources and are primarily associated with particles and exhibit very similar reactivities in the atmosphere. Kamens et al. carried out a set of chamber experiments in which he varied the levels of solar intensity, humidity and temperature to determine the half lives of a selected group of PAH²⁵. The results showed that PAH such as BbF, BkF and BghiP exhibited very similar half-lives compared to reactive PAH such as CcdP, BaA and BaP which exhibited much shorter half-lives. The Canadian Environmental Protection Act (CEPA) has classified all five members of the PAH5 composite as toxic under CEPA article 11c as substances constituting a danger for

life and human health or thought to have toxic effects on the environment due to their carcinogenic and mutagenic nature.

Figure 3-8(b) displays the ratios of the known air transformation products, Benzanthracene-7,12-dione (BD), 2-NP, and 2-NFA, to the PAH5 composite value. The ratio in most cases significantly deviates from 1. Since BD, 2-NP and 2-NFA are atmospheric transformation products, it is not surprising that they exhibit unique transformation profiles compared to the PAH5 profile.

Figure 3-9 shows the relative loadings data for the PAH composite sample. Relative loadings values in Figure 3-9 ranges from 100 (lowest transformed sample) to about 3 (highest transformed sample). This plot is therefore a transformation profile of the PAH5 composite at Simcoe and Toronto. An interesting observation is the diurnal pattern at Simcoe and at Toronto. The periods of highest transformation are observed mostly during the day-time. This indicates that the day-time transformation profiles are different from that of the night-time profiles at both Simcoe and Toronto. Since the photolysis of particle-bound PAH depends on atmospheric conditions such as light intensity, temperature, humidity and ozone concentration, it is not surprising to observe transformation profiles in night samples that are different from day samples.

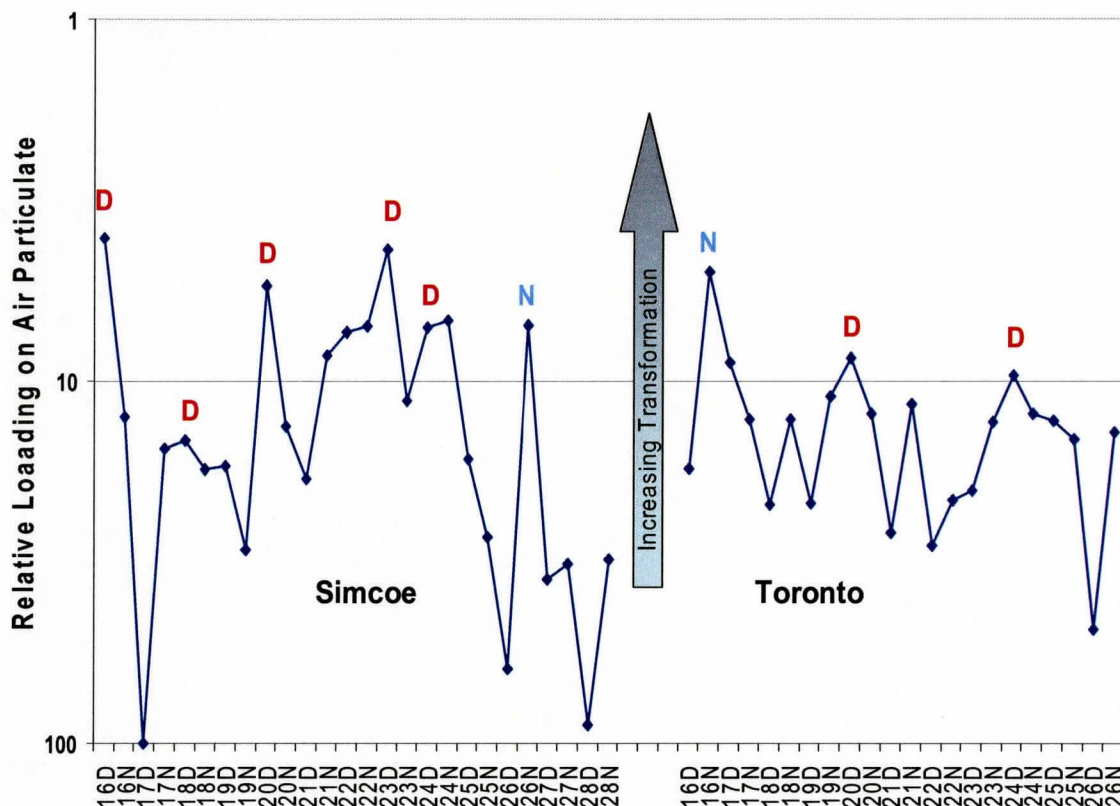


Figure 3-9. Relative loadings values of PAH5 composite at Simcoe and Toronto.

3.3.1 Principal Component Analysis of PAC Data from Toronto and Simcoe.

In order to further explore the differences in the day and night transformation profiles at each site, a principal components analysis (PCA) was carried out. Since some of the polycyclic aromatic compounds (PAC) were not detected in every sample during the sampling period, the data matrix was reduced from 20 to 14 PAC and from 14 to 11 sampling days to obtain a complete data set. Of the 14 PAC, 10 were PAH which included BghiF, BaA, BbF, BkF, BjF, BeP, BaP, Per, IcdP, and BghiP. The remaining 4 PAC were three NPAH (1-NP, 2-NP, 2-NFA) and BD. The latter is the oxidized product of BaA. The data set was comprised of the relative particulate loadings values for each

variable. In this case the variables were the species of interest (PAC) which were coded according to sampling time (day/night) as well as site (Toronto/Simcoe).

The outcome of the principal components analysis for the Simcoe/Toronto data matrix yielded 7 principal components that accounted for 100% of the variance in the data set. A set of plots of the first 3 components which accounts for 85% of the variance is shown in Figures 3-10 (a) to (d). In these plots each marker represents a given polycyclic aromatic compound from 11 samples collected at Simcoe and Toronto during the day and night.

Table 3-5. The 7 principal components for the Toronto/Simcoe data set along with the percentage variance.

Component	% of Variance	Cumulative %
1	44.7	44.7
2	25.0	69.7
3	15.7	85.4
4	8.7	94.1
5	3.5	97.6
6	1.5	99.1
7	0.9	100.0

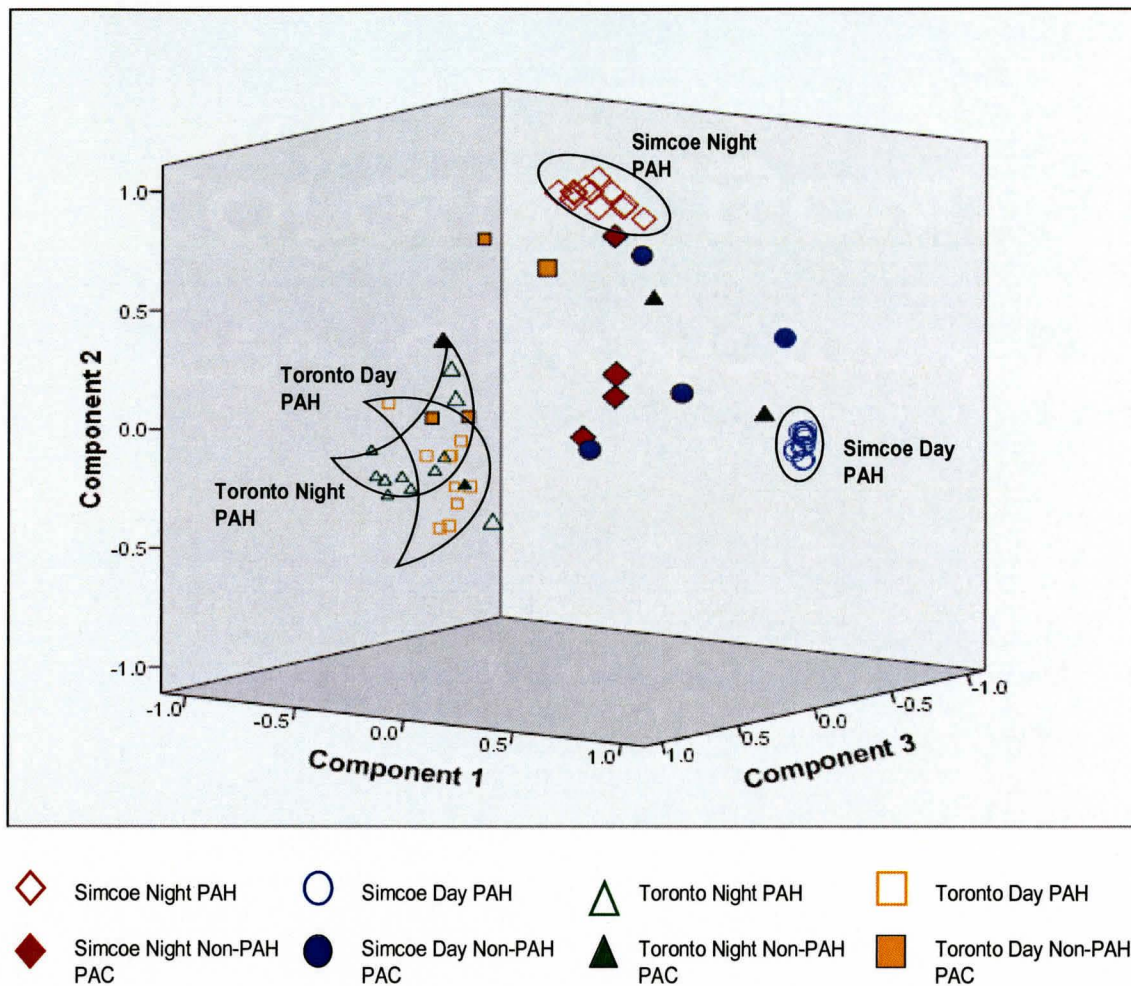


Figure 3-10(a) Principal components plot of data matrix from Toronto and Simcoe (Components 1, 2 and 3).

Figure 3-10(a) shows a 3D plot of components 1, 2 and 3. The open symbols are the 11 PAH while the filled symbols are the 4 PAC. One observation is that the PAH from Simcoe day and night samples are clearly separated from each other; the Toronto day and night samples are also separated but to a lesser degree. The PAH at Simcoe show high degrees of correlation since both groups form very tight clusters. The Toronto day and night samples are less tightly clustered but their relative separations are significant.

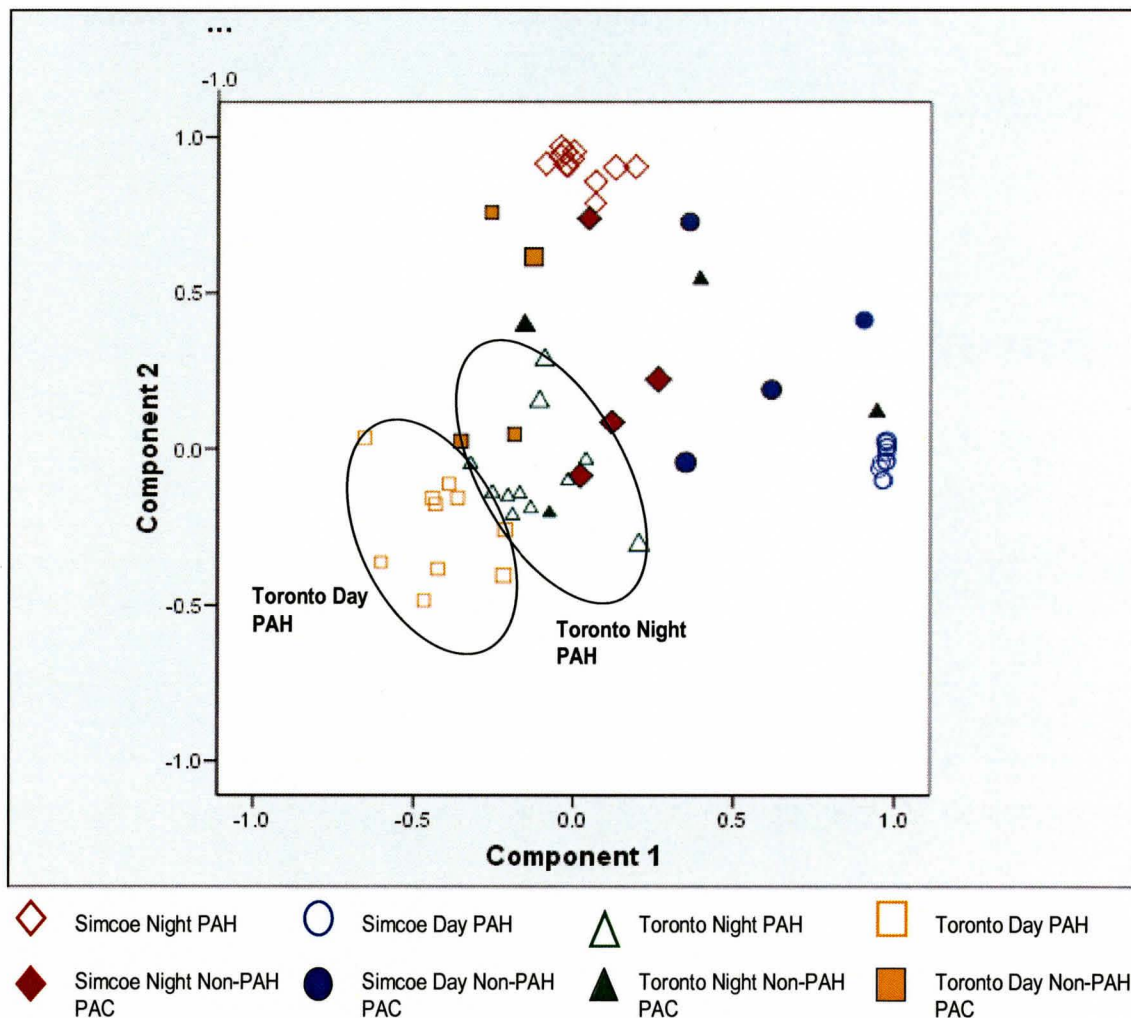


Figure 3-10(b) Principal components plot of data matrix from Toronto and Simcoe (Components 1 and 2).

Figure 3-10(b) displays components 1 and 2 of the Simcoe/Toronto data set. The Toronto day and night PAH samples appear to be better separated in this angle of view. The non-PAH PAC from each group seems to be spread around and seem to show little correlation to the corresponding PAH.

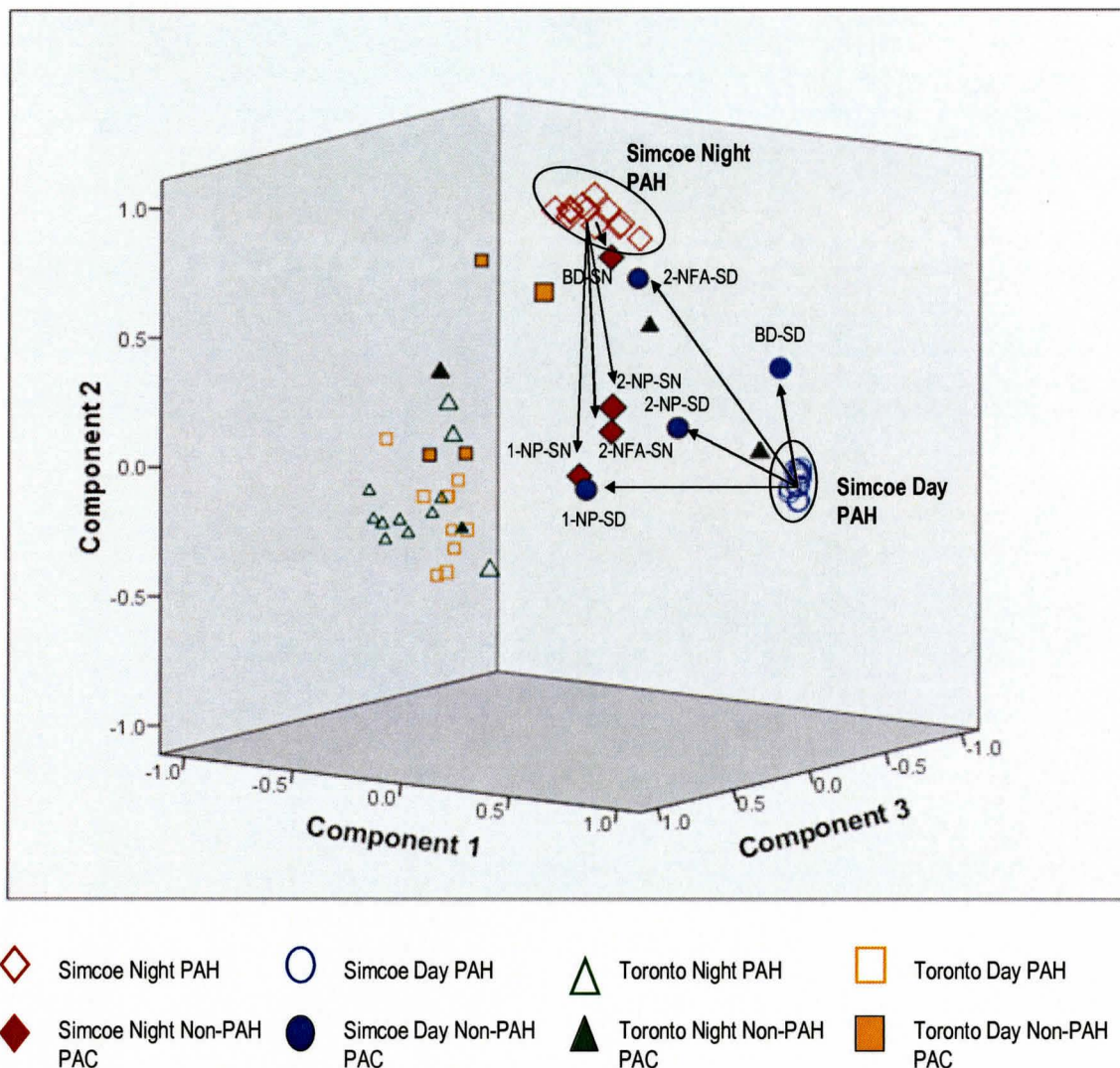
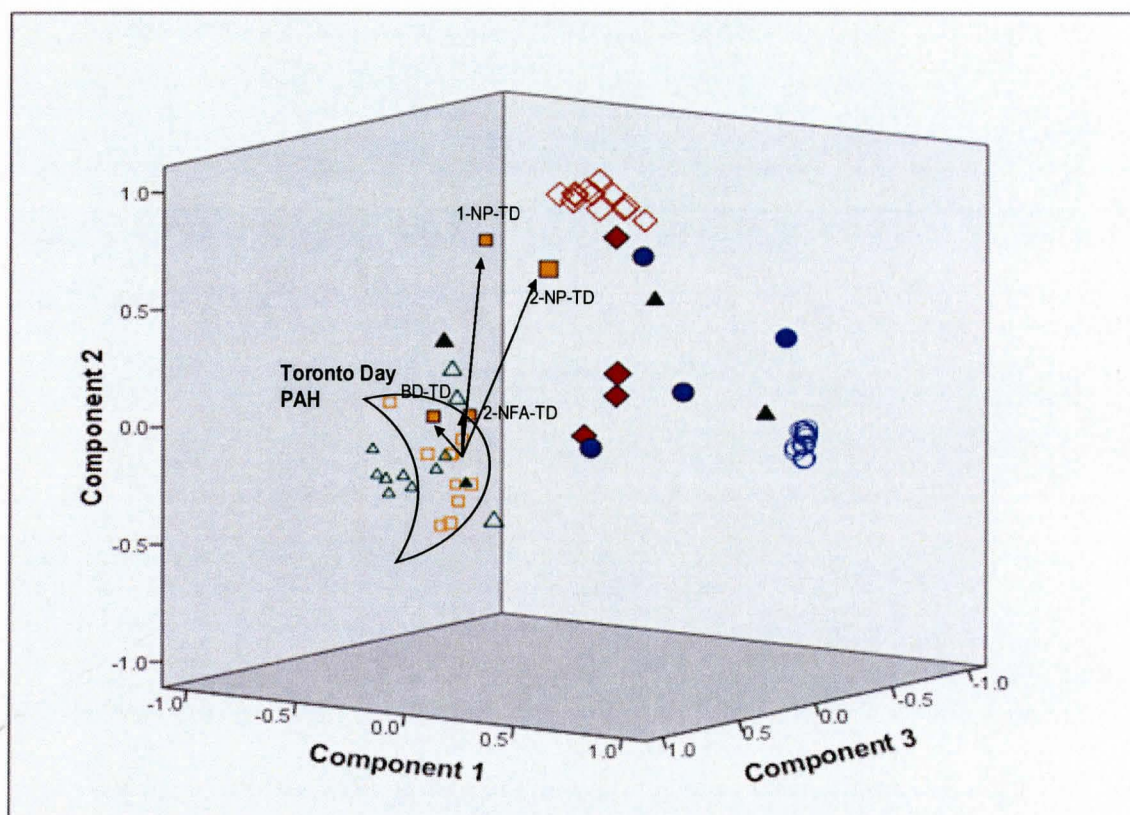


Figure 3-10(c) Principal components plot of data matrix from Toronto and Simcoe (components 1, 2 and 3) highlighting the distribution of the non-PAH with respect to the PAH cluster at Simcoe day and night.

Figure 3-10(c) shows the location of the 4 non-PAH PAC with respect to an arbitrary center of the PAH for Simcoe day and night. The three NPAH from each site are well removed from their PAH cluster. Though 1-NP is a source emission product it does not correlate with the PAH from each group which are all combustion emission

products. 2-NFA from each group also does not show any correlation to the corresponding PAH; 2-NFA is a major air transformation product and thus it is not surprising that it behaves differently from the PAH. The BD at Simcoe day is removed from the PAH cluster but the BD at Simcoe night is located close to the PAH. Since BD is produced from the oxidation of the parent PAH it is most likely that BD is oxidized more during the day than at night and thus BD levels at night correlate well with the PAH.



- | | | | |
|--|--|---|---|
|  Simcoe Night PAH |  Simcoe Day PAH |  Toronto Night PAH |  Toronto Day PAH |
|  Simcoe Night Non-PAH PAC |  Simcoe Day Non-PAH PAC |  Toronto Night Non-PAH PAC |  Toronto Day Non-PAH PAC |

Figure 3-10(d) Principal components plot of data matrix from Toronto and Simcoe (components 1, 2 and 3) highlighting the distribution of the non-PAH with respect to the PAH cluster at Toronto day.

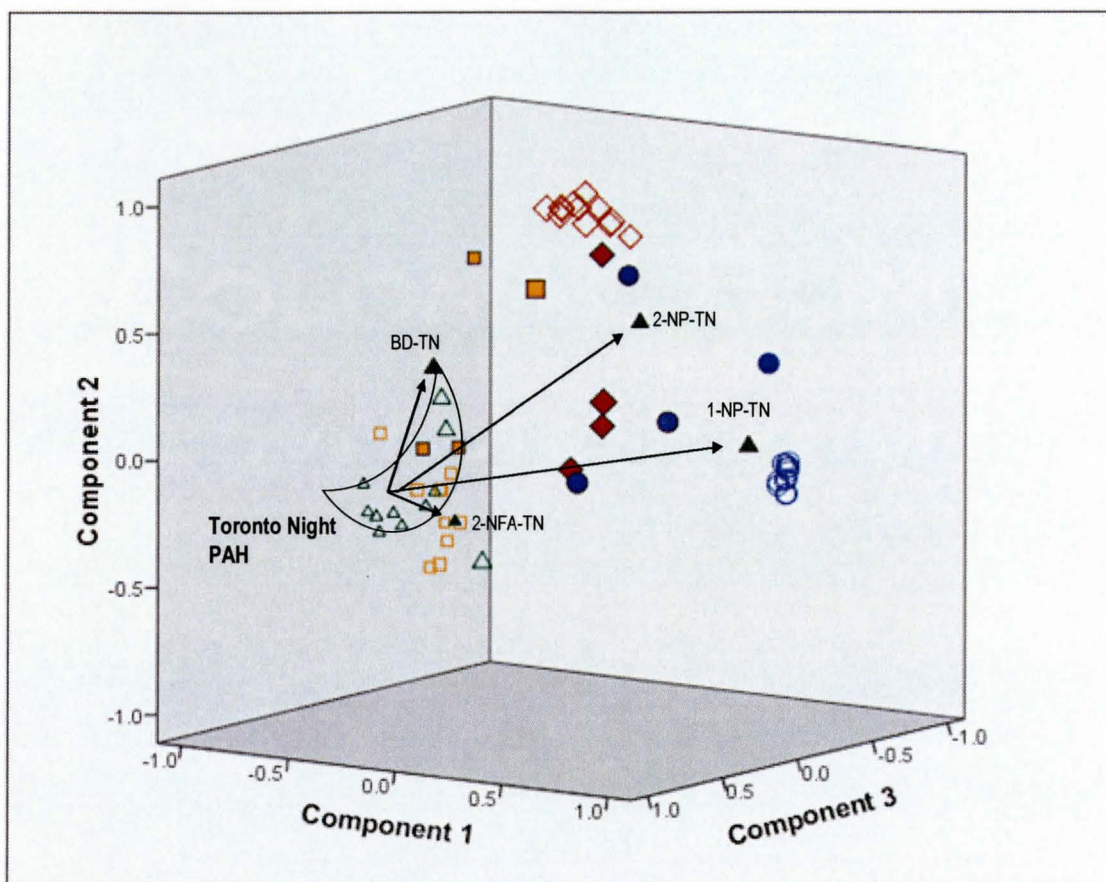


Figure 3-10(e) Principal components plot of data matrix from Toronto and Simcoe (components 1, 2 and 3) highlighting the distribution of the non-PAH with respect to the PAH cluster at Toronto night.

Figures 3-10(d) and 3-10(e) show the locations of the non-PAH PAC with respect to the PAH at Toronto day and night. Similar to the Simcoe samples, the 1-NP does not show any correlation with the PAH. The 2-NFA species from the Toronto samples appear to be modestly correlated with the PAH cluster. The BD at Toronto day and night samples seem to correlate well with the PAH cluster.

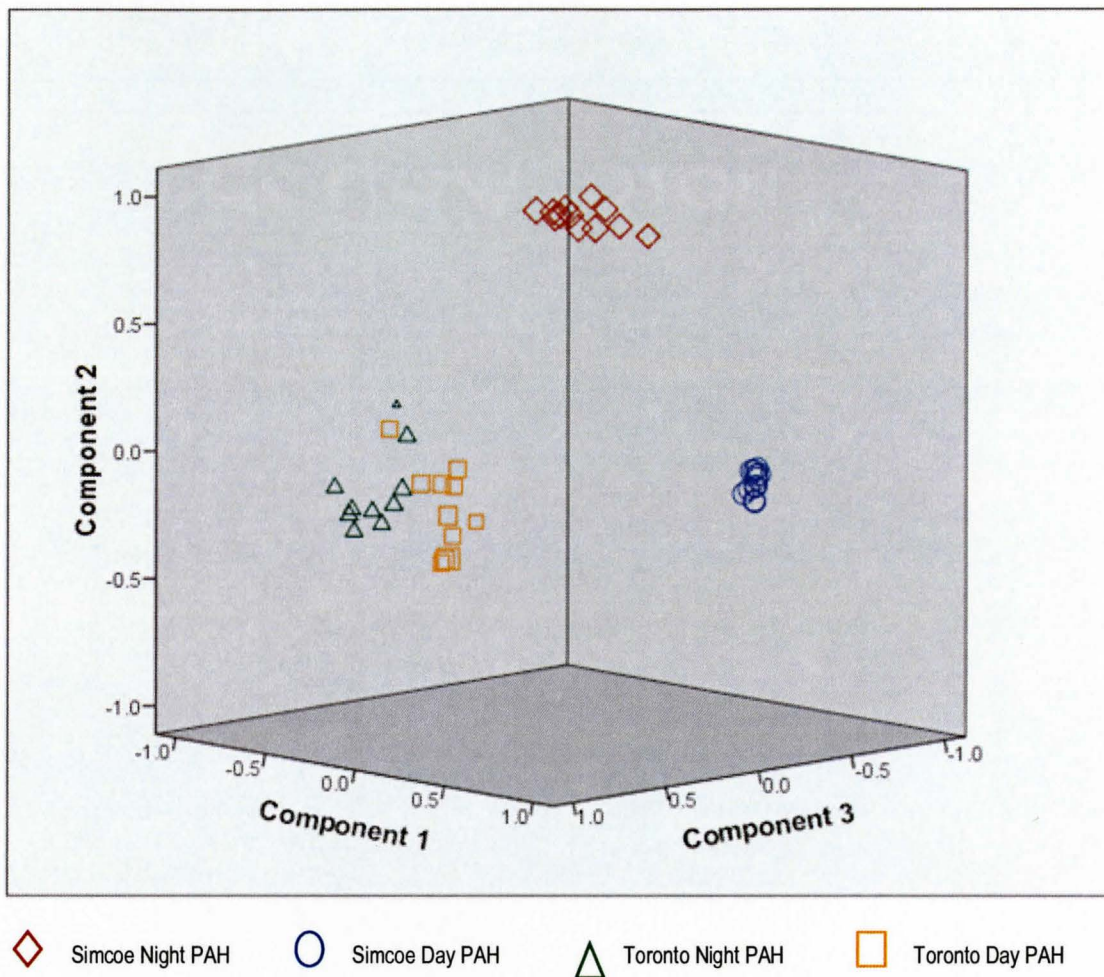


Figure 3-10(f) Principal components plot of only PAH data from Toronto and Simcoe (components 1, 2 and 3).

Figure 3-10(f) displays the 3D principal component plot of only the PAH data from the Toronto and Simcoe day and night samples. The plot shows the clear separation of the PAH from the day and night samples at Simcoe and Toronto. The rotated component matrix for the PAH data from the Toronto and Simcoe samples is shown in Table 3-6. The table shows the variance, as a fraction, that each component explains in the PAH data matrix from the 4 sampling groups. The suffix of each PAH label describes

the site (Simcoe/Toronto) and time (Day/Night) of collection. The results show that component 1 seems to correlate primarily with the PAH from the Simcoe day samples. Similarly component 2 seems to correlate with the Simcoe night PAH while components 3 and 4 are linked to the Toronto day and Toronto night PAH, respectively.

It is expected that the day-time transformation pattern of PAH would be different from that of the night-time transformation pattern. As was discussed in section 1.3, the day-time transformation of PAH is linked to OH radical pathway whereas any night-time transformation processes is linked to NO₃ radical pathway¹². Figure 3-10(f) also displays differences between the two sampling sites as the Simcoe samples collected during the same time period differ from that of the Toronto samples. This finding once again highlights the differences between an urban and rural site with respect to local emission sources and transformation.

Table 3-6. Rotated component matrix for the PAH data from the Toronto and Simcoe samples.

PAH	Component				
	1	2	3	4	5
BghiF-SD	0.953				
BghiF-SN		0.971			
BghiF-TD			0.501		
BghiF-TN			0.676		0.369
BcPh-SD	0.966				
BcPh-SN		0.906			
BcPh-TD				0.833	
BcPh-TN			0.864		
BaA-SD	0.958				
BaA-SN		0.858			
BaA-TD				0.821	
BaA-TN			0.933		
BbF-SD	0.977				
BbF-SN		0.931			
BbF-TD				0.859	
BbF-TN			0.885		
BkF-SD	0.975				
BkF-SN		0.954			
BkF-TD				0.886	
BkF-TN			0.945		
BjF-SD	0.977				
BjF-SN		0.939			
BjF-TD				0.830	
BjF-TN			0.944		
BeP-SD	0.975				
BeP-SN		0.915			
BeP-TD				0.810	
BeP-TN			0.905		
BaP-SD	0.961				
BaP-SN		0.952			
BaP-TD				0.755	
BaP-TN			0.621		0.224
Per-SD	0.972				
Per-SN		0.905			
Per-TD				0.754	
Per-TN			0.822		
IcdP-SD	0.975				
IcdP-SN		0.914			
IcdP-TD				0.706	
IcdP-TN			0.884		
Pic-SD	0.976				
Pic-SN		0.789			
Pic-TD				0.795	
Pic-TN			0.877		

Figure 3-11 displays the relative loadings values of the PAH5 composite along with that of 1-NP at Simcoe and Toronto during the sampling period. The loadings pattern at Simcoe indicates a lower loading average for the 1-NP compared to the PAH5 composite. This pattern seems to indicate that 1-NP is more transformed than PAH5 composite during most of the sampling period at Simcoe. Since 1-NP is a primary diesel exhaust product, it is likely that the 1-NP is highly transformed during long range transport to Simcoe from the various sources across the transcontinental border. Conversely, the transformation pattern at Toronto indicates that 1-NP at Toronto appears to be less transformed, most likely due to the constant input of 1-NP to the atmosphere from numerous local sources within Toronto.

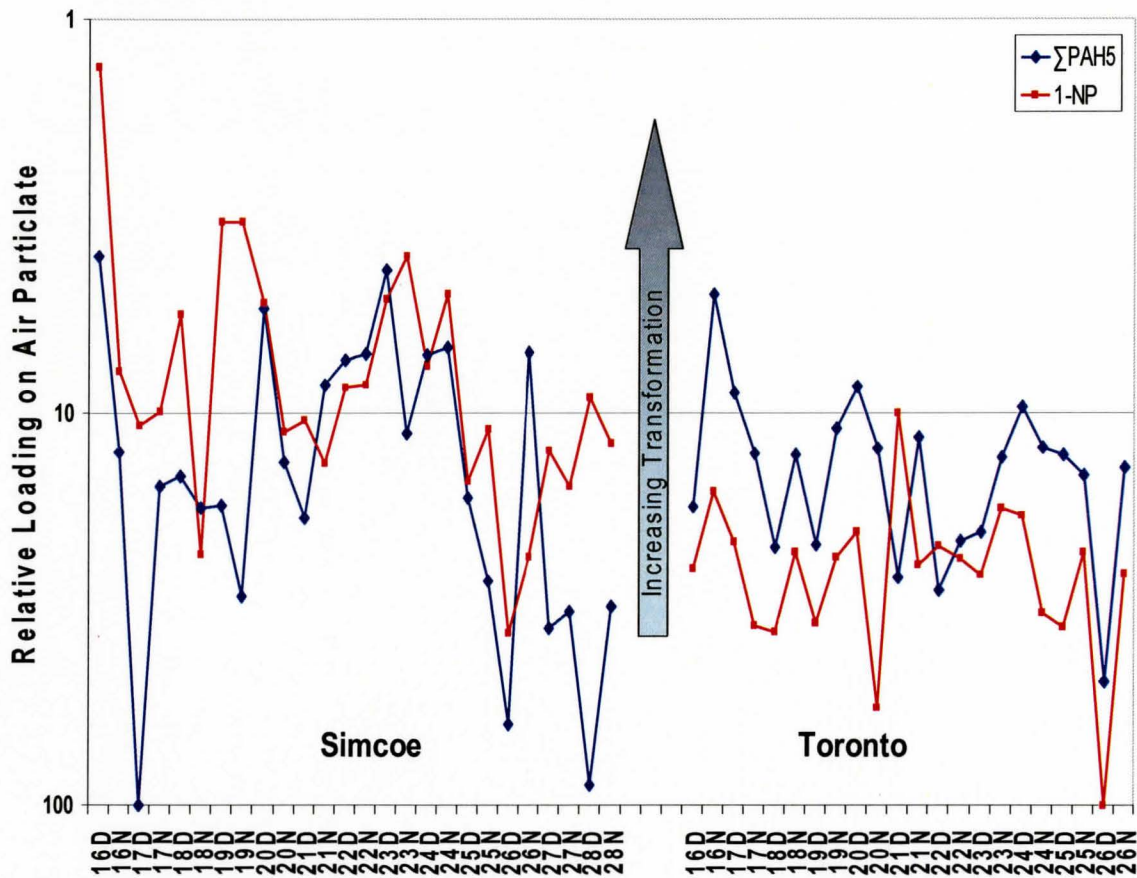


Figure 3-11. Relative loadings profile of 1-NP and PAH5 at Simcoe and Toronto during the sampling period.

3.3.2 Mean Relative Loadings of PAC at Toronto and Simcoe

Figure 3-12 displays the mean relative loading value of each target analyte in the Toronto Day (TD) and the Toronto Night (TN) samples. The mean relative loading values in the Toronto day samples are higher than those in the night samples. The three atmospheric transformation products (BD, 2-NP, and 2-NFA) are the only PAC where the night minus day value (green line) is positive, indicative of a net production. The higher mean relative loading values during the day seem to indicate that there is a significant input of PAH into the atmosphere during the day. Furthermore, the average relative loading profile of the Toronto day samples is flat which is indicative of a site that is located in close proximity to sources.

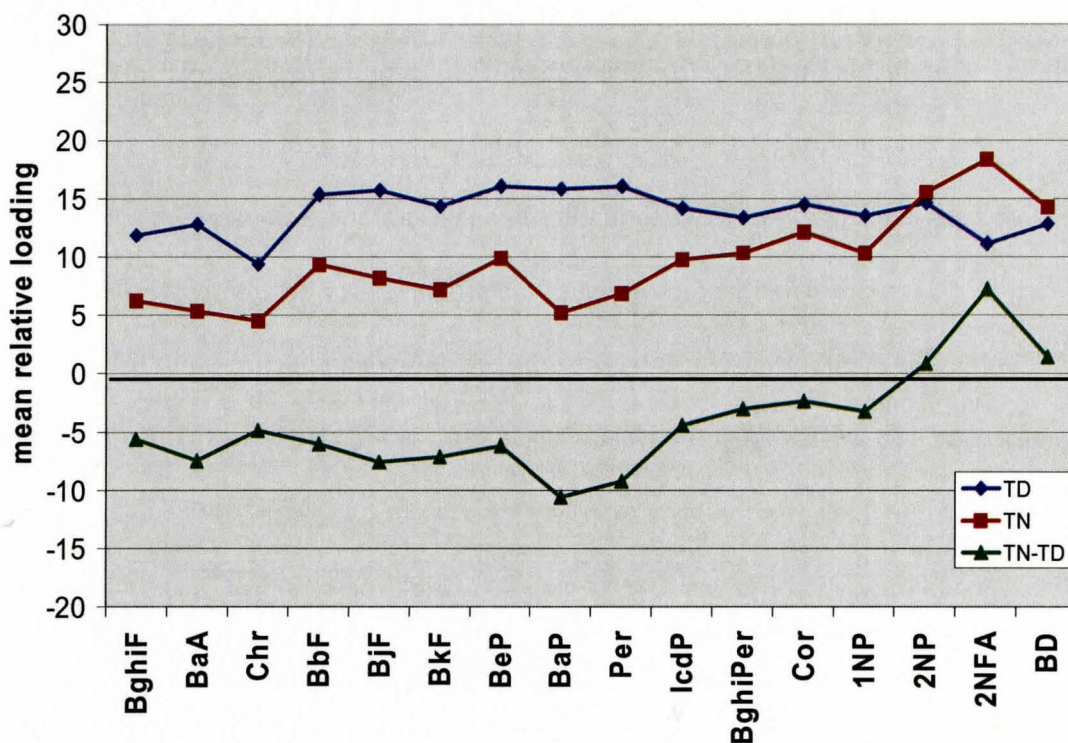


Figure 3-12. Mean relative loadings values of the PAC in the Toronto day (TD) and Toronto night (TN) samples, along with the differences in loadings (green line).

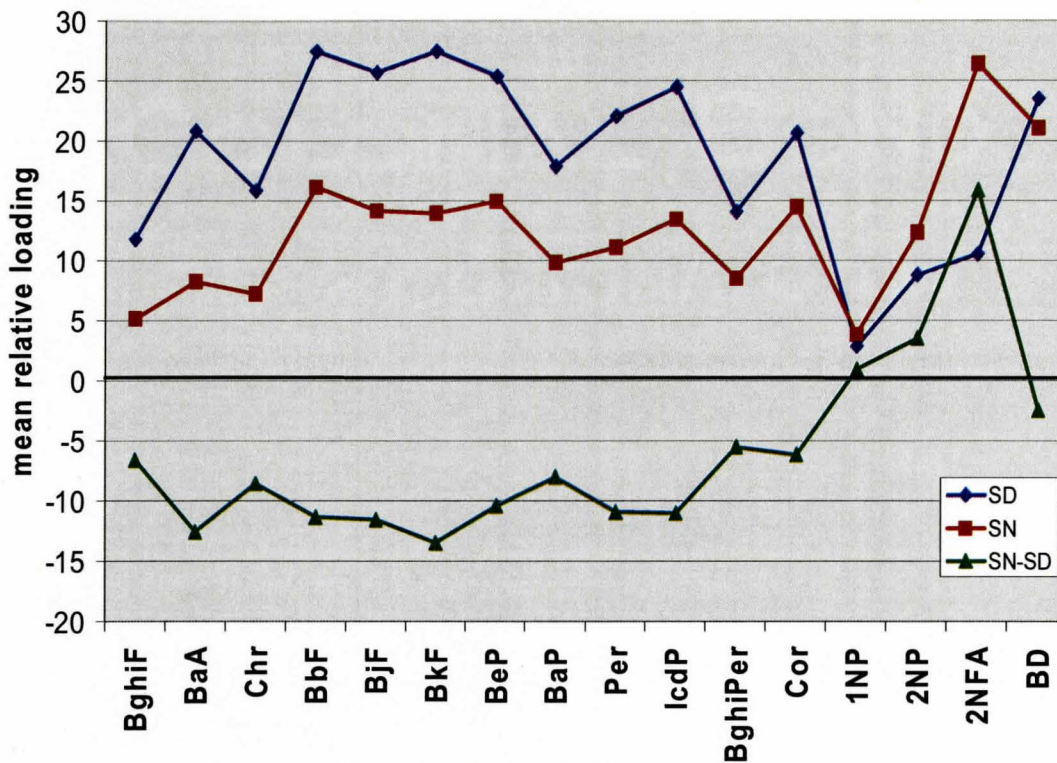


Figure 3-13. Mean relative loadings values of the PAC in the Simcoe day (SD) and Simcoe night (SN) samples along with the differences in loadings (green line).

Figure 3-13 displays the mean relative loading value of each target analyte in both the Simcoe Day (SD) and Simcoe Night (SN) samples. The Simcoe day samples appear to have higher mean relative loadings values compared to those of the Simcoe night samples, again with the exception of the atmospheric transformation products (2-NP and 2-NFA). Similar to the Toronto samples, there are higher average loading of PAH during the day at the Simcoe site than at night. Since it is believed that there are no major local sources of PAH at Simcoe, it is most likely that there is a constant replenishment of PAH carried in by the air mass moving across lake Erie from the U.S. to Simcoe during the

day-time. Interestingly, the 1-NP values show the lowest relative loadings of all analytes, consistent with net loss due to transformation.

Another interesting observation between the Toronto and Simcoe samples is that the profiles of the day/night differences at Simcoe and Toronto are nearly identical for the range of analytes (Figure 3-14). At both sites, the atmospheric transformation products (BD, 2-NP and 2-NFA) have positive mean relative loadings differences compared to the PAH which display negative differences.

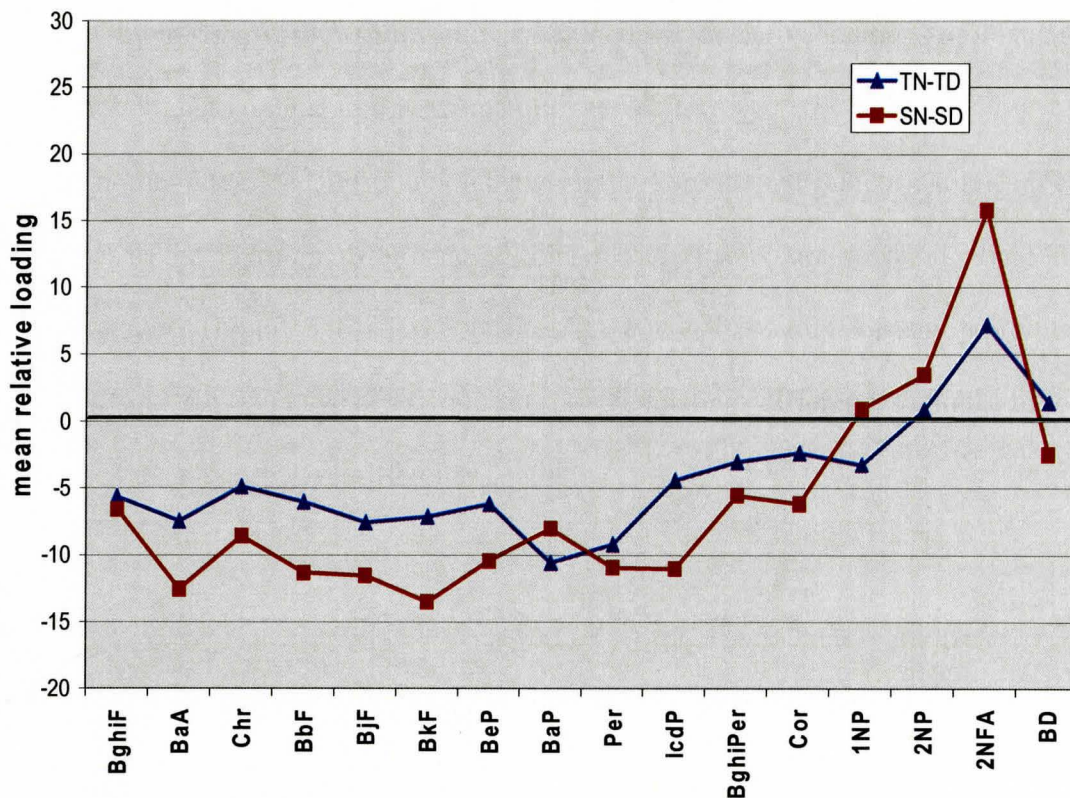


Figure 3-14. Day and night difference in the relative loadings values of the PAC at Toronto and Simcoe.

In summary, the polycyclic aromatic compound (PAC) data from Toronto and Simcoe collected during the day and night time enabled comparison of the transformation pattern of an urban site to a rural site as well as to explore differences in day-time and night-time chemistry. The elemental carbon data was used to convert concentration values of each PAC to loadings values, thereby removing the dispersion effect. Analysis of loadings values gives a more accurate representation of transformation since loadings values are only affected by transformation and not by dispersion. Comparison of loadings data during the sampling period showed that 5 PAH (BjF, BkF, BbF, BeP and BghiP) behaved in a very similar manner. The relative loadings plot of the PAH5 composite at Simcoe and Toronto during the sampling period clearly showed a diurnal pattern indicative of atmospheric transformation.

In order to further examine the diurnal differences in transformation, a principal component analysis was performed on the PAC data. The resulting plots showed that PAH collected from Toronto and Simcoe were grouped on different regions of the plot. The plots also showed that the PAH collected during the day and night at each site were also located in different regions of the plot. The principal component analysis further highlighted the differences in transformation in PAH collected at an urban site (Toronto) and rural site (Simcoe) and differences in day-time and night-time chemistry.

3.4 Loadings of Polycyclic Aromatic Carbons on Air Particulate at Slocan, Langley and Sumas Sites.

The concentration data for a set of polycyclic aromatic compounds (PAC) from the Slocan, Langley and Sumas sites were also available as day and night samples as part of the Pacific 2001 study. The concentration values were converted to loadings values with the use of elemental carbon data from Dr. J. Brook (Environment Canada) for all samples at Slocan, Langley and Sumas. Similar to the Toronto/Simcoe data set, loadings values were converted to relative loadings values which allowed for the direct comparison of species at all sites using a single scale (Section 3-3).

Similar to the Toronto/Simcoe data, the Pacific 2001 data showed that the same set of five PAH had very similar loadings patterns. The 'PAH5' composite is the mean relative loading value of B_jF, B_kF, B_bF, BeP, and B_{ghi}P. Figure 3-15 shows the ratio of the relative loadings of each of these individual PAH to the PAH5 composite at the three main sites in the Pacific 2001 study. In almost all cases the ratio is very close to 1 showing the similarity in the relative loadings as well as transformation pattern among these five PAH.

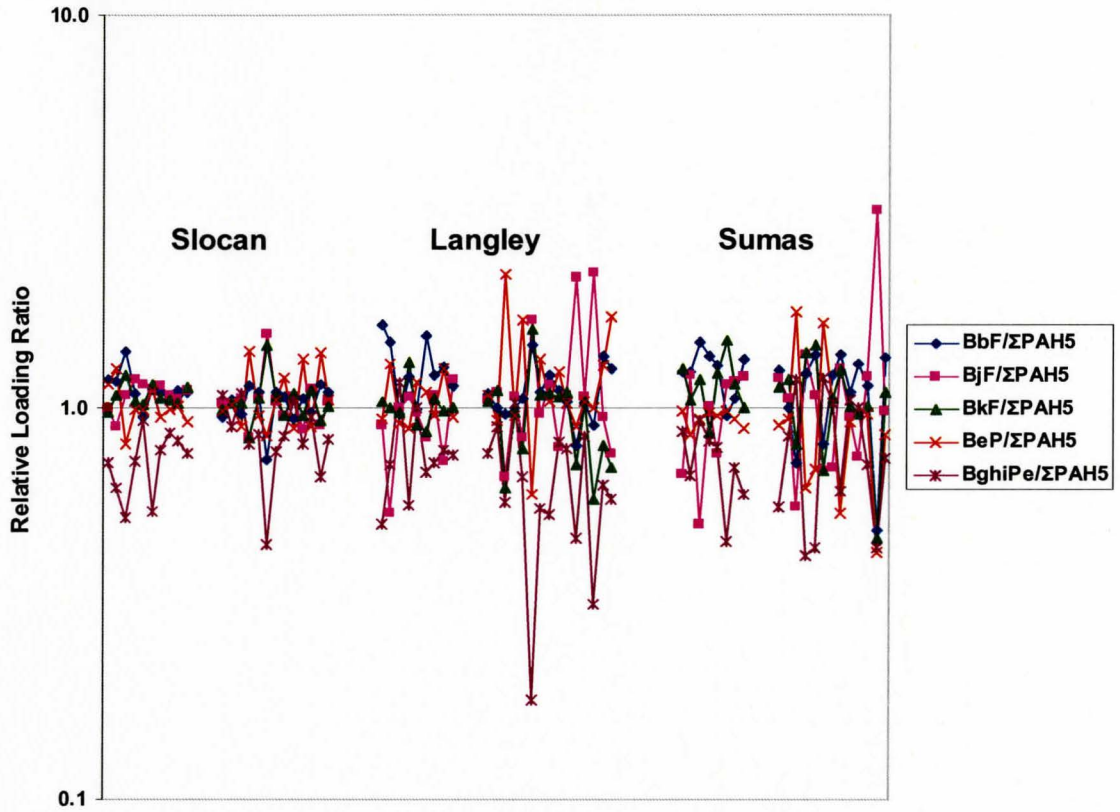


Figure 3-15. Relative loading ratio of BbF, BkF, BjF, BeP & BghiP to PAH5 composite at Slocan, Langley and Sumas.

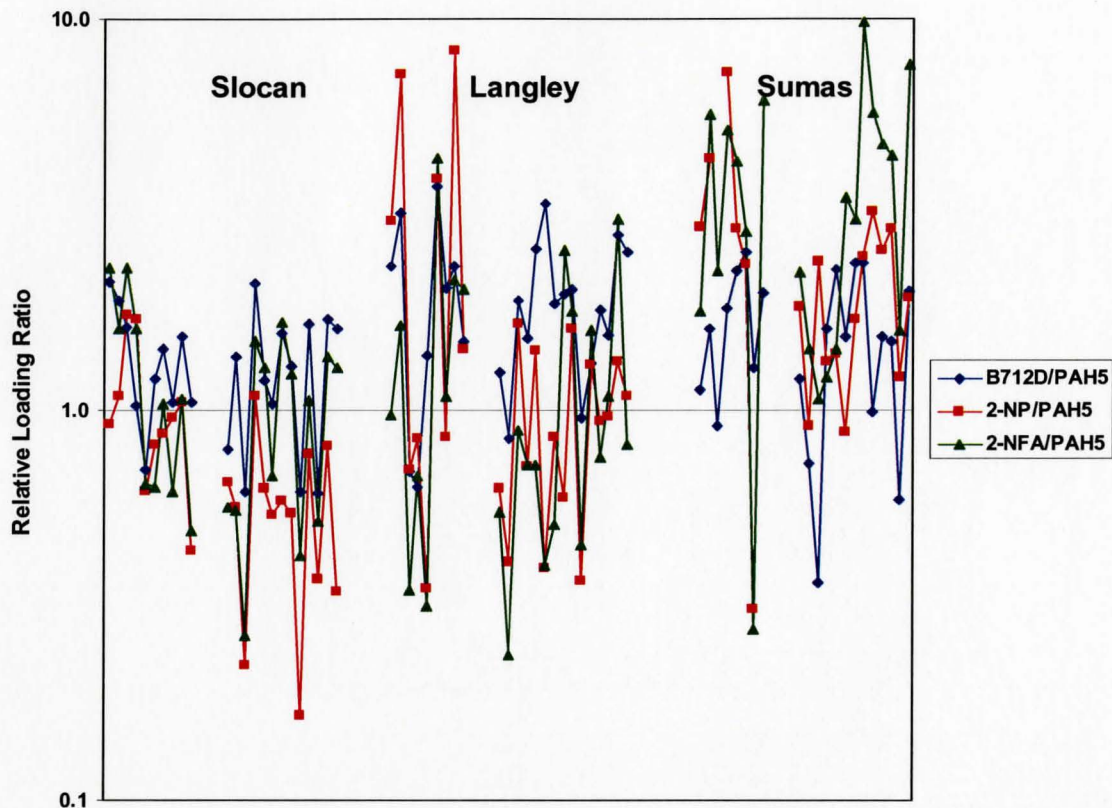


Figure 3-16. Relative loading ratio of BD, 2-NP and 2-NFA to the PAH5 composite at Slocan, Langley and Sumas.

The relative loadings ratios of BD, 2-NP and 2-NFA to the PAH5 composite showed large deviations (Figure 3-16). Similar to the case at Toronto/Simcoe, the relative loadings profile and thus the transformation profile of these three atmospherically transformed products tend to be rather different from that of the PAH5 composite. The PAH that make up the PAH5 composite are all combustion emission products.

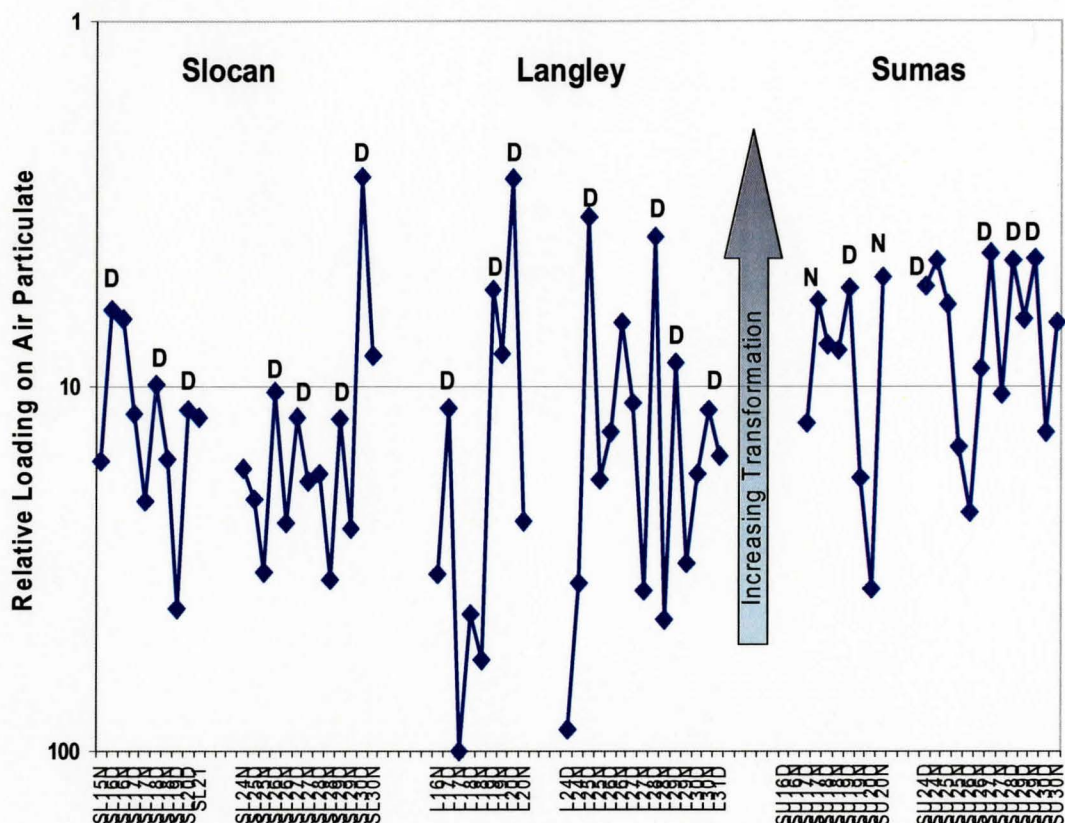


Figure 3-17. The transformation pattern of the PAH5 composite based on relative loadings data at Slocan, Langley and Sumas. 'D' indicates day samples where as 'N' indicated night samples.

The transformation pattern of the PAH5 composite values at the Slocan, Langley and Sumas sites is displayed in Figure 3-17. An important observation from this figure is the clear diurnal pattern. At all three sites there is clearly an increase in the level of transformation (lower relative loading) of the PAH5 composite during the day-time. The difference is most prominent in the Langley samples and is less so at Slocan and Sumas.

3.4.1 Principal Components Analysis of PAC Data from Slocan, Langley and Sumas

The difference in the relative loadings and thus the level of transformation between the day and night samples was examined using principal components analysis. A complete data set comprising of 14 PAC and 11 sampling days was introduced for principal component analysis. Of the 14 PAC, 10 were PAH which included BghiF, BaA, BbF, BkF, BjF, BeP, BaP, Per, IcdP, and BghiP. The remaining 4 compounds were three NPAH (1-NP, 2-NP, 2-NFA) and BD which is the oxidized product of BaA. The data set was comprised of the relative particulate loadings values for each variable. In this case the variables were the species of interest (PAC) which were coded according to sampling time (day/night) as well as site (Slocan/Langley/Sumas).

The outcome of the PCA for the aforementioned data matrix yielded 5 principal components that accounted for 100% of the observed variance among the variables. A set of plots of the first 3 components which accounts for 86% of the variance is shown in Figures 3-19(a) to 3-19(d). In these plots each marker represents a given polycyclic aromatic compound from 11 samples collected at each site in the Pacific 2001 study. The open symbols are PAH; closed symbols are NPAH and BD.

Table3-7. The 5 principal components for the Slocan, Langley and Sumas data set along with the percentage variance.

Component	% of Variance	Cumulative %
1	40.1	40.1
2	24.3	64.4
3	21.1	85.5
4	8.9	94.4
5	5.6	100.0

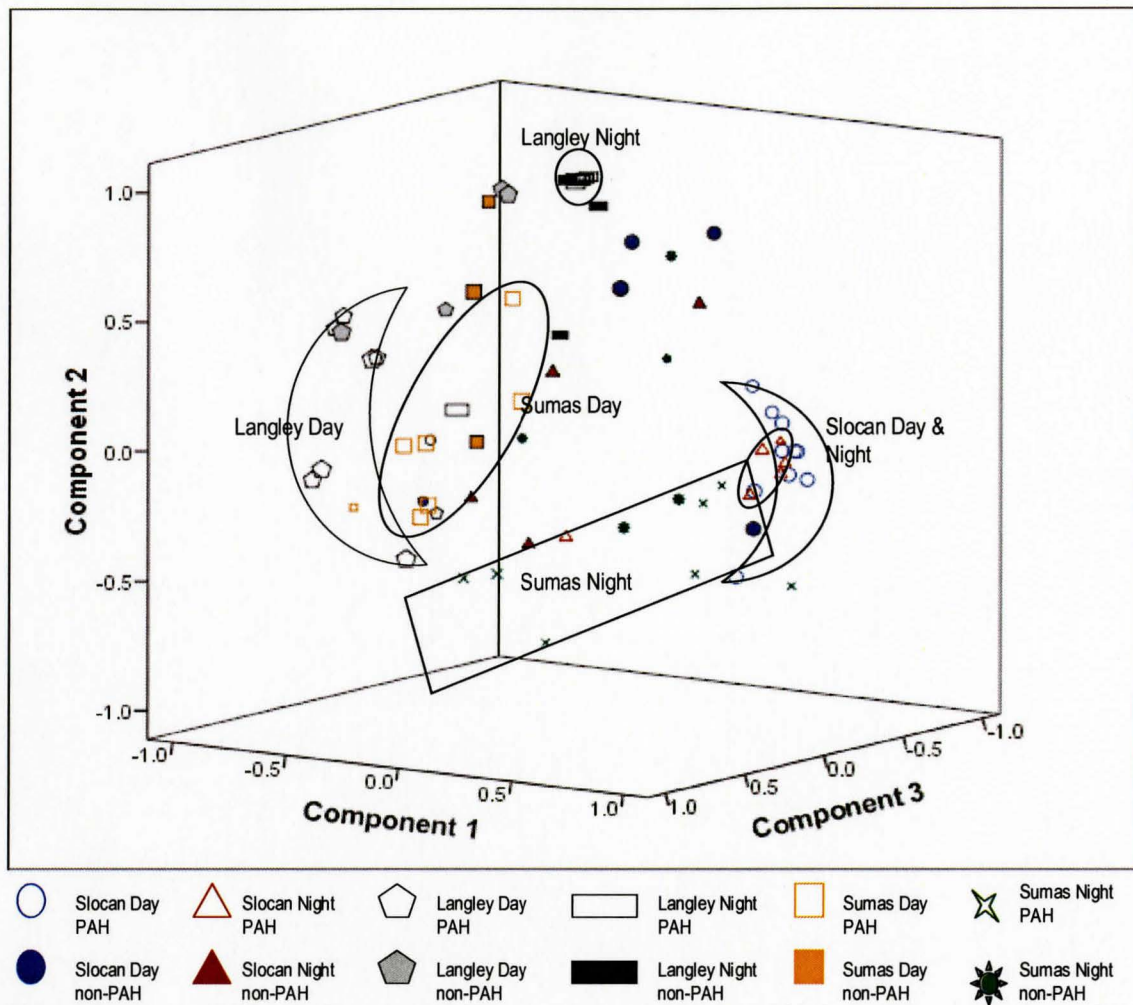


Figure 3-18(a) Principal components plot of the data matrix from the Slochan, Langley and Sumas sites (Components 1, 2, and 3).

Figure 3-18(a) shows the separation of the PAC along components 1, 2 and 3. The day and night PAH data from Langley and Sumas are well separated from each other. The Slochan day and night PAH samples are closely clustered but are separated, less so than the other groups. The non-PAH data from each sampling group appear to be spread around the plot.

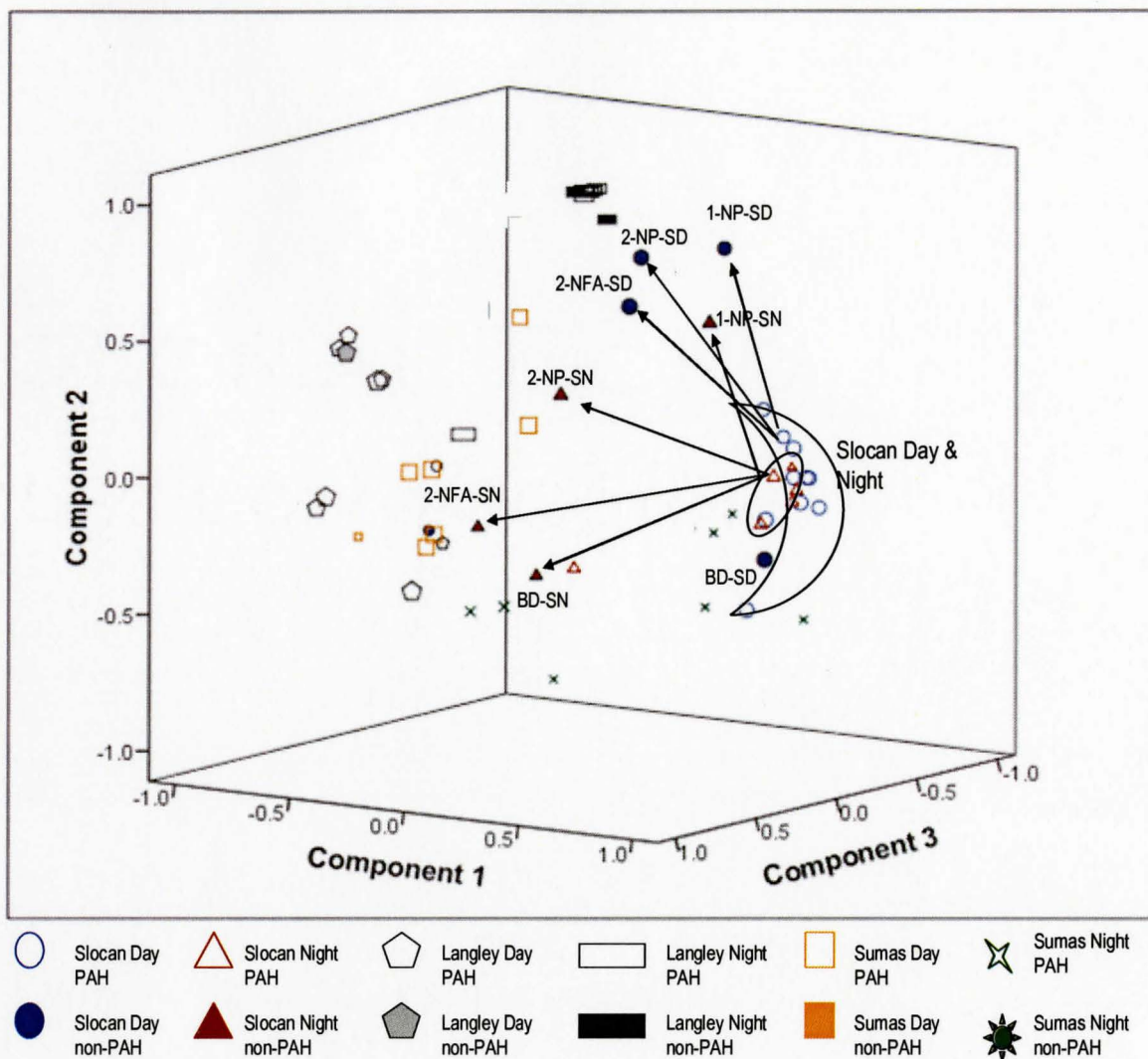


Figure 3-18(b) Principal components plot of the data matrix from the Slokan, Langley and Sumas sites (Components 1, 2, and 3) highlighting the distribution of the non-PAH with respect to the PAH cluster at Slokan day and night.

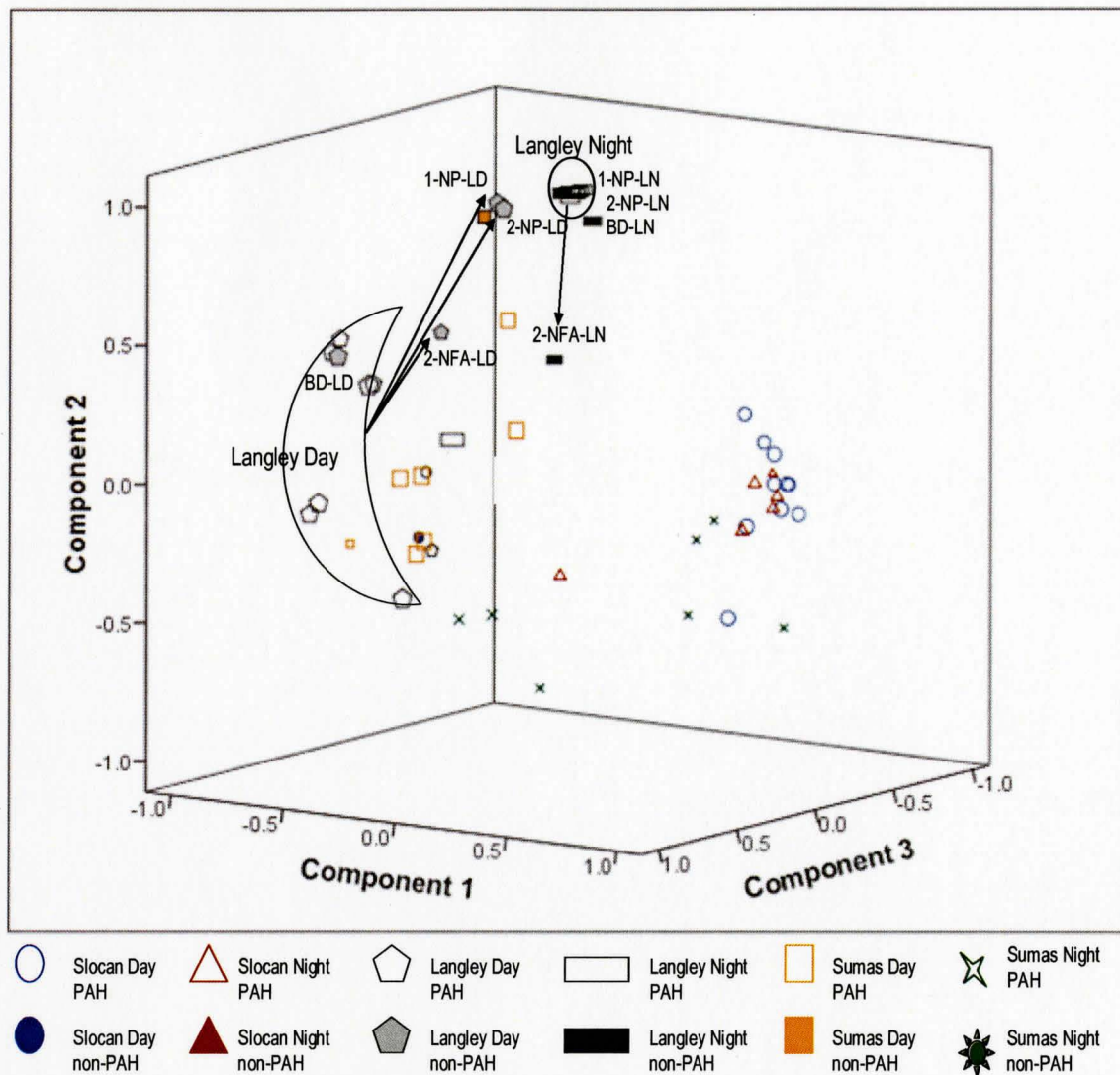


Figure 3-18(c) Principal components plot of the data matrix from the Slocan, Langley and Sumas sites (Components 1, 2, and 3) highlighting the distribution of the non-PAH with respect to the PAH cluster at Langley day and night.

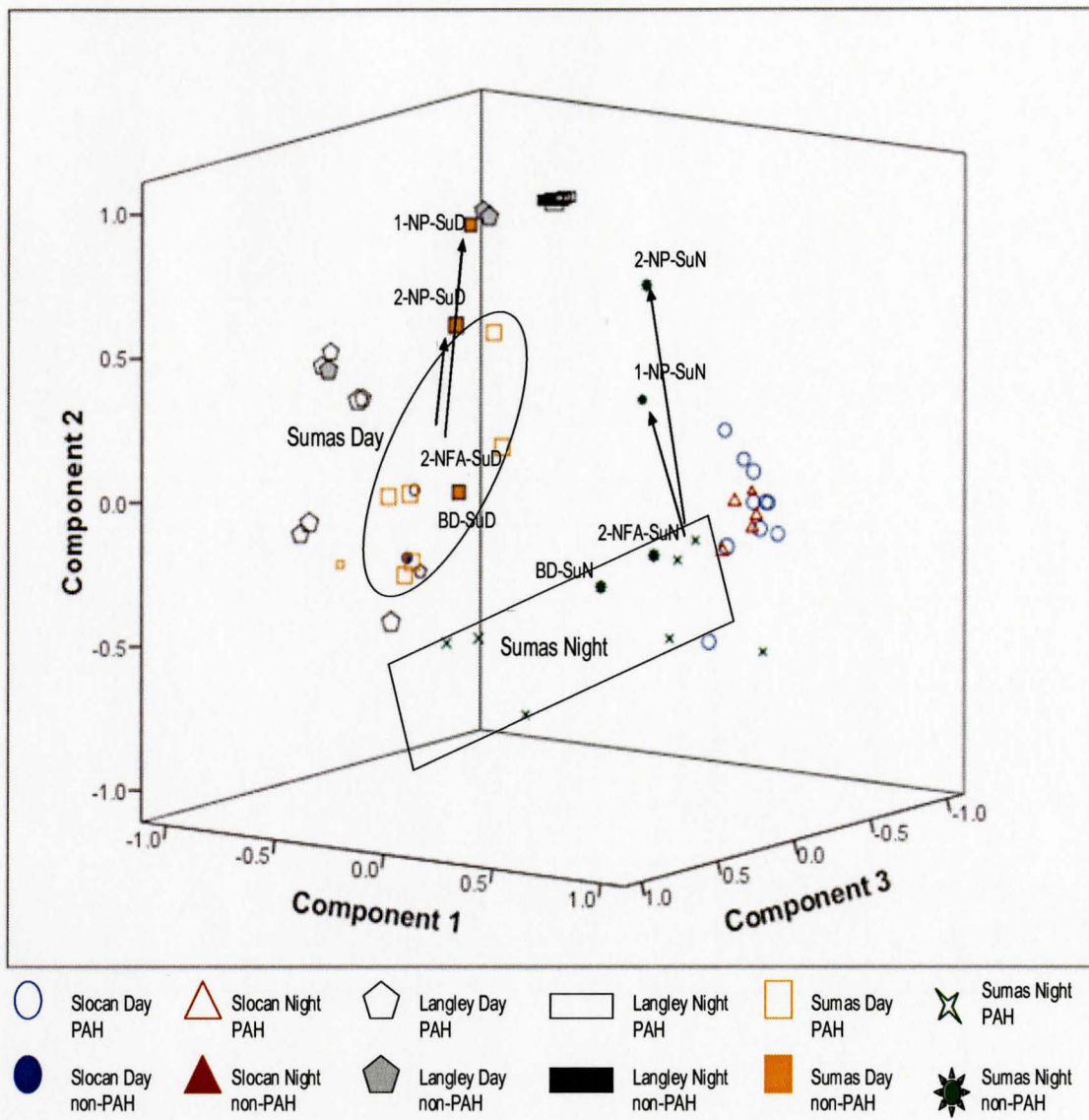


Figure 3-18(d) Principal components plot of the data matrix from the Slochan, Langley and Sumas sites (Components 1, 2, and 3) highlighting the distribution of the non-PAH with respect to the PAH cluster at Sumas day and night.

Figures 3-18(b)-(d) shows the relationship between the non-PAH PAC and the corresponding PAH from each sampling group. The BD is closely correlated with the corresponding PAH cluster with the exception of the Slocan night samples. The 1-nitropyrene (1-NP) data shows little correlation with the PAH cluster except for the Langley night samples. Though 1-NP is a source emission product it does not seem to show any correlation to PAH which are also source emission products. It appears that with the exception of the day and night samples at Sumas, the 2-nitrofluoranthene (2-NFA) of each sampling group are located well outside the corresponding PAH cluster. 2-NFA is a major atmospheric transformation product and displays a transformation profile different from the PAH.

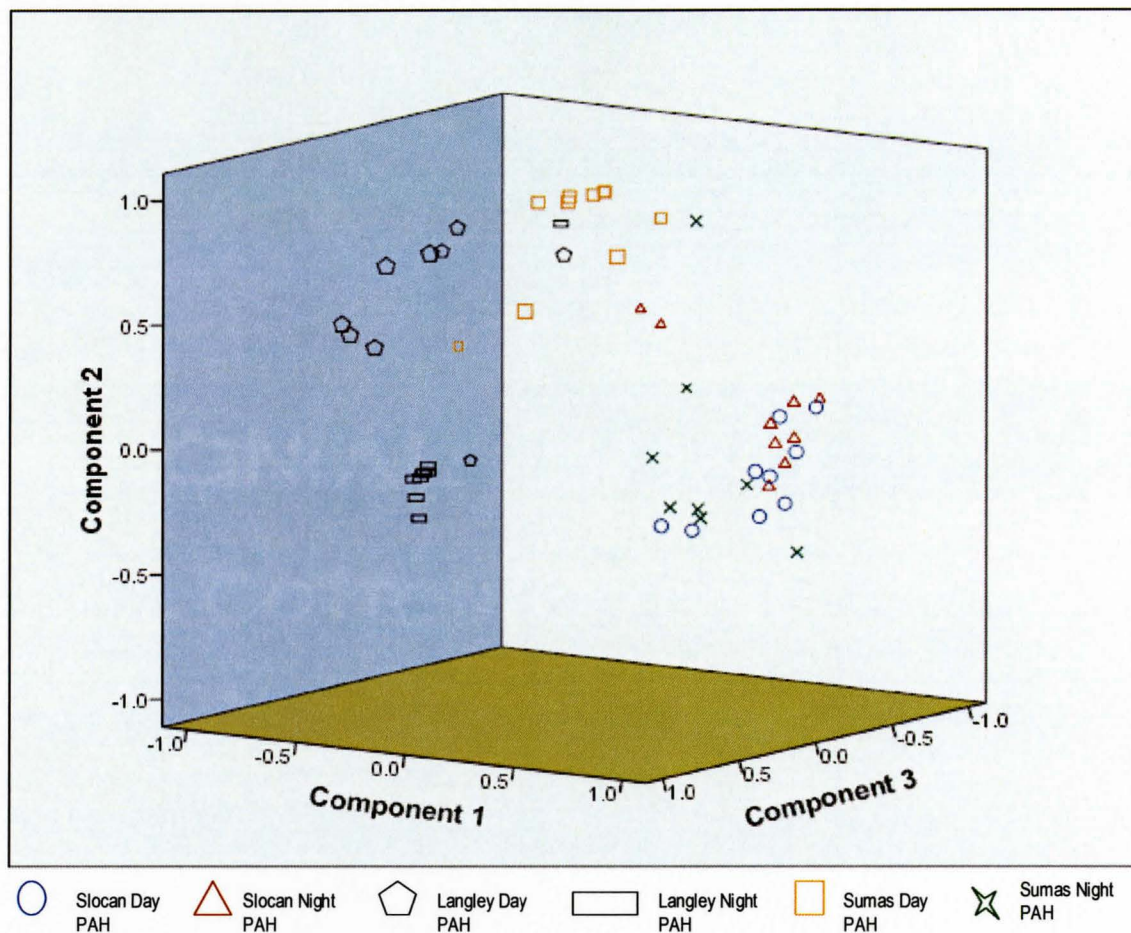


Figure 3-19 Principal components plot of the PAH data from the Slocan, Langley and Sumas sites (Components 1, 2, and 3).

Figure 3-19 shows the three dimensional plot (components 1, 2 and 3) of only the PAH data from the Pacific 2001 samples. It is easy to see the separation of the PAH from the Langley day and night samples as well as from the Sumas day and night samples. The Slocan day and night samples appear to be somewhat overlapped. The rotated component matrix for the PAH data from the Pacific 2001 samples is shown in Table 3-8. The table shows the variance as a fraction that each component accounts for in the PAH data matrix from the 6 sampling groups. The suffix of each PAH label describes the site

(Slocan/Langley/Sumas) and time (Day/Night) of collection. It can be seen that component 1 seems to correlate primarily with the PAH from Slocan day and night samples. These PAH are closely clustered in the principal components plot (Figure 3-19). The Langley day and night samples seem to correlate with components 1 and 2, respectively. The variance of the Sumas day and night samples are explained in most part by components 3 and 4. As a result the day and night PAH from Langley and Slocan are separated in the principal components plot (Figure 3-19).

Table 3-8. Rotated components matrix for the PAH from Pacific 2001 samples.

PAH	Component				
	1	2	3	4	5
BghiF-LD	-0.772				
BghiF-LN		0.988			
BghiF-SuD			0.959		
BghiF-SuN				0.622	
BghiF-SID	0.844				
BghiF-SIN	0.861				
BaA-LD	-0.696				
BaA-LN		0.979			
BaA-SuD			0.965		
BaA-SuN				0.681	
BaA-SID	0.923				
BaA-SIN	0.898				
Chr-LD			0.683		
Chr-LN			0.886		
Chr-SuD			0.938		
Chr-SuN	0.646				
Chr-SID	0.927				
Chr-SIN			0		0.776
BbF-LD	-0.776	0.406	0.414		
BbF-LN		0.993			
BbF-SuD			0.948		
BbF-SuN				0.889	
BbF-SID	0.913				
BbF-SIN	0.950				
BjF-LD	-0.779	-0.400			
BjF-LN		0.997			
BjF-SuD	-0.821				
BjF-SuN				0.824	
BjF-SID	0.633				
BjF-SIN	0.980				
BkF-LD	-0.643				0.602
BkF-LN		0.997			
BkF-SuD			0.970		
BkF-SuN				0.848	
BkF-SID	0.703				
BkF-SIN	0.990				
BeP-LD	-0.578		0.778		
BeP-LN		0.989			
BePSuD			0.781		
BeP-SuN			0.859		
BeP-SID	0.986				
BeP-SIN	0.958				

In comparing the PCA plots of the two studies several similarities can be observed between the data and the transformation patterns of the Toronto/Simcoe samples and the Pacific 2001 samples. In both cases, the sites located closest to the emission sources (Toronto and Slocan) showed smaller differences between the day and night samples. This is most likely due to the constant input of PAH to the atmosphere that impacts the samples collected from these sites. As the air mass moves away from the source towards the rural areas (Langley/Sumas or Simcoe) there are clear differences in the patterns between the day and night samples.

3.4.2 Mean Relative Loadings of PAC at Slocan, Langley and Sumas Sites.

Figure 3-20 displays the mean relative loading values of the PAC from the Langley Day (LaD) and Langley Night (LaN) samples. Contrary to the Toronto and Simcoe samples, the Langley night samples appear to be less transformed (higher loadings) than the Langley day samples. It is likely that the day samples are photochemically transformed or degraded thus yielding lower loadings values compared to the night samples.

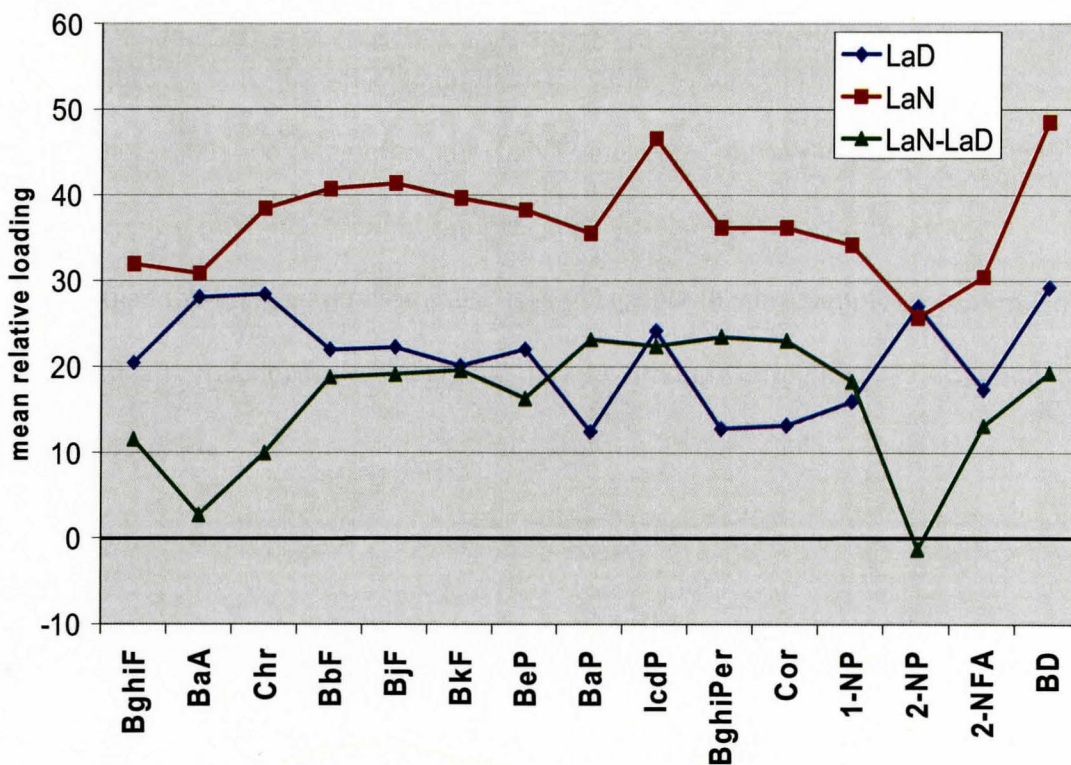


Figure 3-20. Mean relative loadings values of the PAC in the Langley Day (LD) and Langley Night (LN) samples along with the differences in loadings (green line).

Similar trend is observed with the day and night samples collected from the Slocan site (Figure 3-21). Both sites are classified as Urban/Suburban and seem to display transformation profiles that are very similar to one another (Figure 3-23).

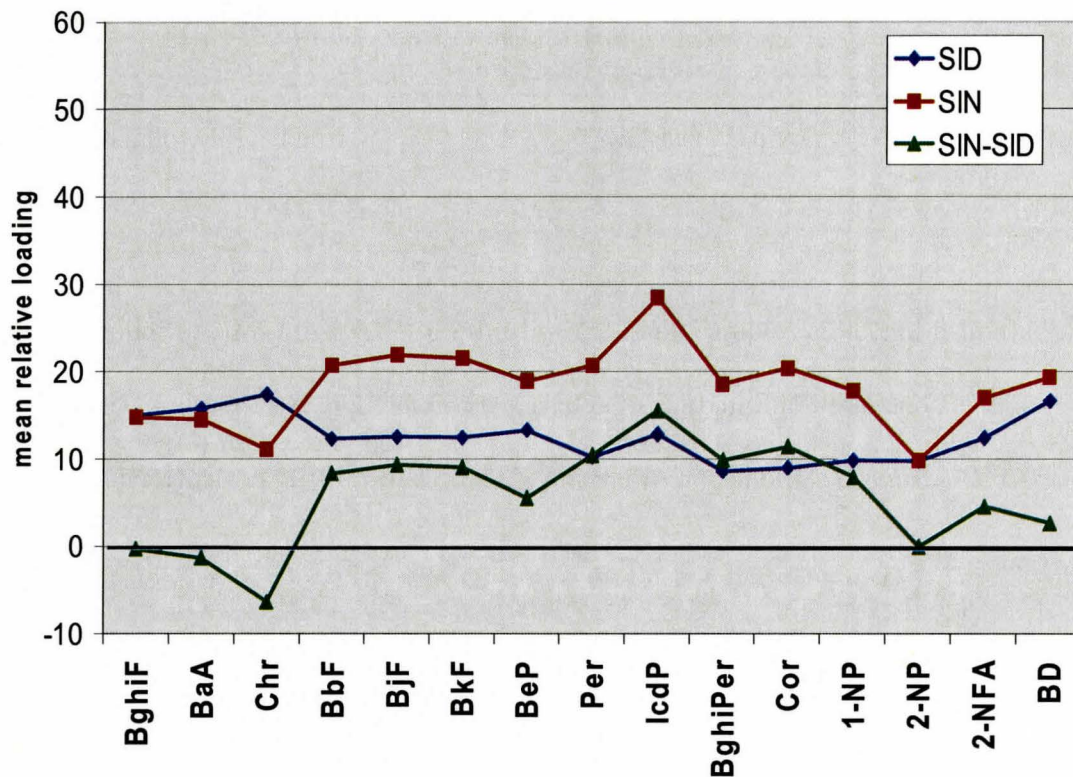


Figure 3-21. Mean relative loading value of the PAC in the Slocan Day (SID) and Slocan Night (SIN) samples along with the differences in loadings (green line).

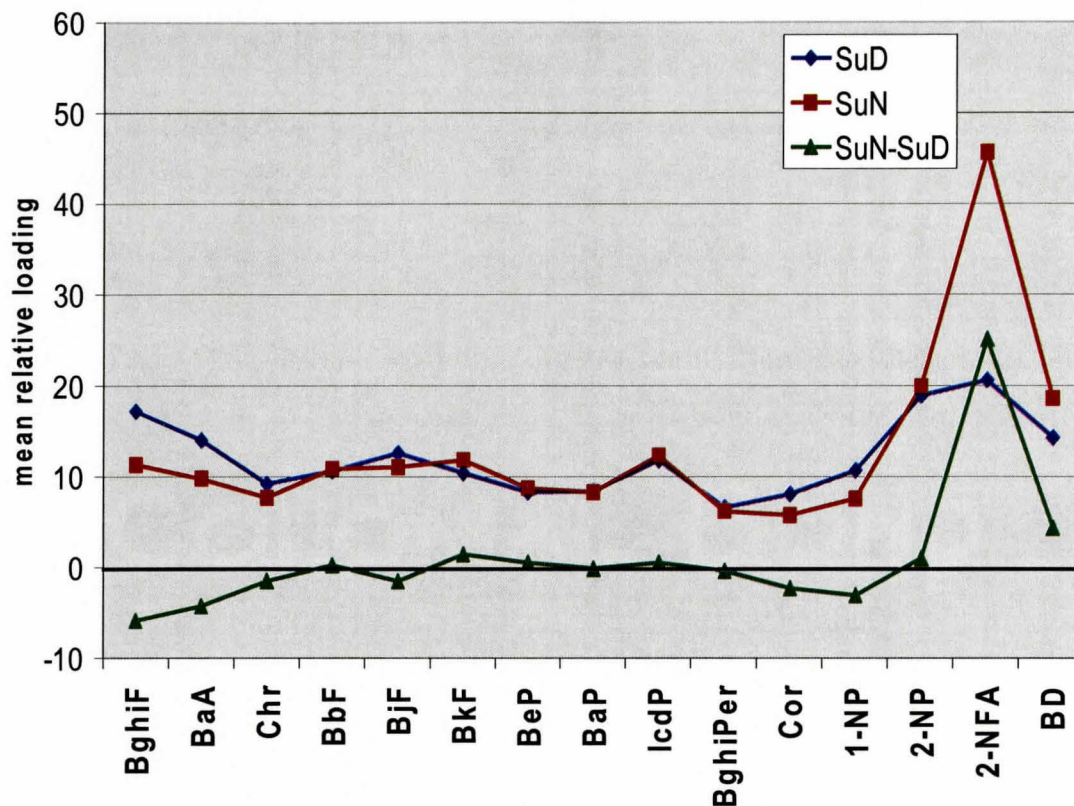


Figure 3-22. Mean relative loading value of the PAC in the Sumas Day (SuD) and Sumas Night (SuN) samples along with the differences in loadings (green line).

The mean relative loadings values from the Sumas site yield a very different profile compared to that from Slocan and Langley. The Sumas profile is similar to the profiles observed at Simcoe and Toronto. Sumas is a rural site located downwind of both Slocan and Langley. It is expected that the PAC emitted from local sources at Slocan and Langley will be transformed or degraded during transport to the Sumas site. The mean relative loadings values for the day and night samples at Sumas are nearly identical and are much lower than those at Slocan and Langley. Furthermore, there is a sharp increase in the level of 2-NFA in the night samples at Sumas. 2-NFA is an atmospheric

transformation product. The relative amounts of 2-NFA increase on going from Slocan to Langley to Sumas (Figure 3-23).

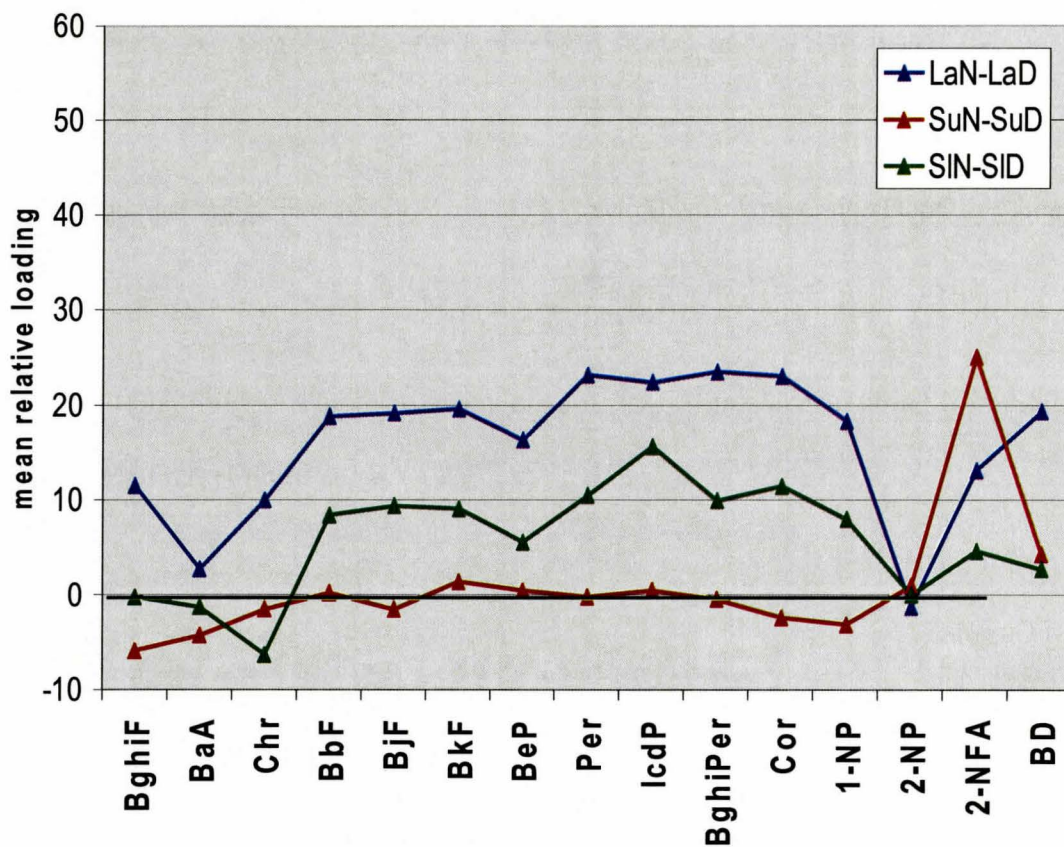


Figure 3-23. Day and night difference in the relative loadings values of the PAC at Langley, Slocan and Sumas.

The PAH from day and night samples from the Pacific 2001 study showed that the transformation profiles during the day and at night are different. The air mass moving onto the Slocan site comes from the west (Pacific Ocean) and this air mass is believed to contain minimal amount of pollutants. Therefore the PAH profile at Slocan is thought to represent the profile of an urban source. This fact is highlighted by the close association of the PAH from the day and night samples at Slocan in the principal components plot (Figure 3-19).

The day and night samples from Langley and Sumas show clear differences in the PAH profiles during the day and night presumably due to atmospheric transformation. It is known that as an air mass is transported over a long distance it is affected by both day-time and night-time chemistries. Sumas is a rural site located downwind of both Slocan and Langley. It is expected that the PAC emitted from local sources at Slocan and Langley will be transformed or degraded during transport to the Sumas site. As a result the Sumas samples exhibited clear differences in PAH profiles compared to Slocan and Langley (Figure 3-23).

4.0 CONCLUSIONS

The profiles of PAH and NPAH were compared in three separate studies involving air samples collected in urban and rural locations across Canada; two of the studies involved day/night sampling. In the Freelton/Pier 25 study performed in the Hamilton, Ontario area the NPAH levels at Pier 25 (urban site) were found to be similar to those at Freelton (rural site) except for the Pier 25 samples collected with impacts from the industrial core of Hamilton. These results were consistent with the PAH data determined by Somers which showed significantly increased levels of PAH at the Pier 25 site compared to the Freelton site under the same conditions²⁸. Since some NPAH are highly mutagenic and carcinogenic compounds that act via reductive metabolism and can be readily metabolized to potent reactive intermediates with all cells, NPAH were considered to be good candidates as agents for mutation induction due to exposures to ambient air. The most potent NPAH are known to be associated primarily with air particulate.

A number of new NPAH standards were prepared to expand the list of existing standards; of these 6 NAPH were detected and quantified in almost all of the samples analyzed. By including these 6 NAPH in the total NPAH levels, a more accurate representation of the total NPAH levels at Pier 25 and Freelton was provided. The newly synthesized NPAH should be used in all future studies that seek to quantify total NPAH levels in ambient air.

The NPAH profiles at Freelton and Pier 25 are very similar if the two most heavily impacted samples (19-23hrs and 24hrs samples) from the Pier 25 site were

removed from the data set. Principal components analysis of the data set with the two heavily impacted samples removed showed that the air masses at Pier 25 and Freelton were not significantly different with respect to NPAH levels and NPAH profiles. The total NPAH levels in the latter 2 samples were significantly higher than in the other samples. Pier 25 is in close proximity to numerous sources of PAH and NPAH emissions (mobile sources and coking operations of steel mills); in addition some PAH would be transformed to certain NPAH isomers via hydroxyl radical reactions during the day-time. Thus the NPAH levels downwind of the city of Hamilton (from direct emissions and transformation processes) were very high compared to Freelton. Principal components analysis of the complete Freelton/Pier 25 data set showed a dramatic difference between the two sites, demonstrating the impacts of the urban/industrial core on air quality.

The second part of the thesis focused on the analysis and interpretation of polycyclic aromatic compound (PAC) data that had been collected during two different large-scale studies, one in Ontario, and the other in the Lower Fraser Valley in British Columbia. Concentration data for a set of PAC (both PAH and NPAH) were obtained for samples collected during the day and night in Ontario during a study at Simcoe (rural) and Toronto (urban) as well as three sites in British Columbia as part of the Pacific 2001 study (Slocan (urban), Langley (suburban/rural) and Sumas (rural)). The conversion of these concentration data into particulate loadings data (using elemental carbon data) allowed us to perform a number of unique interpretations and analyses of the data sets. The loadings data (like the concentration data) showed a range of values over 1000-fold.

The loadings data for each PAH and NPAH were then converted to relative loadings which showed remarkably similar trends.

Comparisons of loadings data in the Toronto/Simcoe data set showed that 5 PAH (BjF, BkF, BbF, BeP and BghiP) had very similar relative loadings patterns consistent with similar degrees of air transformation. When the relative loadings of all PAC species were compared to the PAH5 composite data at Simcoe and Toronto, clear diurnal patterns in transformation were observed. A principal components analysis (PCA) was performed on the Toronto/Simcoe PAC data set. The resulting 3D plots showed that the Toronto and Simcoe data sets were very different from each other and moreover the day and night samples at Simcoe were also very different. The day and night samples at Toronto were proximate. These plots showed that the PAH profiles collected during the day and night were different, consistent with differing degrees of transformation of PAH.

The PAC data from day and night samples from the Pacific 2001 study also showed that the profiles of PAH collected during the day and at night were different at all sites. These differences were smallest at the urban site (Slocan). The air masses moving onto Slocan from the west contains minimal amounts of pollutants since it is blowing in from the Pacific Ocean. Therefore the PAH profile at Slocan is thought to be representative of local emissions sources alone. The close association of the PAH from the day and night samples at Slocan in the principal components plot is consistent with Slocan being close to the sources of pollutants. The day and night samples from Langley and Sumas showed significant differences in their PAH profiles based on the PCA plots. Sumas is a rural site located well downwind of both Slocan and Langley.

Overall, the loadings approach to data analysis of air samples provides a new way of assessing and comparing PAC data in complex data sets, from which it is possible to make direct comparisons of PAH and NPAH profiles over a wide range of concentrations. Future studies should therefore attempt to obtain elemental carbon data such that loadings values could be calculated for each PAC. Clear differences between urban and rural sites as well as day-time and night-time samples can be related to air transformation of PAH.

5.0 REFERENCES

1. Holsen, T.M., Odabasi, M., Vardar, N. *The Science of the Total Environment*, **1999**, 227, 57-67
2. Hoefft, S., Dobbins, R. A., Fletcher, R. A., Benner Jr., B. A. *Combustion and Flame*, **2006**, 144, 773-781
3. Baker, J. E., Bamford, H. A., Bazabeh, D. Z., Schantz, M. M., Wise, S. A. *Chemosphere*, **2003**, 50, 575-587
4. Hayakawa, K., Tang, N., Akutsu, K., Murahashi, T., Kakimoto, H., Kizu, R., Toriba, A. *Atmospheric Environment*, **2002**, 36, 5535-5541
5. Pitts, J. N., Sweetman, J. A., Zielinska, B., Winer A. M., Atkinson, R. *Atmospheric Environment*, **1985**, 19, 1601-1608
6. Kamens, R. M., Fan, Z., Hu, J., Zhang, J., McDow, Stephen. *Environ. Sci. Technol.* **1996**, 30, 1358-1364
7. Kamens, R. M., Fan, Z., Chen, D., Birla, P. *Atmospheric Environment*, **1995**, 29, 1171-1181
8. Nielson, T., Feilberg, A. *Environ. Sci. Technol.* **2000**, 34, 789-797
9. Neilson, T. *Environ. Sci. Technol.* **1984**, 18, 157-163
10. Arrey, J., Zielinska, B., Atkinson, R., Winer, A. M., Ramdhal, T., Pitts Jr., J. N. *Atmospheric Environment*, **1986**, 20, 2339-2345
11. Pitts Jr., J. N., Sweetman, J. A., Zielinska, B., Atkinson, R., Winer, A. M., Hager, W. P. *Environ. Sci. Technol.* **1985**, 19, 1115-1121
12. Arey, J., Atkinson, R. *Environmental Health Perspectives*, **1994**, 102, 117-126
13. Kamens, R.M., Guo, Z., Fulcher, J. N., Bell, D. A. *Environ. Sci. Technol.* **1988**, 22, 103-108
14. Fu, P. P., Herreno-Saenz, D. *Environ. Carcino. & Ecotox.* **1999**, 17, 1-43
15. Atkinson, R., Arrey, J., Zielinska, B., Aschmann, S. M. *International Journal of Chemical Kinetics*, **1990**, 22, 999-1014

16. Arey, J.; Zielinska, B.; Atkinson, R.; Winer, A.M; Ramdahl, T.; Pitts, J.N., Jr. *Atmos. Environ.* **1986**, 20, 2339-2345.
17. Atkinson, R., Arey, J., Taulon, E. C. *International Journal of Chemical Kinetics.* **1990**, 22, 1071-1082.
18. Tang, N., Tabata, M., Mishukov, V.F., Sergineko, Valentine, Toriba, A., Kizu, R., Hayakawa, K. *Journal of Health Science*, **2002**, 48, 30-36
19. Schauer, C., Niessner, R., Poschl, U. *Anal Bioanal Chem.* **2004**, 378, 725-736
20. Sanderson, E.G., Raqbi, A., Vyskocil, A., Farant, J. P. *Atmospheric Environment.* **2004**, 38, 3417-3429
21. Baker, J. E., Larsen, R. K. *Environ. Sci. Technol.* **2003**, 37, 1873-1881
22. Samara, C., Papageorgopoulou, A., Manoli, E., Touloumi, E. *Chemosphere.* **1999**, 39, 2183-2199
23. Arey, J.; Atkinson, R.; Zielinska, B.; McElroy, P.A. *Environ. Sci. Technol.* **1989**, 23, 321-327.
24. Atkinson, R; Arey, J.; Zielinska, B; Aschmann, S.M. *Environ. Sci. Technol.* **1987**, 21, 1014-1022.
25. Atkinson, R.; Aschmann, S.M.; Arey, J.; Zielinska, B.; Schuetzle, D. *Atmos. Environ.* **1989**, 23, 2679-2690.
26. Atkinson, R.; Arey, J. *Chem. Rev.* **2003**, 103, 4605-4638.
27. Arey, J.; Zielinska, B.; Atkinson, R.; Winer, A.M; Ramdahl, T.; Pitts, J.N., Jr. *Atmos. Environ.* **1986**, 20, 2339-2345.
28. Quinn, J. S., McCarry, B. E., Somers, C. M., Malek, F. *Science.* **2004**. 304, 1008-1010
29. Boden, A.R. Ph. D. Thesis, McMaster University, **2001**.
30. Zhang, W. M.Sc. Thesis, McMaster University, **2002**.
31. Yang, R. M.Sc. Thesis, McMaster University, **2005**.
32. Feilberg, A; Nielsen, T. *Atmospheric Environment*, **2002**, 36, 4617-4625.

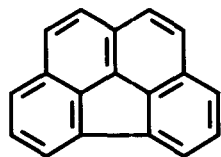
33. Feilberg, A; Neilsen, T. *Environ.Sci.Technol.* **2000**, 34, 789-797.
34. Baker, J.E., Offenber, J.H. *Atmospheric Environment*, **2002**, 36, 1205-1220.
35. Halsall, C.J., Sweetman, A. J., Barrie, L. A. Jones, K. C. *Atmospheric Environment.* **2001**, 35, 255-267.
36. Cecinato, A. *J. Sep. Sci.* **2003**, 26, 402-408
37. Feilberg, A., Nielsen, T., Binderup, M., Skov, H., Poulsen, M. W. B. *Atmospheric Environment.* **2002**, 36, 4617-4625.
38. Kamens, R. M., Leach, K. B., Strommen, M. R., Jang, M. *Journal of Atmospheric Chemistry.* **1999**, 33, 241-264.
39. Ramdahl, T., Becher, G., Bjorseth, A. *Environ. Sci. Technol.* **1982**, 16, 861-865.
40. Scheepers, P. T. J., Velders, D. D., Martens, M. H. J, Noordhoek, J., Bos, R. P. *Journal of Chromatography.* **1994**, 677, 107-121.
41. Pitts Jr., J. N., Cauwenberghe, K. A. V., Grosjean, D., Schmid, J. P., Fitz, D. R. *Science.* **1978**, 202, 515-519.
42. Gibson, T. L. *Mutation Research.* **1983**, 122, 115-121.
43. Durant, J. L., Busby, W. F., Lafleur, A. L., Penman, B. W., Crespi, C. L. *Mutation Research.* **1996**, 371, 123-157.
44. McCarry, B. E., Marvin, C. H., Morris, W. A., Versteeg, J. K., Bryant, D. W., Legzdins, A. E. *Atmospheric Environment.* **1995**, 29, 3441-3450.
45. Hisamatsu, Y., Nishimura, T., Tanabe, K., Matsushita, H. *Mutation Research.* **1986**, 172, 19-27.
46. Moller, L., Cui, X., Eriksson, L. C. *Mutation Research.* **1999**, 442, 9-18.
47. Gorse, R. A., Riley, T. L., Ferris, F. C., Pero, A. M., Skewes, L. M. *Environ. Sci. Technol.* **1983**, 17, 198-202.
48. Pitts Jr., J. N., Sweetman, J. A., Zielinska, B., Atkinson, R., Winer, A. M., Harger, W. P. *Environ. Sci. Technol.* **1985**, 19, 1115-1121
49. Arey, J., Atkinson, R., Sasaki, J., Aschmann, S. M., Kwok, E. S. C. *Environ. Sci. Technol.* **1997**, 31, 3173-3179.

50. Feilberg, A., Kamens, R. M., Strommen, M. R., Neilsen, T. *Atmospheric Environment*. **1999**, 33, 1231-1243.
51. McCarry, B. E., Lant, M. S., Quilliam, M. A., Messier, F., D'Agostino, P. A. *Spectros. Int. J.* **1984**, 3, 33-43
52. Ciccioli, P., Cecinato, A., Brancaleoni, E., Frattoni, M., Zacchei, P. *Journal of Geophysical Research*. **1996**, 101, 19567-19581.
53. Ramdahl, T., Arey, J., Atkinson, R., Pitts Jr., J. N., Zielinska, B., Winer, A. M. *Nature*. **1986**, 321, 425-427.
54. Atkinson, R., Plum, C. N., Carter, W. P. L., Winer, A. M., Pitts Jr., J. N. *J. Phys. Chem.* **1984**, 88, 1210-1215.
55. Kamens, R. M., Fan, Z., Zhang, J., Hu, J. *Environ. Sci. Technol.* **1986**, 30, 2821-2827.
56. Zielinska, B., Arey, J., Atkinson, R., Ramdahl, T., Winer, A. M., Pitts Jr., J. N. *J. Am. Chem. Soc.* **1986**, 108, 4126-4132.
57. Niederer, M. *Environ. Sci. & Pollut. Res.* **1998**, 5, 209-216.
58. Albinet, A., Leoz-Garziandia, E., Budzinski, H., Villenave, E. *Journal of Chromatography A*. **2006**, 1121, 106-113.
59. Baker, J. E., Crimmins, B. S. *Atmospheric Environment*. **2006**, 40, 6764-6779.
60. www.ec.gc.ca/air/smog_e.shtml
61. www.epa.gov/air/urbanair/pm/what1.html
62. Yaghi, B., Abdul-Wahab, S. A. *J. Environ. Monit.* **2003**, 5, 950-952.
63. Fang, G. C., Chang, C. N., Chu, C. C. *The Science of the Total Environment*. **2003**, 308, 157-166.
64. www.pca.state.mn.us/air/emissions/pm10.html.
65. Legzdins, A. E. Ph. D. Thesis, McMaster Univeristy, **1996**.
66. Silvers, K. J., Couch, L. H., Rorke, E. A., *Biochem. Pharmacol.* **1997**, 54, 927.

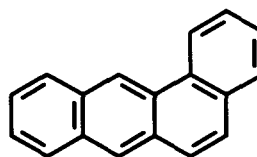
67. Takamura-Enya, T., Suzuki, H., Hisamatsu, Y. *Mutagenesis*. **2006**, 21, 399-504.
68. Fu, P.P. *Drug Metab. Rev.* **1990**, 22, 209-268.
69. Debnath, A. K., Debnath, A. G., Shusterman, A. J., Hansch, C. *Environ. Mol. Mutagen.* **1992**, 19, 37-52.
70. Hopke, P. K. *Receptor Modeling in Environmental Chemistry*. **1985**, 91-103.

APPENDIX A. Compound Names, Molecular Masses and Structures of Selected Polycyclic Aromatic Compounds

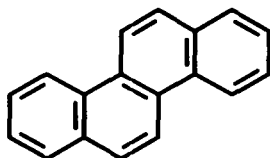
PAH:



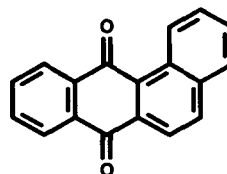
1. benzo[ghi]fluoranthene
M.W.226



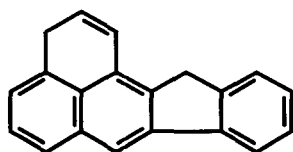
2. benz[a]anthracene
M.W.228



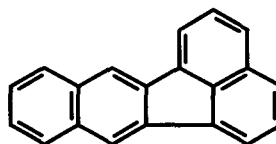
3. chrysene
M.W.228



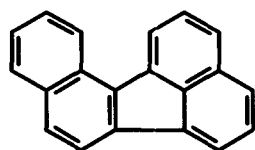
4. benz[a]anthracene-7,12-dione
M.W.258



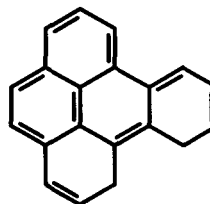
5. benzo[b]fluoranthene
M.W.252



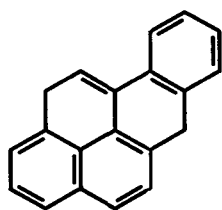
6. benzo[k]fluoranthene
M.W.252



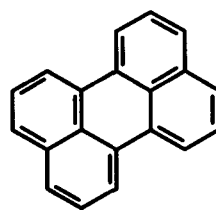
7. benzo[j]fluoranthene
M.W.252



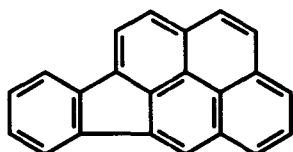
8. benzo[e]pyrene
M.W.252



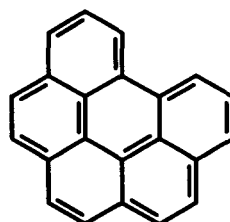
9. benzo[a]pyrene
M.W.252



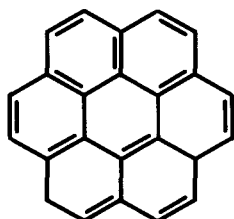
10. perylene
M.W.252



11. indeno[1,2,3-cd]pyrene
M.W.276

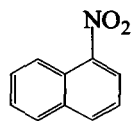


12. benzo[ghi]perylene
M.W.276

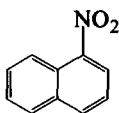


13. coronene
M.W.300

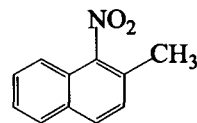
NPAH:



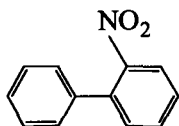
1) 1-nitronaphthalene
M.W.173



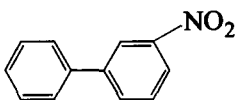
2) 2-nitronaphthalene
M.W.173



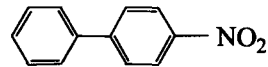
3) 2-methyl-1-nitronaphthalene
M.W. 187



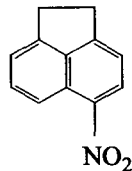
4) 2-nitrobiphenyl
M.W.199



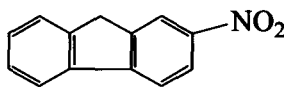
5) 3-nitrobiphenyl
M.W.199



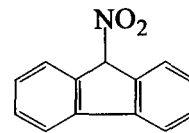
6) 4-nitrobiphenyl
M.W.199



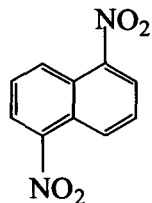
7) 5-nitroacenaphthene
M.W. 199



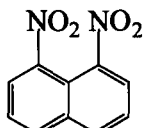
8) 2-nitrofluorene
M.W. 211



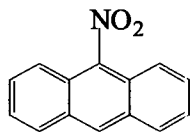
9) 9-nitrofluorene
M.W. 211



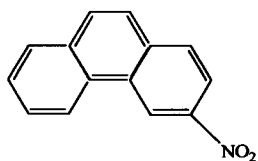
10) 1,5-dinitronaphthalene
M.W. 218



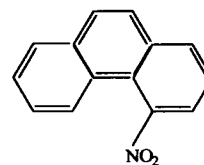
11) 1,8-dinitronaphthalene
M.W. 218



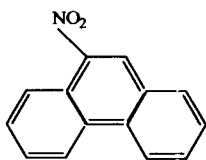
12) 9-nitroanthracene
M.W. 223



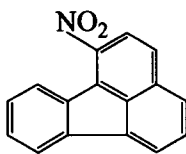
13) 3-nitrophenanthrene
M.W. =223



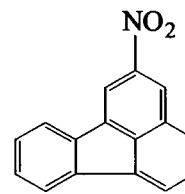
14) 4-nitrophenanthrene
M.W. 223



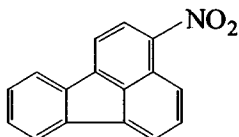
15) 9-nitrophenanthrene
M.W. 223



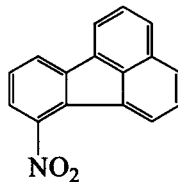
16) 1-nitrofluoranthene
M.W.247



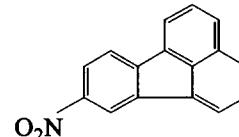
17) 2-nitrofluoranthene
M.W.247



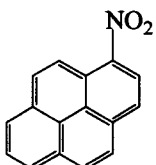
18) 3-nitrofluoranthene
M.W. 247



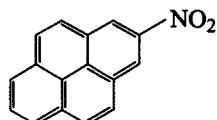
19) 7-nitrofluoranthene
M.W. 247



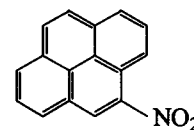
20) 8-nitrofluoranthene
M.W. 247



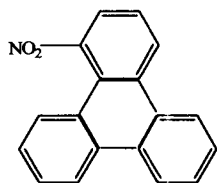
21) 1-nitropyrene
M.W. 247



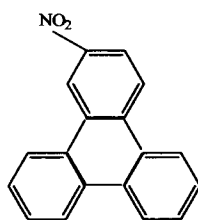
22) 2-nitropyrene
M.W. 247



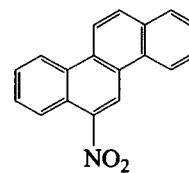
23) 4-nitropyrene
M.W. 247



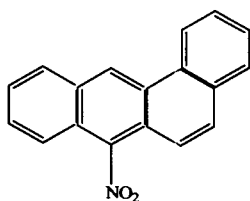
24) 1-Nitrotriphenylene
M.W. 273



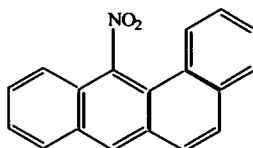
25) 2-Nitrotriphenylene
M.W. 273



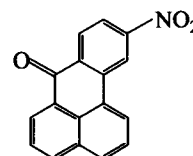
26) 6-nitrochrysene
M.W. 273



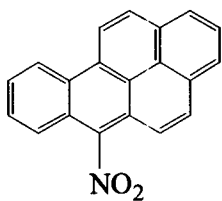
27) 7-nitrobenz[a]anthracene
M.W. 273



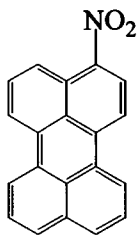
28) 12-Nitrobenz[a]anthracene
M.W. 273



29) 3-nitrobenzanthrone
M.W. 275



30) 6-nitrobenzo[a]pyrene
M.W. 297



31) 3-nitroperylene
M.W. 297

Appendix B. Concentrations (pg/m³) of the 23 NPAH compounds detected in the Freelton and Pier 25 samples.

Appendix B.1 Concentrations (pg/m³) of the 23 NPAH compounds detected in the Freelton samples.

ND: denotes samples in which PAC was not detected.

NPAH	Hours Downwind of Industrial Site					
	0hrs	1-3hrs	4-9hrs	10-18hrs	19-23hrs	24hrs
1-nitronaphthalene	ND	ND	0.22	0.11	ND	ND
2-methyl-1-nitronaphthalene	0.26	ND	0.01	0.01	0.12	0.19
2-nitronaphthalene	0.04	ND	0.18	0.11	ND	ND
2-nitrobiphenyl	ND	0.14	0.08	0.07	0.07	0.09
3-nitrobiphenyl	ND	0.14	0.06	0.06	0.09	0.07
4-nitrobiphenyl	2.04	ND	0.38	0.39	0.28	0.4
5-nitroacenaphthene	ND	3.54	0.09	0.09	0.11	0.14
1,8-dinitronaphthalene	0.06	0.05	0.05	0.02	0.05	0.12
9-nitroanthracene	1.74	5.29	1.1	0.86	0.99	1.07
4-nitrophenanthrene	0.29	0.14	0.03	0.02	0.07	0.1
9-nitrophenanthrene	0.07	0.16	0.05	0.04	0.09	0.16
3-nitrophenanthrene	0.78	1.36	0.48	0.42	0.38	0.57
2-nitrofluoranthene	12.49	18.92	6.38	11.83	4.08	13.8
3-nitrofluoranthene	0.74	1.92	2.32	0.19	0.27	0.36
4-nitropyrene	0.07	0.06	ND	ND	ND	0.16
8-nitrofluoranthene	0.54	ND	ND	ND	ND	0.25
1-nitropyrene	1.29	2.07	1.08	0.38	0.38	0.56
2-nitropyrene	0.64	1.98	ND	ND	ND	0.48
12-nitrobenzanthracene	0.23	0.16	ND	0.11	0.07	0.61
7-nitrobenzanthracene	0.8	0.81	0.22	0.43	0.14	1.21
1-nitrotriphenylene	0.27	0.66	ND	0.1	0.16	2.13
6-nitrochrysene	6.83	0.61	ND	0.35	0.55	0.53
3-nitrobenzanthrone	4.99	0.51	1.67	0.51	0.82	0.7
Total	34.17	38.52	14.4	16.08	8.72	23.69

Appendix B.2 Concentrations (pg/m³) of the 23 NPAH compounds detected in the Pier 25 samples.

ND: denotes samples in which PAC was not detected.

NPAH	Hours Downwind of Industrial Site					
	0hrs	1-3hrs	4-9hrs	10-18hrs	19-23hrs	24hrs
1-nitronaphthalene	ND	ND	0.13	0.04	1.28	15.86
2-methyl-1-nitronaphthalene	ND	ND	0.01	ND	0.12	0.23
2-nitronaphthalene	ND	ND	0.13	0.03	0.65	0.56
2-nitrobiphenyl	0.07	0.04	0.05	ND	0.17	0.18
3-nitrobiphenyl	0.11	0.07	0.09	0.03	0.29	0.25
4-nitrobiphenyl	ND	ND	0.43	ND	ND	0.71
5-nitroacenaphthene	3.4	0.46	0.47	0.5	2.14	23.78
1,8-dinitronaphthalene	0.05	ND	0.13	0.03	0.13	0.2
9-nitroanthracene	7.35	5.51	7.18	0.65	35.75	60.28
4-nitrophenanthrene	0.2	0.16	0.22	0.07	0.55	1.58
9-nitrophenanthrene	0.32	0.18	0.36	0.12	0.64	2.45
3-nitrophenanthrene	1.57	1.03	1.65	0.44	5.56	5.45
2-nitrofluoranthene	12.76	18.73	17.4	5.29	53.37	60.06
3-nitrofluoranthene	1.84	0.83	2.02	1.75	1.51	10.88
4-nitropyrene	0.11	0.21	0.33	0.11	ND	0.65
8-nitrofluoranthene	0.23	ND	0.48	ND	ND	ND
1-nitropyrene	4.06	2.83	2.71	1.53	8.19	15.6
2-nitropyrene	2.96	1.57	2.2	ND	7.63	18.2
12-nitrobenzanthracene	0.15	0.17	0.91	ND	1.91	ND
7-nitrobenzanthracene	1.13	1.23	2.98	0.47	9.37	7.84
1-nitrotriphenylene	0.29	0.12	1.21	0.59	ND	ND
6-nitrochrysene	2.61	0.48	2.65	ND	6.01	7.27
3-nitrobenzanthrone	2.41	0.43	1.37	0.32	2.13	2.43
Total	41.61	34.04	45.12	11.97	137.38	234.45

Appendix C. Relative Loadings ($\mu\text{g/g C}$) of PAC in $\text{PM}_{2.5}$ collected at Simcoe and Toronto

Appendix C.1 Relative Loadings ($\mu\text{g/g C}$) of PAC in $\text{PM}_{2.5}$ collected at Simcoe

Sample	Polycyclic Aromatic Compound															
	BghiF	BaA	Chry	BD	BbF	BJF	BkF	BeP	BaP	Pery	IcdP	BghiP	Cor	1-NP	2-NP	2-NFA
sim0716D	5.5	3.3	5.2	5.4	4.1	3.3	4.5	3.9	2.6	2.1	3.7	4.3	1.0	1.3	1.4	3.5
sim0716N	10.4	6.7	12.2	26.3	15.4	9.8	11.1	14.8	7.4	8.4	10.6	12.0	ND	7.8	25.6	30.9
sim0717D	114.3	111.5	99.6	71.7	100.0	100.0	100.0	100.0	100.0	100.0	121.4	115.6	64.0	10.8	28.2	15.4
sim0717N	10.6	9.1	14.2	25.2	17.0	12.7	13.7	14.9	12.3	16.6	13.8	18.7	16.4	10.0	43.5	37.9
sim0718D	4.8	9.4	19.5	24.6	18.7	11.2	13.0	17.6	8.6	9.4	10.6	12.2	6.8	5.6	16.3	5.7
sim0718N	14.1	19.8	15.8	32.7	18.1	11.7	13.5	24.5	23.6	10.3	12.7	19.7	17.5	23.0	31.3	79.9
sim0719D	9.7	6.4	14.0	42.4	20.2	13.3	15.7	18.7	7.9	10.9	18.7	18.2	16.8	3.3	17.9	16.1
sim0719N	23.2	24.1	31.6	29.9	30.4	30.5	31.2	28.3	29.2	26.7	28.2	26.2	15.8	3.3	9.0	2.5
sim0720D	10.4	4.3	13.0	10.7	6.4	3.5	5.0	6.1	6.0	2.6	4.5	6.2	3.7	5.3	ND	3.3
sim0720N	11.4	8.3	7.1	20.8	14.9	11.9	13.8	14.0	50.3	11.7	12.5	12.3	ND	11.2	36.7	21.1
sim0721D	19.5	5.4	7.6	16.0	21.9	17.2	19.1	19.0	26.2	12.5	15.5	15.7	ND	10.5	27.5	5.0
sim0721N	7.9	3.7	9.0	12.1	9.6	7.3	8.5	9.3	9.6	4.2	9.2	7.9	ND	13.5	9.3	3.8
sim0722D	8.6	4.0	21.6	12.0	8.1	6.6	6.8	7.9	4.7	4.9	6.7	7.2	ND	8.7	18.9	4.1
sim0722N	5.7	2.1	9.1	13.8	8.0	5.5	6.3	6.9	9.3	3.7	7.7	8.6	ND	8.5	13.9	6.4
sim0723D	6.2	3.0	7.2	7.0	4.4	4.0	3.9	4.5	5.2	3.4	3.3	4.9	1.3	5.2	5.6	3.0
sim0723N	8.7	1.8	3.1	11.0	10.1	9.0	11.9	10.1	7.8	6.2	15.1	15.5	14.3	4.0	11.6	7.3

ND: denotes samples in which PAC was not detected.

Appendix C.1 Relative Loadings ($\mu\text{g/g C}$) of PAC in $\text{PM}_{2.5}$ collected at Simcoe (Cont.)

Sample	Polycyclic Aromatic Compound															
	BghiF	BaA	Chry	BD	BbF	BJF	BkF	BeP	BaP	Pery	lcdP	BghiP	Cor	1-NP	2-NP	2-NFA
sim0724D	11.8	4.6	9.3	8.1	7.4	6.6	6.5	6.8	5.4	6.1	4.5	8.4	3.2	7.7	13.9	8.1
sim0724N	10.6	9.1	14.8	15.3	7.6	5.1	7.1	6.9	6.2	3.3	6.5	7.3	5.1	5.0	ND	14.7
sim0725D	23.5	11.4	25.0	22.8	17.2	12.2	15.0	17.7	15.4	10.2	14.0	20.2	17.7	15.0	24.5	22.2
sim0725N	15.4	8.9	11.0	33.0	30.0	24.9	27.7	28.0	23.9	25.4	22.9	24.4	14.9	11.1	60.4	27.3
sim0726D	48.4	29.5	21.8	128.3	70.3	50.6	63.0	67.1	33.7	45.3	60.3	60.2	46.0	36.5	111.4	103.3
sim0726N	10.8	5.7	6.0	8.6	8.6	6.4	6.2	7.2	13.6	4.8	5.9	6.7	5.7	23.3	ND	5.1
sim0727D	37.1	30.1	50.1	23.4	39.9	35.1	38.1	35.5	29.0	29.2	29.4	27.9	14.5	12.5	ND	8.7
sim0727N	12.3	12.5	33.5	54.1	43.8	23.7	28.1	39.7	11.6	16.3	23.8	25.2	15.7	15.4	19.2	96.8
sim0728D	69.4	88.5	100.4	48.8	96.2	88.8	98.0	90.3	82.9	87.9	78.6	71.8	32.6	9.2	15.0	19.3
sim0728N	20.1	20.6	32.4	40.9	34.8	25.1	29.6	33.9	23.0	26.9	30.2	32.2	25.5	12.0	13.0	40.2

ND: denotes samples in which PAC was not detected.

Appendix C.2 Relative Loadings ($\mu\text{g/g C}$) of PAC in $\text{PM}_{2.5}$ collected at Toronto.

Sample	Polycyclic Aromatic Compound															
	BghiF	BaA	Chry	BD	BbF	BJF	BkF	BeP	BaP	Pery	IcdP	BghiP	Cor	1-NP	2-NP	2-NFA
tor0716D	21.7	10.0	10.4	6.6	13.2	13.3	18.6	14.4	13.3	14.4	17.0	27.5	22.5	24.9	28.2	9.1
tor0716N	8.9	2.2	4.8	9.2	4.6	3.3	4.3	4.7	2.3	2.1	4.4	8.2	10.8	15.9	15.0	11.8
tor0717D	21.5	6.4	7.4	8.0	6.4	5.8	8.5	7.8	6.6	ND	7.3	16.0	20.5	21.4	20.6	7.3
tor0717N	11.8	3.7	6.3	11.4	6.9	5.5	6.9	10.9	6.9	10.2	9.9	33.6	47.6	35.0	33.9	11.3
tor0718D	35.2	19.7	23.4	15.2	16.9	14.5	20.4	22.1	24.5	20.2	18.4	35.8	42.7	36.1	19.0	7.3
tor0718N	12.3	6.7	15.0	15.6	14.1	7.5	9.7	14.5	5.3	5.9	12.5	18.2	23.7	22.6	36.3	14.0
tor0719D	20.8	24.0	32.7	18.3	24.2	20.7	22.5	22.3	90.4	24.4	16.1	18.9	16.6	34.3	48.8	10.9
tor0719N	12.4	4.9	10.3	22.0	9.4	5.6	7.7	11.8	4.3	7.2	11.7	20.4	29.1	23.4	38.7	22.4
tor0720D	11.8	7.6	12.6	11.6	7.9	5.5	7.3	8.6	18.7	6.0	7.7	13.6	17.2	20.1	6.0	14.2
tor0720N	14.5	3.9	5.8	23.6	10.8	6.7	9.4	12.6	4.4	4.9	10.4	22.1	37.8	56.4	22.9	30.4
tor0721D	26.8	20.9	21.5	18.4	28.2	22.9	25.0	26.8	26.0	25.3	26.8	28.2	27.4	10.0	11.9	5.9
tor0721N	12.2	4.2	5.2	17.2	9.8	6.5	8.6	11.3	5.4	9.4	12.2	21.7	32.9	24.4	37.1	20.5
tor0722D	34.1	18.6	26.7	21.1	31.9	25.2	29.9	30.4	26.1	28.7	28.1	24.3	22.3	21.9	26.4	10.6
tor0722N	17.3	12.2	12.6	27.7	24.7	15.9	17.4	22.6	10.3	17.3	25.8	25.6	4.4	23.5	28.6	50.2
tor0723D	29.7	14.8	14.8	14.3	20.2	14.7	16.9	20.2	17.8	19.0	20.9	28.4	32.7	26.0	27.6	15.9
tor0723N	11.2	10.4	8.1	11.0	12.5	11.4	13.2	12.7	10.2	13.6	12.7	15.1	13.7	17.5	14.1	16.3

ND: denotes samples in which PAC was not detected.

Appendix C.2 Relative Loadings ($\mu\text{g/g C}$) of PAC in $\text{PM}_{2.5}$ collected at Toronto site (Cont.)

Sample	Polycyclic Aromatic Compound															
	BghiF	BaA	Chry	BD	BbF	BjF	BkF	BeP	BaP	Pery	lcdP	BghiP	Cor	1-NP	2-NP	2-NFA
tor0724D	15.0	6.8	9.1	9.7	8.4	6.1	7.8	9.9	5.0	7.8	7.8	16.0	22.5	18.2	18.1	8.2
tor0724N	17.0	13.2	8.9	12.0	8.7	6.4	9.0	11.7	15.8	8.1	9.9	25.7	32.9	32.4	44.1	10.2
tor0725D	19.8	11.2	12.7	9.4	10.6	8.8	11.0	13.1	14.9	15.2	10.0	20.8	24.4	35.2	19.4	9.4
tor0725N	21.9	7.6	19.7	24.7	11.6	10.2	12.5	12.9	21.0	8.7	13.3	25.1	31.5	22.7	33.9	8.9
tor0726D	85.7	42.7	46.5	35.1	34.1	33.8	40.4	48.4	42.0	64.8	33.5	84.4	105.1	143.7	88.7	22.9
tor0726N	30.6	7.7	8.8	12.1	10.3	7.5	10.1	13.0	9.6	9.8	10.9	28.1	32.6	25.7	29.5	5.1

ND: denotes samples in which PAC was not detected.

Appendix D. Relative Loadings ($\mu\text{g/g C}$) of PAC in $\text{PM}_{2.5}$ collected at Slocan, Langley and Sumas.

Appendix D.1 Relative Loadings ($\mu\text{g/g C}$) of PAC in $\text{PM}_{2.5}$ collected at Slocan.

Sample	Polycyclic Aromatic Compound															
	BghiF	BaA	Chry	BD	BbF	BjF	BkF	BeP	BaP	Pery	IcdP	BghiP	Cor	1-NP	2-NP	2-NFA
SL0815N	15.8	8.8	21.1	35.2	19.6	16.5	16.1	19.1	0.4	ND	19.0	12.0	13.1	23.5	15.2	38.4
SL0816D	7.6	7.9	11.6	12.5	7.6	5.8	7.0	8.2	1.5	2.8	6.9	4.1	4.1	8.1	7.1	10.6
SL0816N	6.2	4.0	5.8	11.4	9.8	7.5	8.5	5.7	4.5	4.9	9.0	3.7	3.9	16.5	12.3	16.2
SL0817D	14.5	13.1	15.2	12.8	13.5	14.7	12.9	12.3	4.4	5.4	14.2	9.1	8.4	17.3	21.3	20.1
SL0817N	10.2	14.6	10.2	14.5	19.5	23.8	21.0	20.4	26.8	26.0	30.6	19.1	19.5	24.5	12.7	13.4
SL0818D	10.9	15.8	15.0	13.2	12.2	12.2	12.5	12.1	13.1	9.4	12.7	5.9	4.6	6.4	8.9	6.9
SL0818N	8.9	8.3	8.5	23.6	18.1	18.8	17.4	15.5	10.2	10.6	25.3	12.8	12.6	12.2	14.2	17.0
SL0819D	34.2	24.0	25.9	42.8	42.7	44.3	42.9	40.6	13.3	14.9	59.0	35.3	38.2	30.5	39.2	25.5
SL0820D	10.3	8.2	8.9	18.3	13.1	12.5	12.2	12.0	5.6	6.1	16.7	9.7	10.1	10.4	12.4	12.6
SL0821	7.6	7.1	5.6	13.0	13.6	13.8	14.1	11.4	4.6	5.1	17.9	9.5	10.3	11.3	5.4	6.1
SL0824N	17.5	14.8	11.8	13.0	15.4	16.8	16.3	16.2	16.1	15.5	25.0	17.6	18.6	13.1	10.7	9.3
SL0825D	30.2	26.7	20.0	28.0	21.4	21.1	21.0	20.9	19.0	24.0	26.6	18.3	20.3	12.0	11.5	11.3
SL0825N	17.1	17.8	10.9	19.2	30.0	32.9	31.9	27.8	31.9	31.1	48.4	33.7	38.6	21.4	6.9	8.3
SL0826D	11.9	14.1	20.0	22.1	11.8	8.7	8.8	14.6	9.4	6.9	12.0	8.5	9.7	6.3	11.3	15.7
SL0826N	17.4	14.9	14.4	28.3	25.9	24.9	25.0	22.6	16.3	14.9	37.3	20.2	23.3	19.0	14.9	30.3

ND: denotes samples in which PAC was not detected.

Appendix D.1 Relative Loadings ($\mu\text{g/g C}$) of PAC in $\text{PM}_{2.5}$ collected at Slocan (Cont.).

Sample	Polycyclic Aromatic Compound															
	BghiF	BaA	Chry	BD	BbF	BjF	BkF	BeP	BaP	Pery	IcdP	BghiP	Cor	1-NP	2-NP	2-NFA
SL0827D	14.4	16.7	18.3	13.9	9.9	20.8	19.4	11.4	6.6	16.7	9.4	6.0	5.5	7.8	7.2	9.1
SL0827N	14.3	11.5	14.6	29.3	20.6	19.4	19.9	19.5	10.0	10.6	24.2	14.4	15.8	14.4	11.0	31.4
SL0828D	24.8	25.3	28.9	22.5	18.6	16.6	16.7	20.7	16.9	15.0	19.0	14.8	16.4	18.0	9.5	21.6
SL0828N	33.6	30.0	15.5	20.3	30.5	34.7	35.6	29.1	59.8	50.0	46.3	34.1	39.5	24.8	5.4	13.9
SL0829D	16.2	18.2	21.1	20.7	13.3	11.0	11.9	16.6	13.2	10.5	13.1	10.1	10.8	10.3	9.7	13.3
SL0829N	17.6	22.0	11.7	15.0	23.8	27.4	27.1	21.9	41.1	33.3	34.7	23.2	24.4	18.8	9.1	12.8
SL0830D	4.9	4.7	7.4	4.8	3.2	2.5	2.6	3.9	2.3	2.2	2.4	1.9	1.7	3.4	2.3	3.9
SL0830N	8.2	8.0	9.3	13.6	9.2	8.7	8.5	8.8	6.7	5.8	1.0	7.0	7.2	9.8	2.9	10.8

ND: denotes samples in which PAC was not detected.

Appendix D.2 Relative Loadings ($\mu\text{g/g C}$) of PAC in $\text{PM}_{2.5}$ collected at Langley.

Sample	Polycyclic Aromatic Compound															
	BghiF	BaA	Chry	BD	BbF	BJF	BkF	BeP	BaP	Pery	IcdP	BghiP	Cor	1-NP	2-NP	2-NFA
LA0816N	51.9	40.7	31.6	82.7	57.6	32.0	36.8	33.2	16.2	ND	51.2	17.8	20.1	81.1	108.2	34.2
LA0817D	19.2	18.8	12.5	37.7	17.4	6.3	11.7	15.1	12.1	ND	18.1	8.4	10.1	30.2	85.7	19.3
LA0817N	158.9	129.3	80.5	104.4	144.5	150.6	146.4	137.3	176.7	156.0	ND	174.6	174.3	140.9	105.7	51.9
LA0818D	62.0	82.5	30.9	29.2	54.8	48.6	59.9	40.6	27.1	48.4	73.0	25.7	24.5	18.2	38.6	31.0
LA0818N	25.2	22.0	32.7	77.8	55.8	55.0	50.9	65.4	17.6	24.0	103.6	56.2	55.7	41.4	19.8	17.8
LA0819D	7.3	9.3	9.5	20.7	8.4	4.6	4.8	6.0	4.7	ND	8.6	3.8	4.8	7.6	21.5	24.3
LA0819N	6.6	4.5	6.2	17.1	10.1	9.0	8.9	8.0	3.0	ND	14.1	6.0	6.7	7.0	7.1	9.1
LA0820D	6.0	4.9	4.4	6.2	3.4	2.0	2.6	3.4	3.6	3.9	4.2	2.1	2.7	4.7	22.2	5.7
LA0820N	17.2	11.2	11.2	36.6	27.8	28.9	24.2	22.9	6.1	10.2	38.8	18.5	18.3	17.3	34.8	49.5
LA0824D	67.7	88.0	88.4	112.4	97.9	94.2	93.9	97.3	47.4	44.3	119.1	69.2	69.9	78.3	56.6	49.5
LA0824N	14.4	23.6	15.5	31.1	36.6	40.3	40.8	33.9	59.1	54.4	77.3	32.7	23.7	11.6	15.0	8.7
LA0825D	6.3	12.2	14.6	7.2	3.7	2.5	2.4	8.3	4.2	5.0	2.2	2.2	1.7	2.4	6.3	3.3
LA0825N	7.1	9.1	8.8	27.6	18.1	19.3	17.6	17.2	16.5	16.9	34.5	18.5	17.6	9.5	12.9	13.1
LA0826D	14.9	28.2	42.3	36.9	15.0	12.0	11.2	23.8	13.5	9.1	14.7	9.5	8.9	7.8	20.1	10.3
LA0826N	1.2	13.0	131.0	27.1	11.6	13.4	12.7	1.0	0.5	ND	11.9	1.4	ND	3.4	3.1	3.2

ND: denotes samples in which PAC was not detected.

Appendix D.2 Relative Loadings ($\mu\text{g/g C}$) of PAC in $\text{PM}_{2.5}$ collected at Langley (Cont.).

Sample	Polycyclic Aromatic Compound															
	BghiF	BaA	Chry	BD	BbF	BJF	BkF	BeP	BaP	Pery	IcdP	BghiP	Cor	1-NP	2-NP	2-NFA
LA0827D	9.8	22.2	35.4	23.5	13.8	12.1	13.6	16.8	5.3	14.4	9.8	7.0	3.2	8.7	10.7	6.4
LA0827N	22.6	20.6	34.0	78.5	48.3	45.3	43.2	40.9	17.2	16.8	53.4	21.2	19.6	24.9	23.6	101.4
LA0828D	4.7	6.9	42.6	8.1	4.4	3.2	4.2	4.9	2.9	2.7	5.9	3.3	3.3	3.9	6.5	7.2
LA0828N	51.6	55.3	41.7	44.4	48.3	49.7	50.7	47.7	63.6	53.7	67.4	36.5	28.8	58.4	17.0	21.0
LA0829D	8.2	11.3	10.2	12.1	7.3	19.6	6.6	8.2	4.8	8.4	8.2	4.2	5.6	6.2	11.9	14.7
LA0829N	35.6	38.3	46.3	56.6	32.5	33.5	32.6	32.8	25.1	25.7	42.5	26.7	24.9	38.0	29.5	23.8
LA0830D	18.9	25.3	22.8	28.3	16.4	40.4	10.7	18.1	11.6	15.0	18.9	5.7	12.7	8.2	17.5	19.7
LA0830N	11.6	13.1	15.8	33.4	16.0	11.2	9.5	15.3	7.1	8.7	18.6	7.5	10.1	25.6	15.8	36.6
LA0831D	18.1	37.5	42.1	41.3	20.5	12.5	11.4	27.9	12.5	11.9	8.1	9.5	11.6	11.0	17.7	13.3

ND: denotes samples in which PAC was not detected.

Appendix D.3 Relative Loadings ($\mu\text{g/g C}$) of PAC in $\text{PM}_{2.5}$ collected at Sumas.

Sample	Polycyclic Aromatic Compound															
	BghiF	BaA	Chry	BD	BbF	BjF	BkF	BeP	BaP	Pery	IcdP	BghiP	Cor	1-NP	2-NP	2-NFA
SU0817D	16.6	15.9	11.8	14.6	16.1	8.8	16.3	12.7	14.8	12.9	18.4	11.3	10.8	22.7	38.1	23.2
SU0817N	4.4	3.4	2.7	9.8	7.5	7.4	6.3	5.2	3.6	3.5	7.8	4.1	4.4	8.5	26.7	34.6
SU0818D	10.4	10.0	8.3	7.3	11.8	4.0	9.4	7.5	3.4	7.5	13.5	7.4	6.1	16.3	ND	18.1
SU0818N	7.7	4.9	5.6	15.0	11.1	8.3	7.1	8.0	4.8	4.4	13.4	6.7	6.2	13.6	60.0	42.7
SU0819D	8.9	4.0	7.8	12.7	7.2	4.3	6.8	5.3	2.2	ND	8.9	4.4	4.1	9.7	16.3	24.1
SU0819N	41.5	36.3	13.9	49.4	18.5	22.3	28.9	19.0	16.3	81.5	18.0	8.8	9.1	12.8	45.7	55.6
SU0820D	73.0	52.0	31.6	48.0	39.5	44.1	43.3	35.2	22.1	46.6	39.3	26.4	27.7	74.0	11.6	10.3
SU0820N	7.6	5.6	4.6	10.5	7.0	6.3	5.3	4.7	4.0	3.9	6.7	3.2	3.8	4.1	ND	32.6
SU0824D	10.2	5.6	6.2	6.7	7.0	6.7	6.3	5.1	7.7	3.9	7.8	3.1	3.7	10.5	10.3	12.7
SU0824N	4.2	4.5	3.6	3.6	5.0	5.3	5.9	4.7	5.5	2.7	5.1	4.3	2.1	1.9	4.6	7.2
SU0825D	7.5	6.1	3.8	2.3	4.6	3.6	5.2	11.2	8.8	4.5	5.7	7.5	3.8	4.5	15.3	6.8
SU0825N	9.8	11.7	10.5	25.7	19.5	21.7	22.0	9.9	14.7	12.0	30.1	6.7	7.8	5.0	21.1	19.3
SU0826D	58.1	52.3	20.7	49.8	29.6	23.5	31.5	15.1	14.5	62.7	30.0	9.5	23.6	9.8	30.4	31.0
SU0826N	8.5	5.7	6.0	15.1	7.8	6.7	6.8	15.9	12.9	13.0	9.5	11.6	4.9	2.5	8.6	34.1
SU0827D	9.6	7.2	9.2	9.9	5.1	2.9	4.4	4.3	4.3	3.9	6.2	4.3	5.0	8.4	7.1	12.9

ND: denotes samples in which PAC was not detected.

Appendix D.3 Relative Loadings ($\mu\text{g/g C}$) of PAC in $\text{PM}_{2.5}$ collected at Sumas (Cont.).

Sample	Polycyclic Aromatic Compound															
	BghiF	BaA	Chry	BD	BbF	BjF	BkF	BeP	BaP	Pery	IcdP	BghiP	Cor	1-NP	2-NP	2-NFA
SU0827N	8.1	6.0	7.3	25.4	14.6	13.4	13.3	5.7	5.8	9.4	14.1	6.5	9.1	8.9	26.3	143.1
SU0828D	8.4	4.6	3.5	4.2	4.7	4.1	4.3	4.0	4.0	3.8	5.5	4.5	5.6	6.2	13.9	24.7
SU0829D	12.5	10.7	7.1	10.0	8.4	4.9	6.2	6.5	8.2	4.3	8.5	6.5	6.4	9.7	16.7	31.3
SU0829N	5.6	5.0	12.8	7.4	5.6	5.9	5.0	4.7	3.8	4.1	5.8	3.5	2.2	12.6	14.3	22.2
SU0830D	14.1	10.2	7.3	8.5	7.0	46.2	6.7	6.2	7.2	3.5	9.0	6.4	7.5	10.4	17.4	23.1
SU0830N	8.5	6.0	5.4	13.2	8.8	6.4	7.2	5.6	4.1	4.4	8.7	4.9	7.0	9.1	12.7	50.1

ND: denotes samples in which PAC was not detected.